AIR FORCE INSTITUTE OF TECHNOLOGY

AIR UNIVERSITY
UNITED STATES AIR FORCE

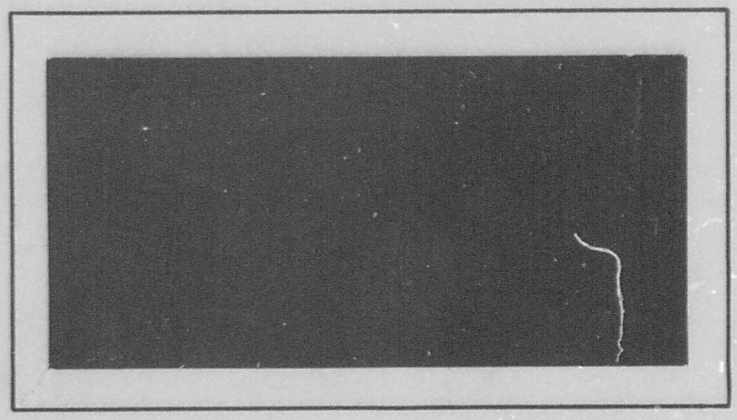

SCHOOL OF ENGINEERING

WRIGHT-PATTERSON AIR FORCE BASE, OHIO

THE APPROXIMATE LONGITUDINAL STABILITY DERIVATIVES OF A VECTORED THRUST VTOL

THESIS

Charles P. Winters
Captain USAF

GAM/AE/68-11

AFLC-WPAFB-MAY 68 35

THE APPROXIMATE LONGITUDINAL STABILITY DERIVATIVES OF A VECTORED THRUST VTOL

THESIS

Presented to the Faculty of the School of Engineering of
the Air Force Institute of Technology
Air University
in Partial Fulfillment of the
Requirements for the Degree of
Master of Science

by

Charles P. Winters, B.S.
Captain USAF
Graduate Aerospace-Mechanical Engineering

March 1968

Acknowledgments

The author wishes to express appreciation to Squadron Leader B. Dickinson and Captain R. VanPutte for their encouragement and assistance and to Mr. E. Flynn and Mr. F. Thomas of the USAF Flight Dynamics Laboratory for suggesting this topic and for their assistance. Appreciation is also extended to Mrs. Imogene Hoffer for her suggestions and for her excellent typing. Last but not least, he wishes to acknowledge his wife for her patience and understanding.

BLANK PAGE

Contents

List of Figures

List of Tables

BLANK PAGE

List of Symbols

A	aspect ratio, b^2/S_w
A_e	effective aspect ratio, b_e^2/S_e
A_{eff}	Datcom parameter used to estimate tail downwash
C_1, C_2, C_3, C_4, C_5	coefficients of the drag polynomial
C_1, C_2	1 - empirical taper ratio constants 2 - example constants used in discussion of control stick displacement
C_{Db}	Datcom parameter used to determine $(C_{DO})_B$
ΔC_{DMIN}	change in the minimum parasite, drag coefficient due to flap deflection
ΔC_{df}	Datcom parameter used to determine ΔC_{DMIN}
$(C_{Di})_w$	induced drag coefficient of the wing alone
$(C_{DO})_{ave}$	average parasite drag coefficient with flaps deflected 50°
$(C_{DO})_B$	parasite drag coefficient of the fuselage alone
$(C_{DO})_W$	parasite drag coefficient of the wing alone (also called C_{Df})
$(C_{DO})_{WB}$	parasite drag coefficient of the wing-body
$(C_D)_{WB}$	drag coefficient of the wing-body
C_f	coefficient of friction
$(C_{L\alpha})_e$	lift-curve slope of the effective lifting surface, per radian
C_{LMAX}	maximum lift coefficient
ΔC_{LMAX}	1 - Datcom parameter used to determine C_{LMAX} 2 - change in maximum lift coefficient due to flap deflection
C_{LMIN}	minimum lift coefficient before wing stall at negative angle of attack
C_{Lo}	wing-body lift coefficient at zero aircraft angle of attack

$(C_{L\alpha})_N$	lift curve slope of aircraft nose section, per radian
$(C_{L\alpha})_t$	lift curve slope of aircraft horizontal tail, per radian
$(C_{L\alpha})_{WB}$	lift curve slope of aircraft wing-body, per radian
$(C_{LMAX})_W$	maximum lift coefficient of the wing alone
$(C_{LMAX})_{WB}$	maximum lift coefficient of the wing-body
$(C_{L\alpha})_\delta$	lift-curve slope of the wing-body with 50° flaps, per radian
$C_{L\alpha W(B)}, C_{L\alpha B(W)}$	wing-body interference factors used to determine the aerodynamic center
C_{LT}	tail lift coefficient
C_{LWB}	wing-body lift coefficient
$C_{Mc/4}$	moment coefficient about the quarter chord of the mean aerodynamic chord
$C_{Ma.c.}$	moment coefficient about the a.c. (caused by flap deflection)
C_T	thrust coefficient, $T/{}^1/_2\rho V^2 S_w$
D_{WB}	drag of the wing-body, lbf
D_T	drag of the horizontal tail, lbf
F_1	total force in OX' direction excepting thrust forces, lbf
F_2	total force in OZ' direction excepting thrust forces, lbf
F_I	force at the air intake caused by induced vertical velocity from jet interference, lbf
F_{R1}, F_{R2}	reaction control forces, lbf
F_u	intake air momentum loss in OX' direction, lbf
F_w	intake air momentum loss in OZ' direction, lbf
I_{yy}	aircraft moment of inertia about the OY, OY' axis, slug ft^2

J	Datcom parameter used to determine $(C_{Di})_w$
K	1 - Datcom parameter used to determine $(C_{L\alpha})_e$, $C_{l\alpha}/2\pi$ 2 - Datcom parameter used to determine $(C_{Di})_w$ 3 - Datcom parameter used to determine C_{LMAX}, $C_{Ma.c.}$ and α_{MIN}
K_b,K'	Datcom parameter used to determine ΔC_{DMIN}
K_N,$K_{W(B)}$,$K_{B(W)}$	Datcom parameters used to determine $(C_{l\alpha})_{WB}$
L_T	tail lift, lbf
L_{WB}	wing-body lift, lbf
M,M_1	1 - total moment excepting reaction control and tail incidence contributions, ft lbf 2 - total moment about OY axis, equations of motion, ft lbf
M_o	1 - moment about the a.c. caused by flap deflection, ft lbf 2 - equilibrium moments, equation of motion, ft lbf $1/I_{yy}\partial M/\partial q$
M_R	reaction control moment, ft lbf
M_{RNF}	reduced reaction control moment caused by reduced thrust in nonaccelerating transition, ft lbf
ΔM	perturbation moment, equations of motion, ft lbf
M_T	moment caused by tail incidence, ft lbf
M_u	$1/I_{yy}\partial M/\partial u$
M_w	$1/I_{yy}\partial M/\partial w$
$M_{\dot{w}}$	$1/I_{yy}\partial M/\partial \dot{w}$
N_F/N_{FD}	per cent of 100% engine speed
RPM_{250}	difference in engine speed between zero and 250 kts airspeed at constant thrust
$RPM_{.95}$	.95 engine speed
RPM_o	linearized engine speed at zero thrust and zero airspeed
RPM_V	engine speed after correction for velocity

RPM_X	engine speed for total thrust at zero airspeed
S_B	maximum flat plate area of the fuselage, ft^2
S_e	effective (exposed) wing area, ft^2
S_{Nref}	flat plate area of the fuselage as seen from the nose of the airplane, ft^2
S_s	total wetted area of the fuselage, ft^2
S_T	total horizontal tail area, ft^2
S_w	total wing area, ft^2
S_{wf}	area of the flaps and area of the wing immediately in front of the flaps, ft^2
T	total thrust, lbf
T_x	total thrust, (T_1+T_2)
$T_{.95}$	thrust at zero airspeed and .95 maximum engine speed
T_1	cold jet, low pressure compressor, thrust, lbf
T_2	hot jet, turbine, thrust, lbf
V, V_∞	velocity of the aircraft, ft/sec
V_B	approximate volume of the aircraft nose section, ft^3
V_i	induced vertical velocity at air intake, ft/sec
V_j	mean exhaust jet velocity, ft/sec
W	weight of the airplane, lbf
X	total forces in the OX direction, lbf
X_o	equilibrium OX forces, equations of motion, lbf
ΔX	perturbation OX forces, equations of motion, lbf
X_u	$1/m\ \partial X/\partial u$
X_w	$1/m\ \partial X/\partial w$
Z	total forces in the OZ direction, lbf
Z_o	equilibrium OZ forces, equations of motion, lbf

ΔZ	perturbation OZ forces, equation of motion, lbf
Z_q	l/m $\partial Z/\partial q$
Z_u	l/m $\partial Z/\partial u$
Z_w	l/m $\partial Z/\partial w$
$Z_{\dot{w}}$	l/m $\partial Z/\partial \dot{w}$
a	Datcom parameter used in the estimation of tail downwash
a_D	slope of the drag curve, per radian
a_T	slope of the tail lift curve, per radian
a_{WB}	slope of the wing-body lift curve, per radian
b	total wing span, in or ft
b_e	effective wing span, in or ft
b_{eff}	Datcom parameter used to estimate tail downwash
b_f	total span of the flaps, in or ft
b_h	total span of the horizontal tail, in or ft
b_i	distance from the fuselage datum line to the inboard flap station, in or ft
b_v	span of the wing tip vortices at any given longitudinal station, ft
b_{vru}	span of the completely rolled up wing tip vortices, ft
c	wing chord, ft or in
$\bar{c}$	mean aerodynamic chord, ft or in
c'	wing chord with flaps deflected 50°, ft or in
c_{de}	Datcom parameter used to determine $[C_D(\alpha)]_B$
c_f	flap chord, in
c_i	wing chord at inboard flap station, ft or in
$c_{l\alpha}$	lift-curve slope of the airfoil section, per radian

ΔC_{lMAX}	change in maximum section lift coefficient due to flap deflection
$(c_{lMAX})_{base}$	Datcom parameter used to determine c_{lMAX}
$\Delta(c_{lMAX})_{base}$	Datcom parameter used to determine Δc_{lMAX}
$c_{mc/4}$	moment coefficient of the airfoil section about the quarter chord
c_r	wing root chord, ft or in
c_{re}	effective wing root chord, ft or in
c_t	wing tip chord, ft or in
c_w	average wing chord at flap position, ft or in
d	diameter of fuselage based on maximum flat plate area and assuming circular fuselage, ft or in
f	1 - fineness ratio, ℓ_B/d 2 - fuel/air mass ratio
g	acceleration of gravity, 32.2 ft/sec^2
h	distance from wing apex to center of mass, ft or in
h_H	height of horizontal tail above fuselage datum line, ft or in
h_{nWB}	distance from wing apex to aerodynamic center of the wing-body, ft or in
h_{R1}	distance from wing apex to the rear reaction nozzle, ft or in
h_{R2}	distance from wing apex to the forward reaction nozzle, ft or in
h_T	distance from wing apex to the aerodynamic center of the tail, ft or in
h_{T1}	distance from wing apex to cold jet nozzles, ft or in
h_{T2}	distance from wing apex to hot jet nozzles, ft or in
i_t	tail incidence, rad or deg
i_w	wing incidence, rad or deg

k	T_2/T_1
k_2-k_1	apparent mass factor used in estimating lift of the fuselage
k_1,k_2,k_3	empirical factors used in estimating maximum lift with flaps deflected 50°
ℓ_{aff}	distance from the wing tip quarter chord point to the horizontal tail quarter chord point, ft or in
ℓ_N	1 - distance from the wing apex to the air intake, ft or in 2 - length of aircraft nose (Datcom)
ℓ_s	control stick displacement, in
m	mass of the airplane, W/g, lbm
$\dot{m}_a$	mass of the air entering the intake, lbm
q	perturbation pitching velocity, rad/sec
t/c	maximum wing thickness to chord ratio
u	perturbation velocity in OX direction, ft/sec
u'	perturbation velocity in OX' direction, ft/sec
u_o	component of free stream velocity in OX direction
u_x	component of free stream velocity in OX' direction, ft/sec
u_{xx}	component of u_x in OX direction, ft/sec
u_{xz}	component of u_x in OZ direction, ft/sec
w	perturbation velocity in negative OZ direction
w'	perturbation velocity in negative OZ' direction
w_a	weight of air entering intake, lbf
w_b	weight of reaction control bleed air available, lbf
w_o	component of free stream velocity in OZ direction
w_Z	component of free stream velocity in OZ' direction, ft/sec
w_{zx}	component of w_Z in OX direction, ft/sec

w_{zz}	component of w_z in OZ direction, ft/sec
x_3, x_4	distances used in the calculation of c_i, ft or in
$x_{a.c.}$	Datcom notation for h_{nWB}
y	difference between airfoil ordinate at 6% chord and 15% chord as a percentage of the chord
z_e	distance from the c. g. to the engine centerline measured perpendicular to the fuselage datum line
z_t	distance from the c. g. to a line perpendicular to the fuselage datum line through the horizontal tail a. c., ft
z_{WB}	distance from the c. g. to the fuselage datum line measured perpendicular to the fuselage datum line, ft
β	Mach number parameter, $\sqrt{1-M^2}$
Γ	wing dihedral angle, deg
Δ	empirical factor used in calculating C_{Di}
Θ	angle of climb measured positively from OX' clockwise to the free stream velocity, deg
$\Lambda_{c/2}, \Lambda_{c/4}$	sweepback angle of the wing at the half chord and quarter chord loci respectively, deg
$\Lambda_{LE}, \Lambda_{TE}$	sweepback angle of the wing leading edge and trailing edge respectively, deg
α	aircraft angle of attack measured from OX counter-clockwise positive to the relative wind, rad
α_{ClMIN}	minimum angle of attack before stall at negative angle of attack
α_o	aircraft angle of attack at zero lift coefficient, rad
α_{oCl}	section angle of attack at zero section lift coefficient, rad
α_t	tail angle of attack measured positive counter-clockwise from tail chord to relative wind, rad
α_w	angle of attack of the wing only, rad

δ_j	nozzle notation angle measured positive clockwise from engine centerline to thrust centerline, deg
ϵ	tail downwash, rad or deg
ϵ_0	tail downwash at zero angle of attack, rad or deg
θ_0	constant aircraft attitude angle measured positive clockwise from OX' to fuselage datum line, deg
θ_{0T}	engine offset angle measured positively clockwise from the fuselage datum line to the cengine centerline, deg
λ	taper ratio, c_t/c_r
μ	viscosity of air
ξ_{ru}	distance required for complete rollup of wing-tip vortices, measured parallel to the wing root chord from wing-tip quarter chord point, in semispans
ρ	density of air, lbm/ft^3
ϕ_{TE}	streamwise trailing edge angle, rad

BLANK PAGE

THE APPROXIMATE LONGITUDINAL STABILITY DERIVATIVES OF A VECTORED THRUST VTOL

I. Introduction

The development of the vertical take-off and landing, VTOL, airplane has necessitated the increased study of low-speed, nonlinear aerodynamics. This area of aerodynamics has been neglected in the past and for the good reason that airplanes did not fly at very low speed and at extreme angle of attack. A great amount of investigation has been undertaken recently on the aerodynamics of pistoned powered VTOL's. There is much less information available on the aerodynamics and stability of turbo-jet powered VTOL's. The object of this study is to investigate the stability and control of a vectored-thrust, turbo-jet powered VTOL in transition from hover to conventional flight. More particularly, the objective is to estimate the stability of the Hawker Siddeley P-1127, Kestrel fighter.

Several areas were indicated to be of importance. These areas were the axis system to be used, the estimation of the aerodynamic forces and moments, and the derivation of the stability derivatives and the equations of motion. The choice of which area to investigate first was obvious because the definition of the axis system was necessary for the derivation of the derivatives and the equations of motion. It was found that a study of the forces and moments gave a firm basis for a physical appreciation of the stability derivatives.

Because of the logical calculation sequence, the derivatives were next derived and in turn used to solve the equations of motion.

Axis Systems

Two axis systems, stability and body, were considered as possibly suitable for the calculation of the stability. The stability axes are somewhat conventional in stability calculations. However, stability axes are defined in relation to the velocity of the airplane and, because of the possible low speed and extreme angle of attack of the vectored-thrust VTOL, were considered unsuitable. A body axes system centered at the center of mass and defined by the fuselage datum line with the X and Z axes in the plane of symmetry gives a constant reference for all flight conditions. Because a continuous solution from hovering flight through conventional flight was to be attempted, this body axes system appeared most suitable. The body axes used are represented by the OX, OY, and OZ axes in Fig. 1.

The performance of the airplane could also be solved in this body axis system. However, it was felt that an Earth axis system gave a clearer representation of the performance. The Earth axes permit direct calculation of angle and rate of climb, horizontal velocity and acceleration, and angle of attack. More important than the ease of calculation, is the fact that during transition the airplane is usually flown with a constant reference angle to the horizontal Earth axis. The Earth axes are OX', OY', and OZ' in Fig. 1.

Forces and Moments

A knowledge of the forces and moments on the airplane in all flight conditions is necessary to solve the performance and stability

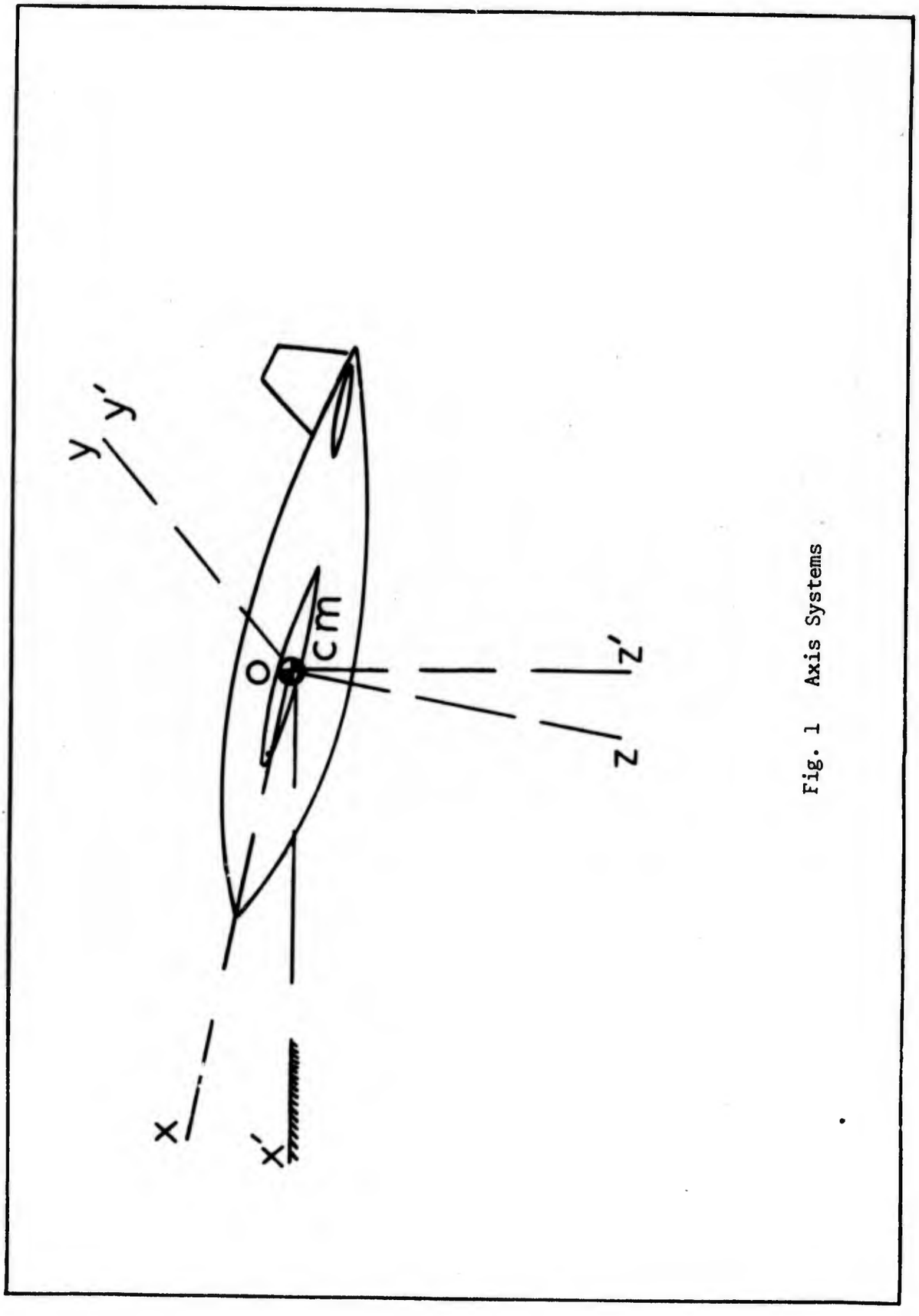

Fig. 1 Axis Systems

problem. A dilemma is present in the performance and stability problem of a VTOL airplane. To get a true solution of the steady flight stability, it is necessary that the forces and moments be found for a nonaccelerating airplane. This solution may be readily found, but the VTOL airplane is seldom flown in the transition speed regime at steady speed. For stability reasons the vectored-thrust VTOL is rapidly accelerated through the transition. The flight conditions and the forces and moments of a rapidly accelerating airplane are very much different from those of an airplane in nonaccelerating transition. The stability solution for the accelerating transition is accurate if all the affects of the acceleration are accounted for in the stability derivatives and the equations of motion. It is very difficult, however, to estimate all the acceleration effects. However, a quasi-steady solution of the accelerating transition may be affected assuming that the aerodynamic forces and moments and the stability derivatives of accelerating flight are not greatly different from those of steady flight at any instant. The quasi-steady solution assumes that the changes in circulation and vorticity occur quickly enough that the forces and moments are negligibly affected.

The steady flight conditions give an accurate stability solution, and the unsteady flight conditions with a quasi-steady solution has inherent errors. However, the airplane is usually flown in the accelerating transition. It was felt that both solutions should be attempted in an effort to answer the following two questions. Is there a large difference in the stability as found for the accelerating airplane as compared to the airplane at steady speed and if so, which more truly represents the stability of the airplane?

In both types of transition there are problems unique to the vectored-thrust VTOL. When the airplane is in transition, the thrust vector and inlet air momentum vector change direction and magnitude. Because of this momentum change, forces and moments will result and some method must be found to approximate them. It is also necessary to find the derivatives of these forces and moments for the stability solution.

The jet interference effects caused by the large negative pressure differential below the airplane produced by the thrust must be investigated. The jet interference will affect the inlet air momentum, wing lift and moment; and horizontal tail downwash, lift and moment. The greatest effect on the stability is caused by the tail and the estimation of the tail downwash is very important. The change of the inlet air momentum is important only at the hover.

The last important problem may be called the nonlinear aerodynamics of the airfoils. Three questions arise from nonlinear aerodynamics. What is the effectiveness of an airfoil at an unstalled angle of attack but at very low airspeed? Is there any way to estimate the effect of an airfoil when it is stalled? At what angle of attack does the airfoil unstall and does it become effective gradually or abruptly? These questions are not easy to answer and are in an area of aerodynamics in which little information is available.

Stability Derivatives

After the forces and moments are known, the knowledge of their variation is used to compute the stability derivatives. This knowledge is necessary for the performance solution and thus the calculation of

the derivatives does not necessitate much additional labor. Most of the symmetry and acceleration assumptions normally used to eliminate certain of the derivatives are applicable.

The form that the derivatives take is dependent upon the dimensionality of the solution. The nondimensional analysis has had some traditional value but is not considered necessary because of the increased use of computers. Nondimensionaling with respect to free stream velocity results in meaningless values at zero and very low speeds. No advantage can be seen to nondimensionalize with an artificial parameter. The dimensional analysis permits a clearer physical appreciation and is considered more practical for VTOL studies.

Equations of Motion

The equations of motion are derived with respect to the body axes and dimensional for consistency with the derivatives. There is no reason to believe that the linearized equations will not give a good approximation of the stability. The accuracy of the approximation of the forces and moments does not warrant the use of the nonlinear equations. The solution of the equations of motion completes the stability solution.

II. P-1127 Description

The P-1127, Hawker-Siddeley, Kestrel fighter is the first operational vectored-thrust VTOL in the world. The tactical fighter was designed to take off and land vertically from prepared surfaces, and also fly supersonic. It also has very short take off and landing characteristics from unprepared surfaces.

The outward appearance of the vectored-thrust VTOL is very similar to that of any fighter. The one distinquishing feature is the position of the exhaust nozzle or nozzles on the bottom or side of the aircraft. The exhaust nozzles of the P-1127 are rotatable from rearward in a line with the engine center line through an angle of 100°. This enables the P-1127 to hover and even fly backward. The P-1127 is powered by a Pegasus V engine with a rated thrust greater than the take off weight of the airplane.

The controls of the P-1127 look similar to most airplanes. The most important of the normal controls for longitudinal calculations is the all movable stabilator, which has maximum incidences of 12° and -10°. The airplane also has reaction controls for yaw, pitch and roll at low speeds. The only important reaction control for longitudinal stability is the pitch control. Pitch reaction control is provided by thrust from nozzles in the nose and the tail. Air for the thrust is provided by bleed air from the low pressure compressor, and the amount of bleed air available is dependent on engine speed. The amount of pitch control used is determined by the pilot with the control stick. The rear nozzle thrust is connected to the tail plane

movement by a hydraulic jack, whereas the forward nozzle thrust is controlled directly by the control stick displacement.

The flaps of the P-1127 are plain and capable of two positions, up and 50° down. The airfoils are all symmetric.

There are several interesting characteristics to be noted about the design of the P-1127. The intakes are necessarily large to permit the large air mass flow of the high by-pass engine. The wings have a large anhedral angle, 12°. Finally, the center of mass is unusually far forward probably because of the position of the engine. The C.G. range is approximately from 0.095 to 0.145 of the mean aerodynamic chord. For a summary of the P-1127 geometry see Fig. 2 which has been reproduced from Reference 1.

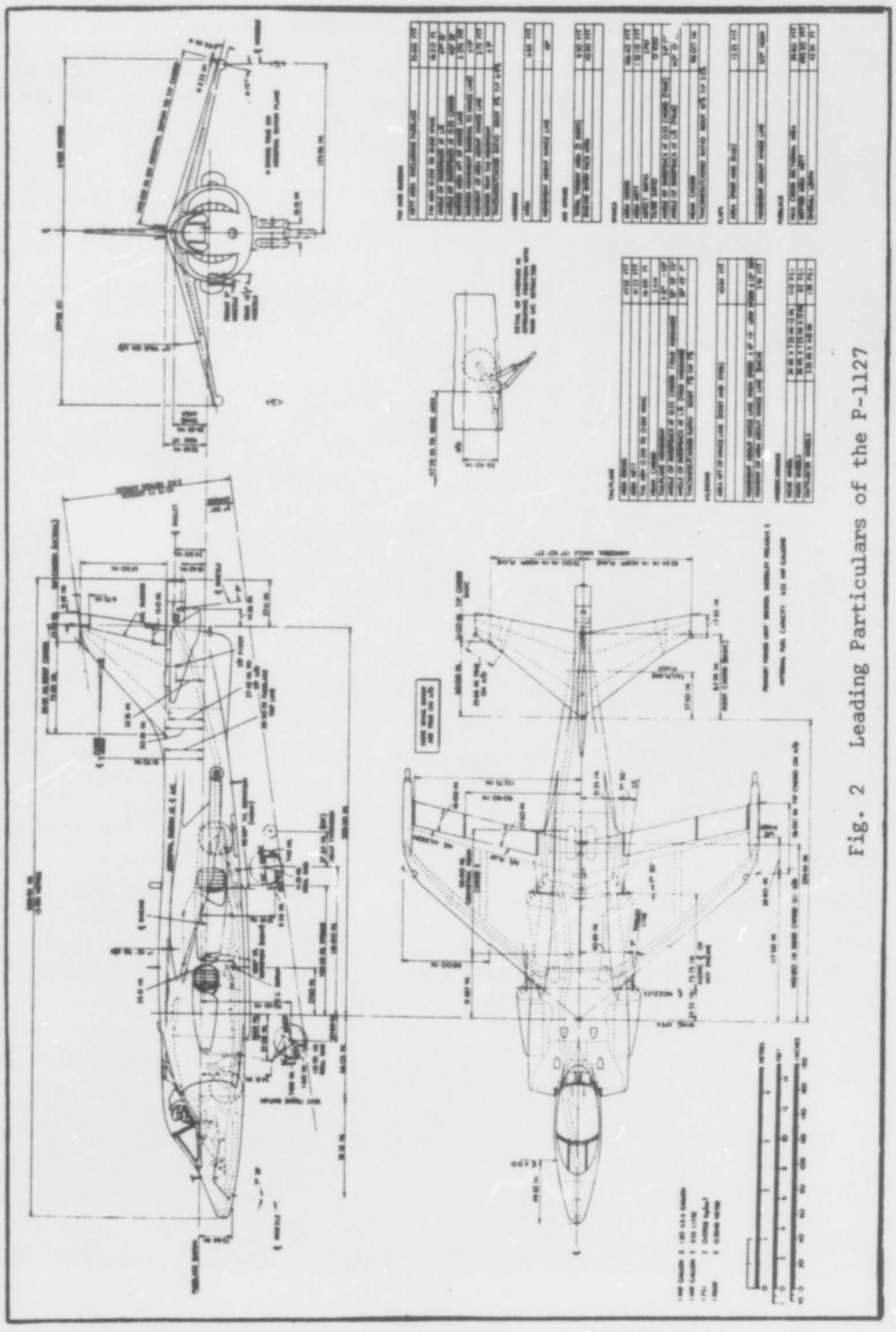

Fig. 2 Leading Particulars of the P-1127

III. Performance Estimation

As previously noted, it was necessary to calculate the performance in two distinctly different transitions. Because of the unique natures of the accelerating and nonaccelerating transitions, two separate calculations were needed. Both transitions were solved in an Earth axis system. The axis system and the various reference velocities and angles are presented in Fig. 3 with arrows indicating positive directions. The forces and moments involved in each transition are the same, however, their treatment in each is different. The forces, moments and moment arms are presented in Fig. 4.

The performance equations for the transitions are the same with the exception of the right side. The X force equation:

$$-L_{WB}\sin\theta - D_{WB}\cos\theta - L_T\sin\theta - F_R\sin\theta_0 +$$

$$(T_1+T_2)\cos(\delta_j+\theta_{0T}+\theta_0) - F_u = 0 \text{ nonaccelerating}$$

$$= (W/g)\, du_x/dt \text{ accelerating}$$

The Z force equation:

$$-L_{WB}\cos\theta + D_{WB}\sin\theta - L_T\cos\theta - (T_1+T_2)\sin(\delta_j+\theta_{0T}+\theta_0) -$$

$$F_R\cos\theta_0 + W + F_I + F_W = 0 \text{ nonaccelerating}$$

$$= (W/g)\, dw_z/dt \text{ accelerating}$$

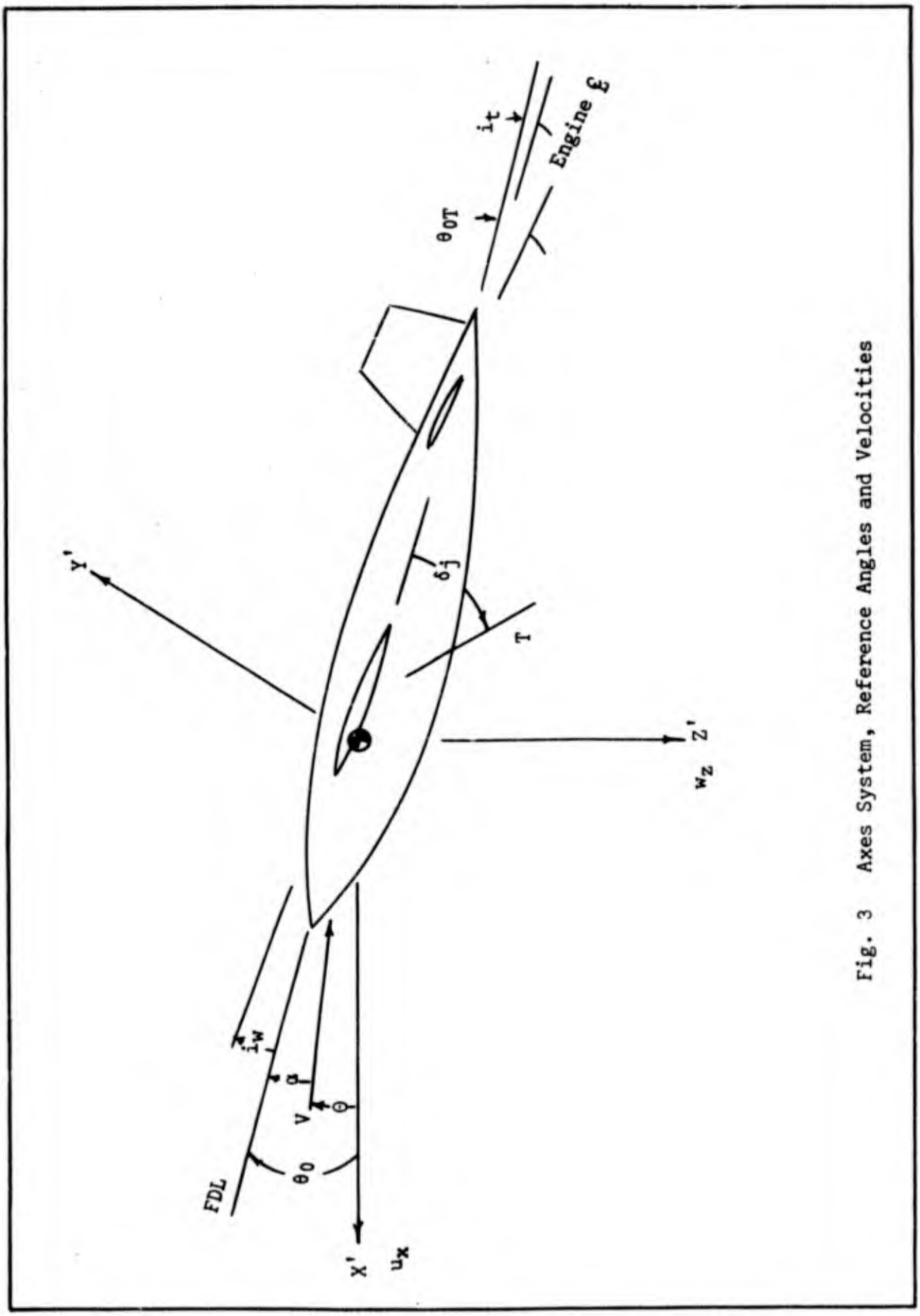

Fig. 3 Axes System, Reference Angles and Velocities

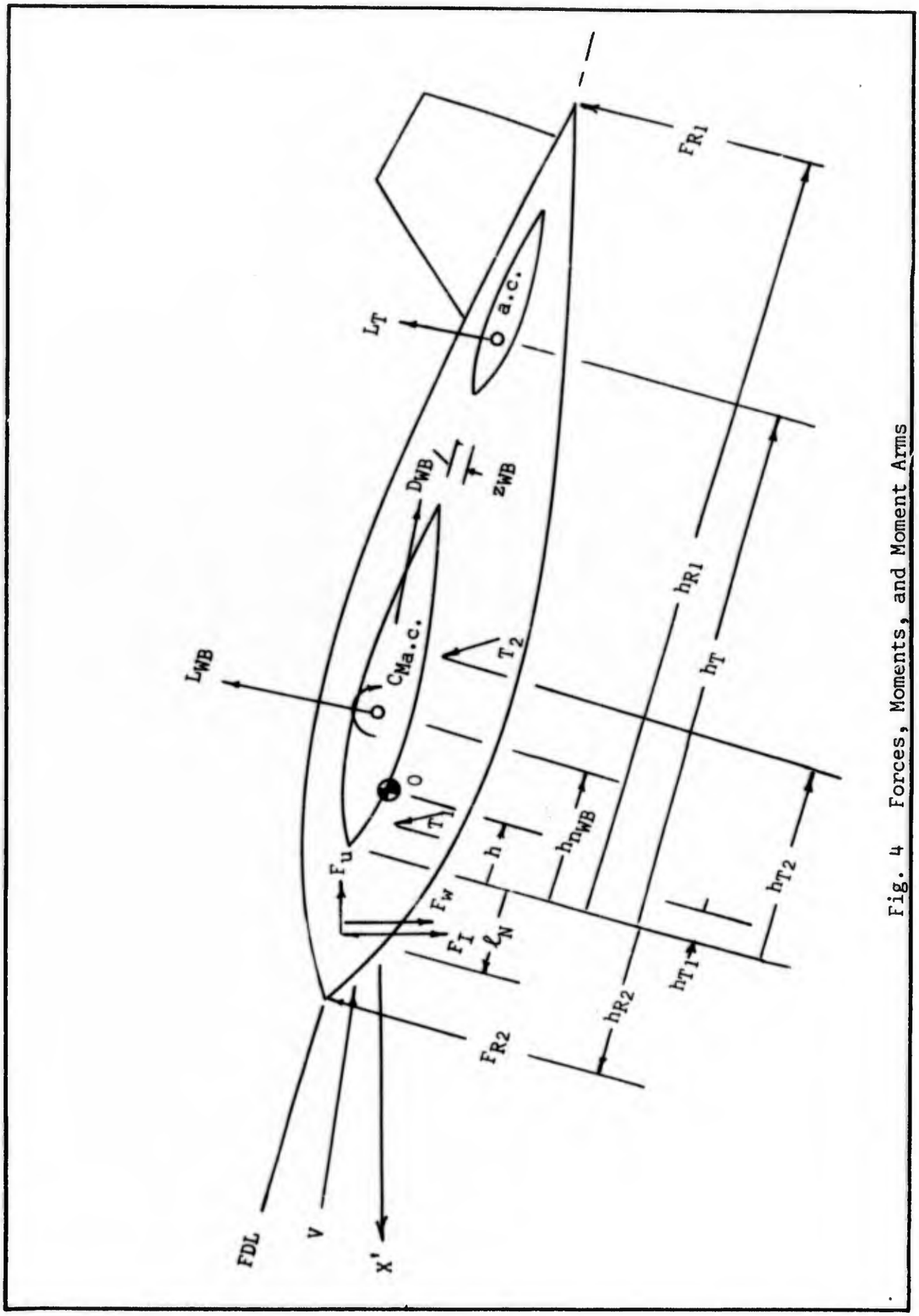

Fig. 4 Forces, Moments, and Moment Arms

The M moment equation:

$$L_{WB}\cos\alpha(h-h_{n_{WB}}) + (\ell_N+h)(F_W-F_I)\cos\theta_0 +$$

$$D_{WB}z_{WB}\cos\alpha + [T_1(h-h_{T1}) + T_2(h-h_{T2})]\sin(\delta_j+\theta_{0T}) -$$

$$L_T(h_T-h) + M_R + M_0 = 0 \text{ nonaccelerating}$$

$$\simeq 0 \text{ accelerating}$$

In most performance estimations only the X and Z equations are used and the tail forces are neglected. In attempt for greater accuracy, the moment equation was included. The inertia term, $I_{yy}\,d\ddot{\theta}/dt$, of the accelerating moment equation was assumed negligible. The forces and moments must be discussed before the method of solution can be understood.

Aerodynamic Lift and Drag

The aerodynamic lift and drag were computed using the USAF Stability and Control Datcom. It was originally desired that this estimation would not be necessary, as experimental lift and drag curves would have been more accurate. However, the use of the Datcom provides an interesting approximation and is representative of the information which would be available in the design of an airplane.

In all calculations an average t/c of .08 for the wing and .07 for the tail was used. The geometric parameters, aspect ratio, tip to root chord ratio, mean aerodynamic chord, etc., were either given by Reference 2 or calculated from the geometry. The employment of the lift and drag in the two transitions is considerably different and must

be discussed in the sections concerning the solution of the performance equations.

The conventional definitions were used:

$$L_{WB} = 1/2\rho V^2 S_W C_{LWB}$$

$$D_{WB} = 1/2\rho V^2 S_W C_{DWB}$$

$$L_T = 1/2\rho V^2 S C_{LT}$$

$$Ma.c. = 1/2\rho V^2 S_W \bar{c} C_{Ma.c.}$$

The problem was then to estimate C_{LWB}, C_{DWB}, C_{LT} and $C_{Ma.c.}$.

$\underline{C_{LWB}}$, $\underline{C_{DWB}}$, $\underline{C_{LT}}$, and $\underline{C_{Ma.c.}}$. The equation:

$$C_{LWB} = a_{WB}(\alpha_W + i_W) = C_{L_0} + a_{WB}\alpha$$

is accurate assuming the usual linear lift curve. The nonlinearity of the lift curve was neglected, which is essentially assuming that at the minimum angle of attack the boundary layer attaches over the entire wing instantaneously. The flapped lift coefficient was computed for fifty degrees (full) flaps only. The P-1127 has no intermediate flap position.

There is no simple expression for the drag coefficient, although it could be represented by a polynomial of form:

$$C_D = C_1\alpha^4 + C_2\alpha^3 + C_3\alpha^2 + C_4\alpha + C_5$$

The tail drag was neglected.

$C_{Ma.c.}$ was estimated using the 65-009 airfoil section moment data from Reference 3. $C_{Ma.c.}$ for zero flap deflection is zero for this

symmetric wing. With 50° flaps $C_{Ma.c.}$ was estimated by:

$$C_{Ma.c.} = c_{ma.c.} (S_{Wf}/S) K$$

The horizontal tail is symmetrical and the incidence is variable so that:

$$C_{LT} = a_T \alpha_t = a_T[(1-\partial\varepsilon/\partial\alpha)\alpha+i_t-\varepsilon_0]$$

The same Datcom method was used for the lift of the tail as for the wing without flap. Once again nonlinearities were neglected.

For a detailed calculation of all the aerodynamic force coefficients see Appendix A.

Tail Downwash. There are two problems in downwash; first the $\partial\varepsilon/\partial\alpha$ and ε_0 in conventional flight must be calculated, and second the $\partial\varepsilon/\partial\alpha$ and ε_0 must be estimated for the transition. The first problem is solved by use of the Datcom and is presented in Appendix A. The solution presented is for an aircraft angle of attack of 3°. Little variation in $\partial\varepsilon/\partial\alpha$ was found from 0° to 6° angle of attack. ε_0 was considered zero for conventional flight as it could not be predicted analytically (Ref 4:23).

An analytic estimation of the downwash in the transition was not attempted. The only accurate method of obtaining the tail downwash is by wind tunnel studies of the aircraft model. Such experimental information was not available so an order of magnitude approximation was attempted. The downwash characteristics of a VTOL similar to the P-1127 were found in Reference 5.

From a study of the data in Reference 5, there appeared to be a correlation between the downwash and the thrust coefficient, C_T, the

free stream exhaust jet velocity ratio, V_∞/V_j, and the nozzle deflection, δ_j. The maximum downwash that could be expected was approximately 10°. This was determined from the fact that a change in the tail incidence of 9° did not quite return the moment to the tail-off value (Ref 5:116). Furthermore, the fact that the moment coefficient increased at the same rate with the tail at zero incidence as with no tail, indicated that the downwash was increasing at the same rate as the angle of attack (Ref 5:12). Thus, when there was maximum downwash, $\partial\varepsilon/\partial\alpha$ was equal to one and the tail did not contribute to the stability. This analysis did not explain the variation of the downwash, however.

It was expected that zero forward speed with the nozzles vertical would result in negligible downwash. Also expected was a maximum downwash at some nozzle angle greater than zero, and that the downwash for either transition would not be the same. $[C_T(V_\infty/V_j)]/\sin\delta_j$ was thought to be a reasonable parameter and resulted in Fig. 5. It appeared from Fig. 5 that anytime $[C_T(V_\infty/V_j)]/\sin\delta_j$ was less than about one, the maximum downwash could be expected. Also as $[C_T(V_\infty/V_j)]/\sin\delta_j$ rapidly increased, $\varepsilon/\varepsilon_{MAX}$ decreased rapidly toward zero.

Information for nozzle deflection of greater than 60° was not available. However, in transition $[C_T(V_\infty/V_j)]/\sin\delta_j$ approaches infinity as δ_j approaches 90° so one would expect $\varepsilon/\varepsilon_{MAX}$ to approach zero (Figs. 6 and 7). As C_T increases and V_∞/V_j decreases at large nozzle deflections, the moment is, in fact, very nearly zero supporting the assumption that the downwash is very nearly zero (Ref 5:43,45,46,52). It was realized that this analysis was very approximate and that only

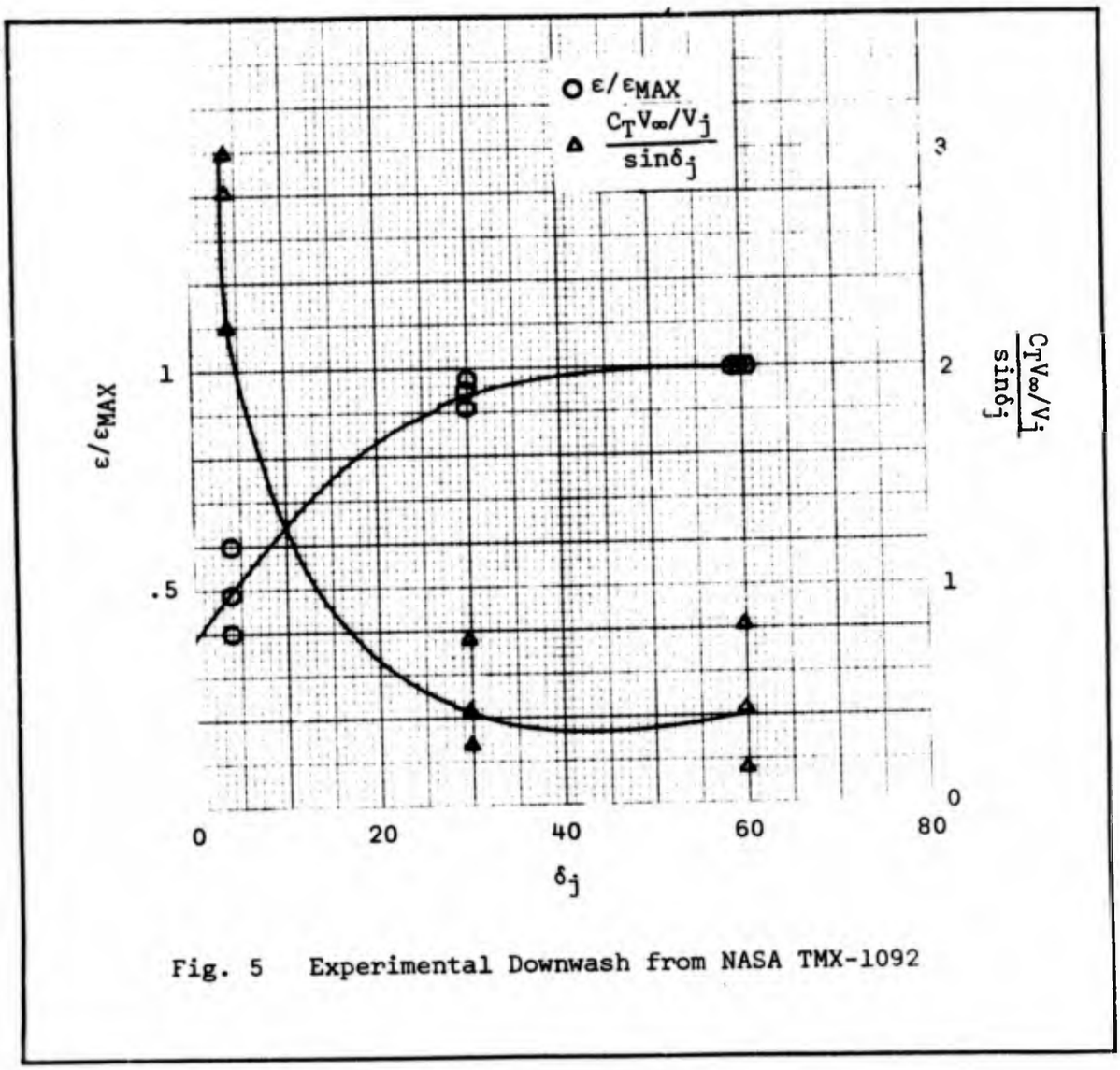

Fig. 5 Experimental Downwash from NASA TMX-1092

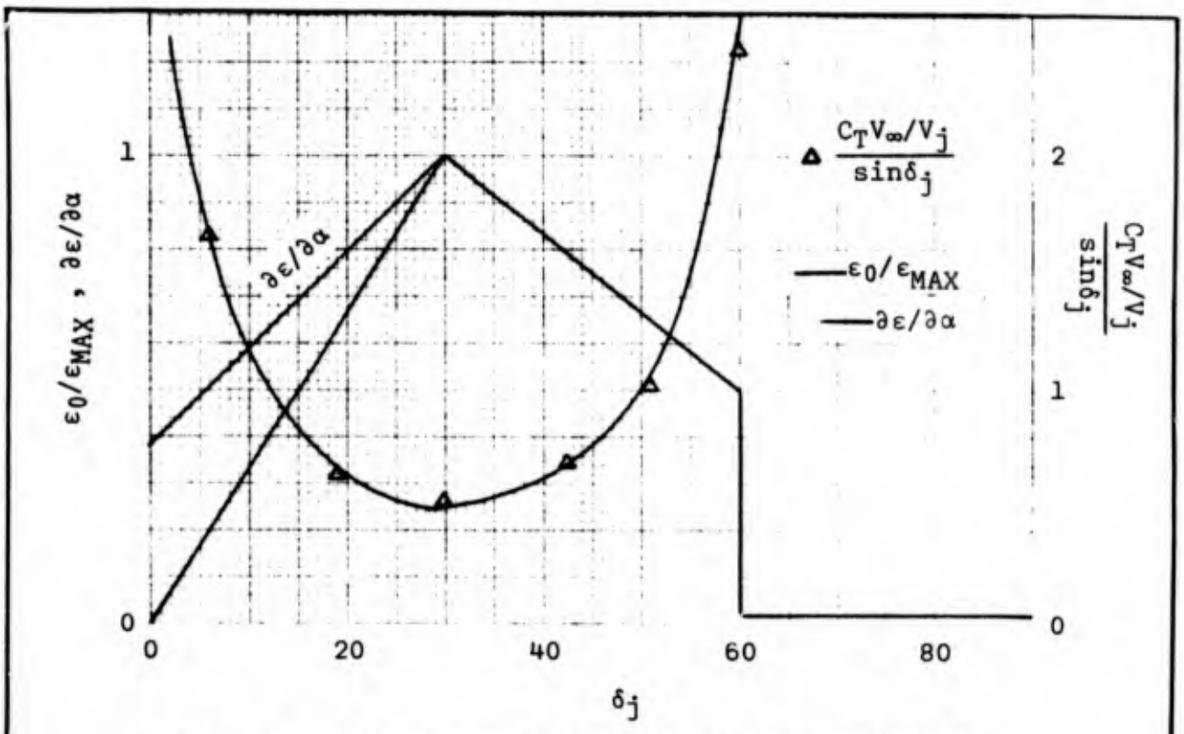

Fig. 6 Tail Downwash (Accelerating Transition)

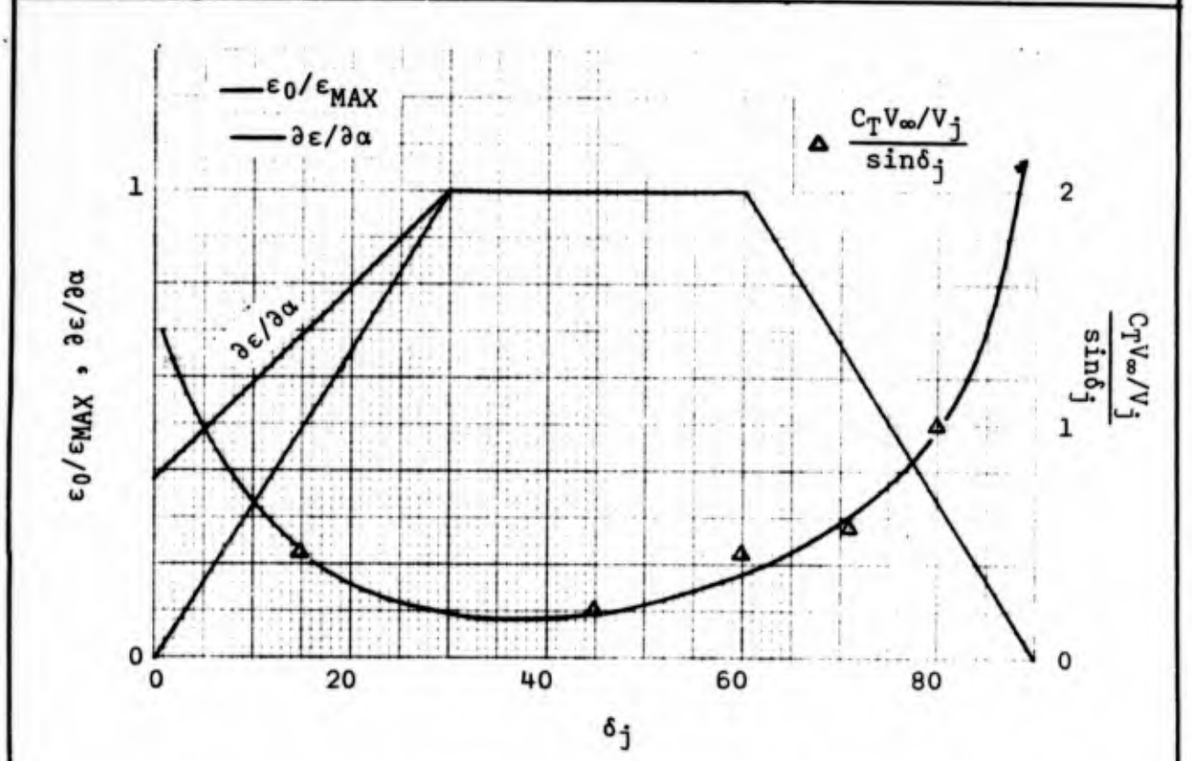

Fig. 7 Tail Downwash (Nonaccelerating Transition)

the trend of the variation of the downwash and perhaps the maximum downwash could be accurately estimated. For this reason, linear variation of downwash with nozzle angle deflection was assumed. There is a discontinuity for the accelerating transition at the 60° nozzle deflection because, above this nozzle deflection, the angle of attack is such that the airfoils are assumed not to be flying (Fig. 7).

It has already been shown that the $\partial\varepsilon/\partial\alpha$ is one when the downwash is maximum. It was assumed that the $\partial\varepsilon/\partial\alpha$ will vary directly as downwash with the exception that the $\partial\varepsilon/\partial\alpha$ becomes the conventional flight value instead of zero when the nozzle deflection is zero. It should be noted that $1-\partial\varepsilon/\partial\alpha$ is a measure of the tail effectiveness.

F_I

When the aircraft is in hovering flight, the jet interference causes a lower pressure below the aircraft than that above. This pressure gradient causes the inlet air to enter the intake at a slight angle. The change in momentum as the air is turned down the duct causes the force, F_I, at the inlet. If the induced vertical velocity is known:

$$F_I = (w_a/g)V_i$$

However, it is most likely that F_I will have to be determined from wind tunnel data. F_I for the P-1127 in hovering flight is about 200 lbf (Ref 2:7). This F_I amounts to an induced vertical velocity of about 17 ft/sec.

F_I is most important at hover; however, it will be present in the transition. It has been assumed that F_I will vary linearly with

nozzle deflection. There is no basis for this assumption except that the force does rapidly become negligible.

F_u and F_w, T_1 and T_2

For a conventional turbo-jet airplane, the inlet momentum losses are usually considered as part of the net thrust; thus:

$$T_{NET} = \dot{m}_a[(1-f)u_e - u_x]$$

where $\dot{m}_a u_x$ is the inlet-air momentum drag. An assumption necessary for this equation is that the air is not turned appreciably from the time it enters the inlet until it exhausts. In a turbo-jet vectored-thrust VTOL, however, the air is turned substantially because of the large negative angles of attack involved in the accelerating transition and the nozzle deflection. This turning of the air at the inlet necessitates a different treatment of the net thrust. The momentum drag is considered separately from the gross thrust. The gross thrust is the mass of exhaust matter multiplied times the exit velocity. The momentum losses are: (Fig. 8)

$$F_w = \dot{m}_a w_z \qquad F_u = \dot{m}_a u_x$$

For conventional, non-VTOL, aircraft thrust for constant RPM is shown as decreasing until about 250 kts then increasing with speed. Gross thrust, as used here, however, steadily increases with speed (Fig. 9). It should be noted that the low pressure, cold jet, thrust, although less at zero velocity, increases more rapidly with speed than does the hot jet thrust.

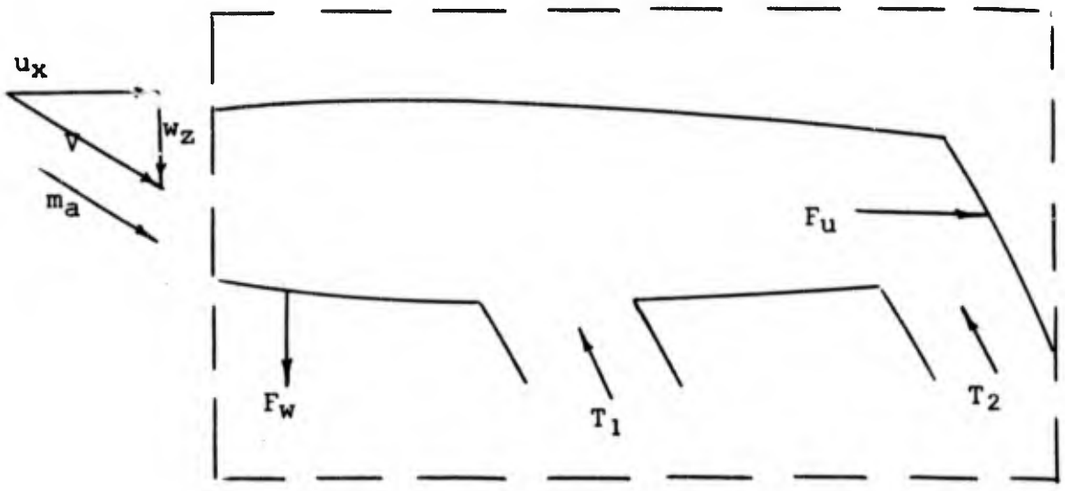

Momentum losses are:

$$F_w = m_a w_z \quad \text{and} \quad F_u = m_a u_x$$

Fig. 8 Intake Air Momentum Losses

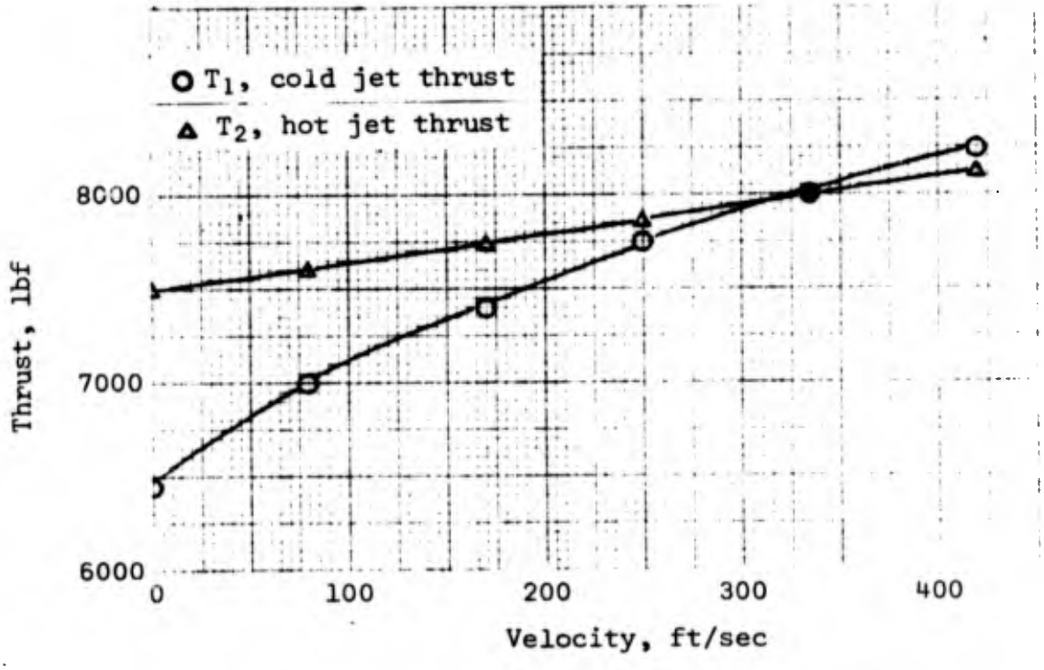

Fig. 9 Thrust Variation with Velocity at 35% of Maximum Engine Speed

It is possible to estimate the gross thrust if fuel and air flow are known. However, this information necessarily comes from the engine manufacturer, and it is assumed that gross thrust information is available. All gross thrust information for this report is from Reference 2.

Thrust data below 85% of maximum engine speed was needed and not available so an extrapolation of the known data was used for the nonaccelerating transition.

F_R and M_R

The longitudinal reaction controls are used to balance the pitching moments at transition speeds. The force, and hence the moment, used is controlled by the control stick in the cockpit. The air for the control jet is supplied from the low pressure compressor bleed air and the amount of bleed air available depends on the nozzle deflection and the engine speed.

The maximum amount of bleed air for any given engine speed is available when the nozzle deflection is 20° or greater. The bleed air available decreases linearly with nozzle angle to zero when nozzles are deflected less than 20°. The force and moment is assumed to vary linearly with the bleed air available to the reaction control (Ref 2:16). The amount of bleed air available varies with engine speed according to the equation:

$$w_b = w_{bMAX} [1-2.14(1-N_F/N_{Fd})] \qquad \text{(Ref 2:12)}$$

Some information about the reaction control forces and/or moments must be available from the manufacturer.

Hawker Siddeley assumes that the bleed air does not reduce the thrust appreciably (Ref 2:4). Both front and rear reaction control jets are producing thrust contributing to lift. When the nozzle deflection is vertical, some of the thrust lost from the engine is regained in the reaction jet if losses are neglected. However, as the nozzles are rotated, thrust is taken from a vector with angle, $\delta j+\theta_{0T}$, to the aircraft and regained in a vector with angle θ_0 to the OZ' axis thus contributing to the lift. This effect is probably negligible unless there is a very large reaction control force.

The variation of all the forces and moments for each transition is considerably different. This variation will be discussed in the solution of the performance equations for each transition.

Accelerating Transition

The accelerating transition is accomplished holding the airplane to a fixed attitude angle with the OX' axis. The engine is held at constant speed and the nozzles rotated at a constant rate. The angles of climb and attack and the velocity are considered variables. The reference values for the calculation were: attitude angle, 6°; RPM, 95%, and rate of nozzle retraction, 3.5° per second. These values were selected because certain performance and stability values were available for comparison for this transition (Ref 2:9,10).

The solution is approximate because the three equations are not solved similtaneously. The equations are not independent because the moment and force equations are coupled by the tail and reaction control terms.

The accelerating transition is started from hovering flight. It is assumed, although physically impossible, that the pilot simultaneously increases the throttle setting to 95% RPM and starts the nozzle retraction at a constant rate of 3.5° per second. This causes the airplane to initially accelerate straight up causing an angle of attack of -90°. As the aircraft accelerates horizontally, the angle of attack rapidly increases to angles at which the airfoil boundary layer is attached. The angle of attack at which the boundary layer is fully attached to the wing was determined by

$$\alpha_{Min} = [(S_W - S_{Wf})/S_W]K\alpha_{C\ell min}$$

Below this angle of attack, it was assumed that the wing was completely stalled and no aerodynamic lift nor moment developed and that only parasitic drag was effective.

The general method of solution is started from the hover and the reaction moment necessary to balance the moment equation is calculated. Using the reaction control force, the X and Z equations are solved for the horizontal and vertical accelerations respectively. From the acceleration, new velocities are found after an interval of time in which the nozzles are retracted. The new angle of climb is found from the velocities and this in turn determines the new angle of attack. This new information is used to once again solve the moment equation and the process is repeated until the angle of attack is -8° at which time the tail incidence angle is also calculated. The solution is repeated until the nozzle angle is zero.

Example Solution. To simplify the moment equation:

$$M + M_T + M_R = 0$$

where:

$$M = L_{WB}\cos\alpha(h-h_{nWB}) + (\ell_N+h)(F_W-F_I)\cos\theta_0 +$$

$$z_{WB}D_{WB}\cos\alpha + [T_1(h-h_{T1}) + T_2(h-h_{T2})]\sin(\delta_j+\theta_{0T}) -$$

$$1/2\rho V^2 S_T a_T (h_T-h)[(1-\partial\varepsilon/\partial\alpha)\alpha-\varepsilon_0] + M_0 = -M_T-M_R$$

The aerodynamic dynamic variables are functions of the angle of attack and, in the case of ε_0 and $\partial\varepsilon/\partial\alpha$, the nozzle angle (Fig. 6). The angle of attack and F_W have been fixed by initial conditions in the solution of the X and Z equations. The nozzle angle is fixed at any instant of time in the transition. The engine speed is held constant and T_1 and T_2 vary only with velocity. The velocity is known from initial conditions on the X and Z equations solution, thus T_1 and T_2 may be found from Fig. 9. The moment arms are known from the aircraft geometry and Datcom solution (Appendix A). The value M may then be calculated.

The incidence of the tail and the reaction force are interdependent by movement of the control stick, ℓ_s. In the solution, the reaction moment variation was used because the reaction force variation was not available. The variation of both the incidence and reaction moment with stick displacement is nearly linear thus both curves were linearized by section. The curves are reproduced from Reference 2 and presented in Fig. 10 and 11. As an example:

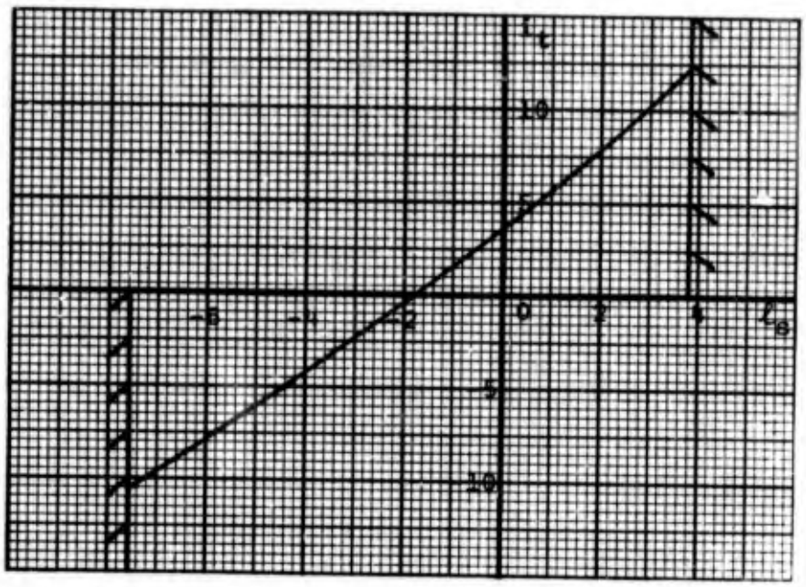

Fig. 10 Tail Incidence vs Control Stick Displacement

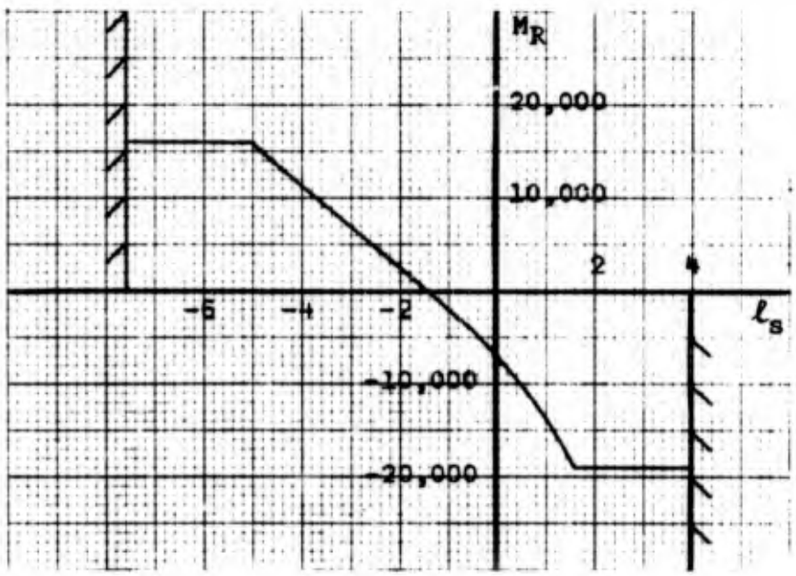

Fig. 11 Reaction Control Moment vs Control Stick Displacement

$$i_t = (\ell_s+2)C_1 \tag{1}$$

$$M_R = (\ell_s+1.4)C_2 \tag{2}$$

$$M_T = -1/2\rho V^2 S_T a_T (h_t-h) \cos\alpha_t \, i_t$$

$$\doteq -T_c i_t \qquad \text{where:} \quad \cos\alpha_t \doteq 1$$

$$T_c = 1/2\rho V^2 S_T a_t (h_T-h)$$

$$M = -M_R - M_T = -(\ell_s+1.4)C_2 + T_c(\ell_s+2)C_1 \quad \text{or}$$

$$\ell_s = (M+1.4C_2 - 2T_cC_1)/(T_cC_1 - C_2)$$

C_1 and C_2 in this example are only representative constants. Now that ℓ_s is known, i_t and M_R are determined from equations (1) and (2). The X and Z equations may now be solved.

The weight is assumed to be constant. F_R is determined by:

$$M_R = (h_{R1}-h)F_{R1} \quad \text{or} \quad M_R = (h_{R2}-h)F_{R2}$$

dependent on the sign of M_R.

The aerodynamic variables L_{WB} and L_T are easily calculated because of their linearity with angle of attack. However, D_{WB} is nonlinear and necessitates the repeated calculation of C_D from the Datcom unless C_D versus angle of attack is plotted. The plotting of the graph enables one to use a computer solution as the C_D-α curve may be linearized by sections or a polynomial may be formed by the least squares method. A standard computer program will compute this polynomial which takes the form of: (Appendices B and C)

$$C_D = C_1\alpha^4 + C_2\alpha^3 + C_3\alpha^2 + C_4\alpha + C_5$$

Knowing all the variables and the velocity the accelerations may be solved.

The solution for the particular velocity, angle of attack, nozzle angle, time from start of transition, etc., is now complete. The calculation for entering conditions of the next time interval must be performed. The new velocity, nozzle angle, thrust and angle of attack are needed prior to resolving the moment equation.

The velocity is found by summing the velocity vectors in the horizontal and vertical directions which are in turn found from the accelerations already calculated. The velocity vectors may be expressed by a Taylor series:

$$w_z\ (NEW) = w_z\ (OLD) + dw_z/dt\Delta t + d^2w_z/dt^2\ (\Delta t)^2 \ldots$$

$$u_x\ (NEW) = u_x\ (OLD) + du_x/dt\Delta t + d^2u_x/dt^2\ (\Delta t)^2 \ldots$$

Using a time interval of one second, it was determined that only the first derivative was necessary. Thus the new velocities become:

$$w_z\ (NEW) = w_z\ (OLD) + dw_z/dt$$

$$u_x\ (NEW) = u_x\ (OLD) + du_x/dt$$

and:

$$V^2\ (NEW) = w_z^2\ (NEW) + u_x^2\ (NEW)$$

It should now be recalled that the rate of nozzle retraction was specified at 3.5° per second so that the new nozzle angle is now

$$\delta_j \text{ (NEW)} = \delta_j \text{ (OLD)} - 3.5^\circ$$

The new angle of attack is found from the new calculated angle of climb and the constant attitude.

$$\Theta = \tan^{-1} (-w_z/u_x)$$

and:

$$\alpha = \theta_0 - \Theta$$

The new thrust is simply found from Fig. 9, entering with the new velocity. Thus the entering parameters for the next solution have been completely specified. The calculations are repeated until the nozzle angle reaches zero and the transition is then completed in about 23 seconds. Because of the repetitive nature of the calculations, the solution lends itself well to the use of a computer. The appropriate 7094 computer program written in Fortran language is presented and explained in Appendix B.

Nonaccelerating Transition

The nonaccelerating transition is accomplished as though the airplane were flown in steps by increments of airspeed. The forces and moments necessary for equilibrium are solved at the hover. The airspeed is then advanced an increment, 10 ft/sec, and the new forces and moments solved. Although not essential, level flight and constant angle of attack were assumed as being the practical way to fly this transition. In the solution, an angle of attack of 6° was used to agree with the constant attitude of the accelerating transition.

Unlike the accelerating transition engine speed, thrust, and nozzle angle are variable.

The general method of solution is similar to the accelerating transition in that the solution of the moment equation is used to solve the force equations. The moment equation is solved for the tail incidence and reaction moment much the same as in the accelerating transition. The X and Z equations are then solved simultaneously for the thrust and nozzle deflection necessary for equilibrium. An example solution is the best way to illustrate the entire procedure.

Example Solution. The moment equation is first solved in hovering flight. There is no velocity so the only moments involved are due to thrust and the induced inlet downwash force, F_I. The moment equation is then solved as before for the incidence and reaction moment. With F_R being found as before, the X and Z equations may be simplified:

$$L_{WB} \sin\theta_0 + D_{WB} \cos\theta_0 + L_T \sin\theta_0 + F_R \sin\theta_0 + F_u$$

$$= -F_1 = (T_1+T_2) \cos(\delta_j+\theta_{0T}+\theta_0)$$

$$-L_{WB} \cos\theta_0 + D_{WB} \sin\theta_0 - L_T \cos\theta_0 - F_R \cos\theta_0 + W + F_I - F_W$$

$$= F_2 = (T_1+T_2) \sin(\delta_j+\theta_{0T}+\theta_0)$$

All of the forces, excepting thrust, may be solved with either the fixed velocity, zero at hover, and angle of attack or by the solution of the moment equation. Dividing the force equations:

$$\tan(\delta_j+\theta_{0T}+\theta_0) = -F_2/F_1$$

and:

$$(T_1+T_2) = F_2/\sin(\delta_j+\theta_{0T}+\theta_0)$$

or:

$$(T_1+T_2) = -F_1/\cos(\delta_j+\theta_{0T}+\theta_0)$$

With the thrust solution, the forces and moments of equilibrium are complete for this fixed velocity and angle of attack.

To once more solve the moment equation, the new velocity is specified:

$$V(NEW) = V(OLD) + \Delta V$$

The angle of attack is unchanged and it is assumed that with small ΔV the thrust and nozzle deflection have not changed appreciably. However, to solve the moment equation, T_1 and T_2 must each be known and only T_1+T_2 has been solved. The equation:

$$(T_1+T_2) = T_1\ (1+k)$$

will solve T_1 if k is known. k is easily found from engine charts as it varies with only velocity and total thrust. For a computer solution, however, some continuous method of solution for k is necessary. By use of a chart such as Fig. 12, an approximate value of k may be found for all flight conditions. (See computer program Appendix C.)

There are two problems to be considered in the nonaccelerating transition. The first is how to treat aerodynamic lift and drag at slow speed. The second is the variation of reaction control force with engine speed.

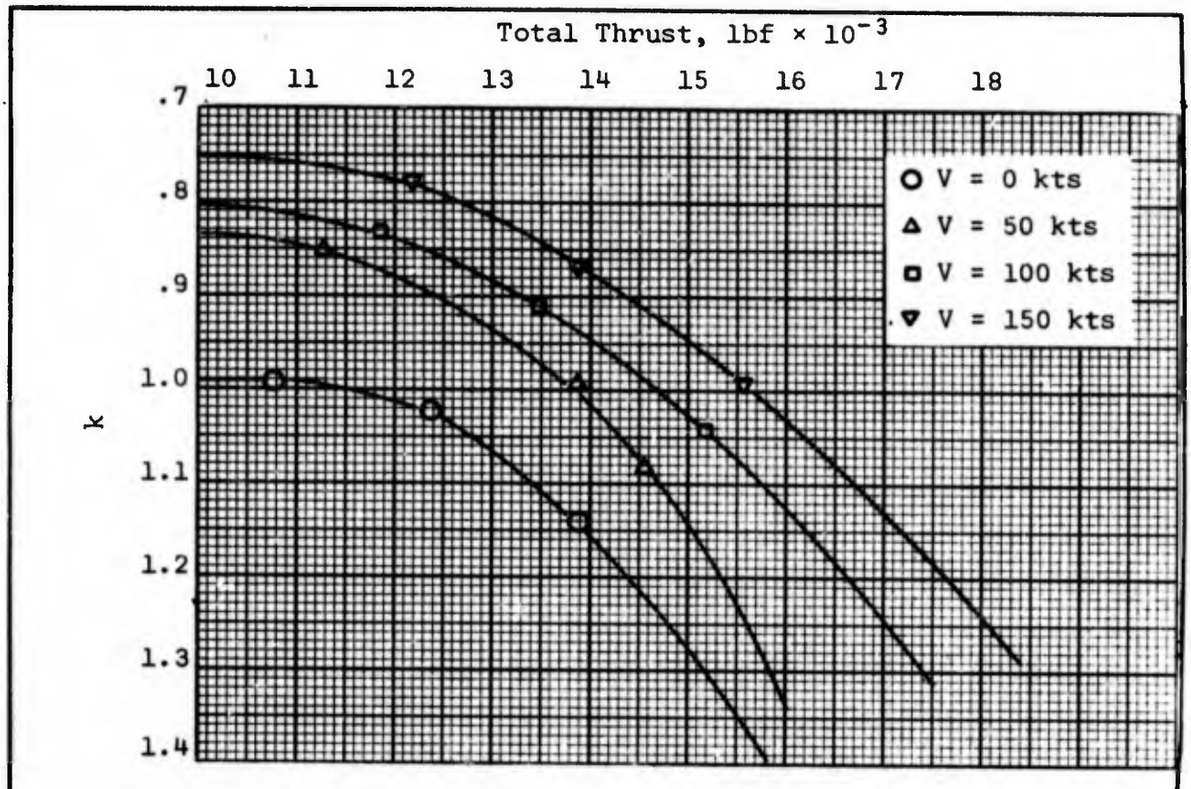

Fig. 12 k, T_2/T_1, vs Total Thrust

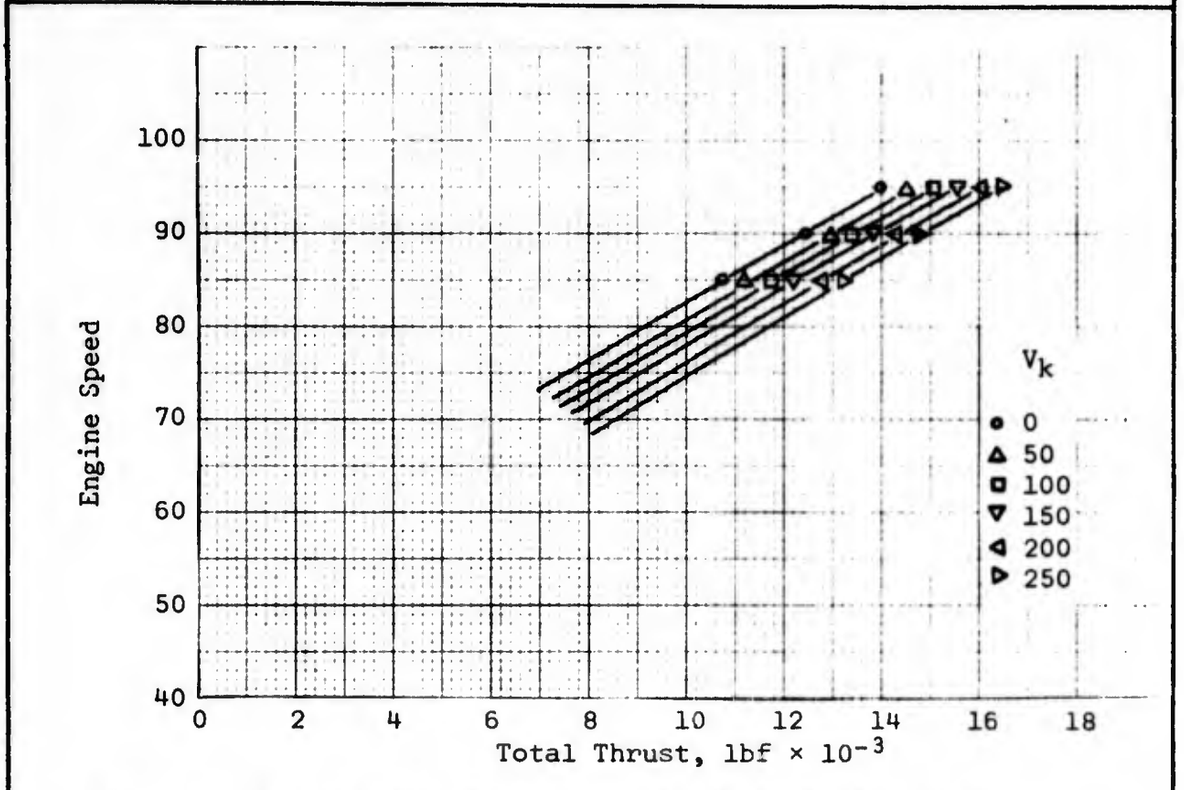

Fig. 13 Engine Speed as a Function of Thrust and Velocity

At very low speeds it is possible that the lift and drag may not be equal to their linear values, i.e.:

$$L_{WB} \neq 1/2\rho V^2 S\, a_{WB}\, \alpha$$

However, with consideration for the magnitude of the thrust and weight, the assumption that the aerodynamic forces are equal to their linear values at low speed is considered to give little error.

In the nonaccelerating transition the thrust and hence, the engine speed, vary and become relatively small toward the end of the transition. It will be remembered that reaction control force varied linearly with bleed air flow and that bleed air varied with RPM:

$$w_b = w_{bMAX}\,[1-2.14\,(1-N_F/N_{FD})]$$

A series of charts could easily be made presenting the variation of reaction control force with control stick displacement for the range of engine speed values. This information would normally be available, however, if only the information at one engine speed, as an example 95% is known, the following method may be used. The reaction control moment and tail incidence for 95% of maximum engine speed are solved as in the accelerating transition. The reaction control moment for the actual engine speed is then compared to that of 95% by the bleed air ratio:

$$w_{b\ .95} = w_{bMAX}\,[1-2.14\,(.05)] = .893\, w_{bMAX}$$

$$w_{bNF} = C_b\, w_{bMAX} \qquad \text{where:} \quad C_b = [1-2.14\,(NF/NFD)]$$

$$w_{bNF} = (C_b/0.893)\, w_{b\ .95}$$

and:

$$M_{RNF} = (C_b/0.893)\, M_{R\ .95}$$

The control stick displacement for this reaction moment is then determined by:

$$\ell_s = (M_{RNF}/C_2) - 1.4$$

and the corresponding i_t by:

$$i_t = (\ell_s+2)C_1$$

The accuracy of this solution may be checked by the balance of the moment equation:

$$M_1 + M_{RNF} + M_T = \text{Error}$$

M_1 is the original moment. When $M_1 + M_{RNF} + M_T = 0$, one has a perfect solution. However, the solution may be iterated to a prescribed error, E, by checking:

$$|M_1 + M_{RNF} + M_T| < E$$

If the error is greater than E, one-half the value of the error is taken and added to M and the calculation repeated.

$$M(NEW) = M(OLD) + \text{Error}/2$$

and:

$$M(NEW) + M_{R\ .95} + M_T = 0$$

This has the effect of increasing or decreasing $M_{R\ .95}$ and hence M_{RNF} depending on the sign of the error and converges the iteration.

The thrust is easily found from the solution, but the RPM must be calculated from the thrust. From Fig. 13 there appears, from the even spacing of points, to be about a linear variation of thrust with speed at any one engine speed. Also there is a linear variation of thrust with engine speed at any one speed. With the total thrust known, it is then possible to determine the RPM by:

$$\frac{T_{.95}-T_x}{T_{.95}} = \frac{RPM_{.95}-RPM_x}{RPM_{.95}-RPM_o} \quad \text{for zero velocity}$$

$$\frac{RPM_x-RPM_V}{RPM_{250}} = \frac{V}{250}$$

or with numbers for the P-1127

$$\frac{[13,950-(T_1+T_2)]}{13,950} = \frac{.95-RPM_x}{.47}$$

$$RPM_x = .95 - \frac{[13,950-(T_1+T_2)]0.45}{13,950}$$

$$RPM_V = \frac{RPM_x-.08V_k}{250} = \frac{RPM_x-.08V_{ft}}{423}$$

The solution of the nonaccelerating transition is repeated until the nozzle is rotated to zero angle. The complexity of the solution demands a computer solution which is presented in Appendix C.

IV. Stability Derivatives

The stability derivatives are functions of the flight conditions at any particular instant in the transition. Since the acceleration effects on the derivatives are assumed to be negligible, the same expressions may be used for both transitions. Since body axes are to be used instead of the Earth axes of the performance solution, the force and moment equations must be changed.

$$X = -F_w \sin\theta_0 - F_I \sin\theta_0 + L_{WB} \sin\alpha - D_{WB} \cos\alpha +$$
$$L_T \sin\alpha_t + (T_1+T_2) \cos(\delta_j+\theta_{0T}) - F_u \cos\theta_0$$

$$Z = F_w \cos\theta_0 + F_I \cos\theta_0 - L_{WB} \cos\alpha - L_T \cos\alpha_t - D_{WB} \sin\alpha -$$
$$F_u \sin\theta_0 - F_{R_1} - F_{R_2} - (T_1+T_2) \sin(\delta_j+\theta_{0T})$$

$$M = -F_{R_1}(h_{R_1}-h) + F_{R_2}(h_{R_2}+h) + (F_w-F_I) \cos\theta_0 (\ell_N+h) -$$
$$F_u \sin\theta_0 (\ell_N+h) + [(F_w-F_I) \sin\theta_0 + F_u \cos\theta_0] z_e +$$
$$(L_{WB} \cos\alpha + D_{WB} \sin\alpha)(h-h_{nWB}) + (D_{WB} \cos\alpha - L_{WB} \sin\alpha) z_{WB} +$$
$$\sin(\delta_j+\theta_{0T})[T_1(h-h_{T_1}) + T_2(h-h_{T_2})] -$$
$$\cos\alpha_t [L_T(h_T-h) + D_T z] + \sin\alpha_t [D_T(h_T-h) + L_T z_T]$$

Many derivatives may be negligible and some moment arms so small as to make the moment negligible. The derivatives of each equation will be derived separately.

X Derivatives

X_u.

$$\frac{\partial X}{\partial u} = -\frac{\partial F_w \sin\theta_0}{\partial u} - \frac{\partial F_I \sin\theta_0}{\partial u} + \frac{\partial L_{WB}\sin\alpha}{\partial u} - \frac{\partial D_{WB}\cos\alpha}{\partial u} +$$

$$\frac{\partial L_T \sin\alpha_t}{\partial u} + \frac{\partial (T_1+T_2)\cos(\delta_j+\theta_{0T})}{\partial u} - \frac{\partial F_u \cos\theta_0}{\partial u}$$

The derivation of each term is performed:

$$\frac{\partial D_{WB}\cos\alpha}{\partial u} = \frac{\partial {}^1/_2\rho V^2 S C_D (u_o+u)/V}{\partial u}$$

$$= \frac{\partial {}^1/_2\rho V S (u_o+u)}{\partial u}$$

$$= {}^1/_2\rho S C_D \left[(u_o+u)\frac{\partial V}{\partial u} + V\frac{\partial (u_o+u)}{\partial u}\right]$$

where: $\frac{\partial C_D}{\partial u} = 0$

$$\frac{\partial V}{\partial u} = \frac{\partial [(u_o+u)^2 + w_o{}^2]^{1/2}}{\partial u} = \frac{u_o+u}{V}$$

where: $\frac{\partial (u_o+u)}{\partial u} = 1$

thus: $\frac{\partial V}{\partial u} = \cos\alpha$

$$\frac{\partial D_{WB}\cos\alpha}{\partial u} = {}^1/_2\rho S C_D \left[(u_o+u)\cos\alpha + V\right] = {}^1/_2\rho V S C_D (1 + \cos^2\alpha)$$

$$\frac{\partial(L_{WB}\sin\alpha)}{\partial u} = \frac{\partial(1/2\rho V^2 S C_{LWB}\, w_o/V)}{\partial u}$$

$$= \frac{\partial(1/2\rho V S C_{LWB}\, w_o)}{\partial u}$$

$$= 1/2\rho S C_{LWB}\, w_o \frac{\partial V}{\partial u}$$

where: $\frac{\partial C_L}{\partial u} = \frac{\partial w_o}{\partial u} = 0$

thus: $\frac{\partial(L_{WB}\sin\alpha)}{\partial u} = 1/2\rho V S C_{LWB} \sin\alpha \cos\alpha$

$$\frac{\partial(L_T \sin\alpha_t)}{\partial u} = \frac{\partial(1/2\rho V^2 S_T C_{LT} \sin\alpha_t)}{\partial u}$$

$$= 1/2\rho S_T [V^2(\sin\alpha_t \frac{\partial C_{LT}}{\partial u} + C_{LT} \frac{\partial \sin\alpha_t}{\partial u}) +$$

$$C_{LT} \sin\alpha_t \frac{\partial V^2}{\partial u}]$$

$$= 1/2\rho S_T (V^2 C_{LT} \cos\alpha_t \frac{\partial \alpha_t}{\partial u} + 2C_{LT} V \sin\alpha_t \cos\alpha)$$

$$\frac{\partial \alpha_t}{\partial u} = \frac{(1 - \partial\epsilon/\partial\alpha)\alpha}{\partial u} = (1 - \partial\epsilon/\partial\alpha)\frac{\partial\alpha}{\partial u}$$

The assumption that C_{LT} is zero until α is in the linear range of the C_{LT} vs α_t curve, permits the approximation:

$$\alpha \approx \frac{w_o}{V} = \frac{w_o}{[(u_o+u)^2 + w_o^2]^{1/2}}$$

Also, for a given transition ϵ_0 and $\partial\epsilon/\partial\alpha$ have been allowed to vary only with nozzle angle.

Thus: $\dfrac{\partial \epsilon_0}{\partial u} = 0$ and $\dfrac{\partial}{\partial u}\left(\dfrac{\partial \epsilon}{\partial \alpha}\right) = 0$

$$\frac{\partial \alpha}{\partial u} = \frac{\dfrac{\partial w_o}{[(u_o+u)^2 + w_o^2]^{1/2}}}{\partial u} = \frac{w_o(u_o+u)}{V^3}$$

$$\frac{\partial(L_T \sin\alpha_t)}{\partial u} = {}^1/_2 \rho V S_T \left[2C_{LT} \sin\alpha_t \cos\alpha + (1 - \partial\epsilon/\partial\alpha)\, C_{LT} \sin\alpha \cos\alpha \cos\alpha_t\right]$$

$$\frac{\partial(T_1+T_2)\cos(\delta_j+\theta_{0T})}{\partial u} = \cos(\delta_j+\theta_{0T}) \frac{\partial(T_1+T_2)}{\partial u}$$

$$= \cos(\delta_j+\theta_{0T}) \frac{\partial(T_1+T_2)}{\partial V} \frac{\partial V}{\partial u}$$

$$= \cos(\delta_j+\theta_{0T}) \cos\alpha \frac{\partial(T_1+T_2)}{\partial V}.$$

$$\frac{\partial(F_u \cos\theta_0)}{\partial u} = \cos\theta_0 \frac{\partial F_u}{\partial u} = \cos\theta_0 \frac{w_a}{g} \frac{\partial u_x}{\partial u}$$

If u_x is thought of as being formed by two velocity vectors u_{xx}, u_{xz} in the X and Z directions then:

$$\frac{\partial u_x}{\partial u} = \frac{\partial(u_{xx}^2 + u_{xz}^2)^{1/2}}{\partial u} = \frac{u_{xx}}{(u_{xx}^2 + u_{xz}^2)^{1/2}}$$

$$= \frac{u_{xx}}{u_x} = \cos\theta_0$$

$$\frac{\partial F_u \cos\theta_0}{\partial u} = \frac{w_a}{g} \cos^2\theta_0$$

similarly:

$$\frac{\partial (F_w \sin\theta_0)}{\partial u} = \frac{w_a}{g} \sin^2\theta_0$$

thus:

$$- \frac{\partial (F_u \cos\theta_0)}{\partial u} - \frac{\partial (F_w \sin\theta_0)}{\partial u} = - \frac{w_a}{g}$$

It may be argued that the air mass flow varies with velocity, but as may be seen in Fig. 14, for constant engine speed, the variation is very small and most of this is due to increased thrust (Ref 2). It is felt that this derivative would be negligible.

F_I has been allowed to vary only with nozzle deflection thus:

$$\frac{\partial F_I}{\partial u} = 0$$

All stability derivatives of F_I are zero and will be neglected henceforth.

Finally:

$$\frac{\partial x}{\partial u} = - \frac{w_a}{g} + {}^1/_2 \rho V S C_{LWB} \sin\alpha \cos\alpha - {}^1/_2 \rho V S C_D (1 + \cos^2\alpha) +$$

$$\rho V S_T C_{LT} [\sin\alpha_t \cos\alpha - {}^1/_2 (1 - \partial\varepsilon/\partial\alpha) \cos\alpha_t \sin\alpha\cos\alpha] +$$

$$\frac{\partial (T_1+T_2)}{\partial V} \cos\alpha \cos(\delta_j + \theta_{0T})$$

$$X_u = \frac{1}{m} \frac{\partial x}{\partial u}$$

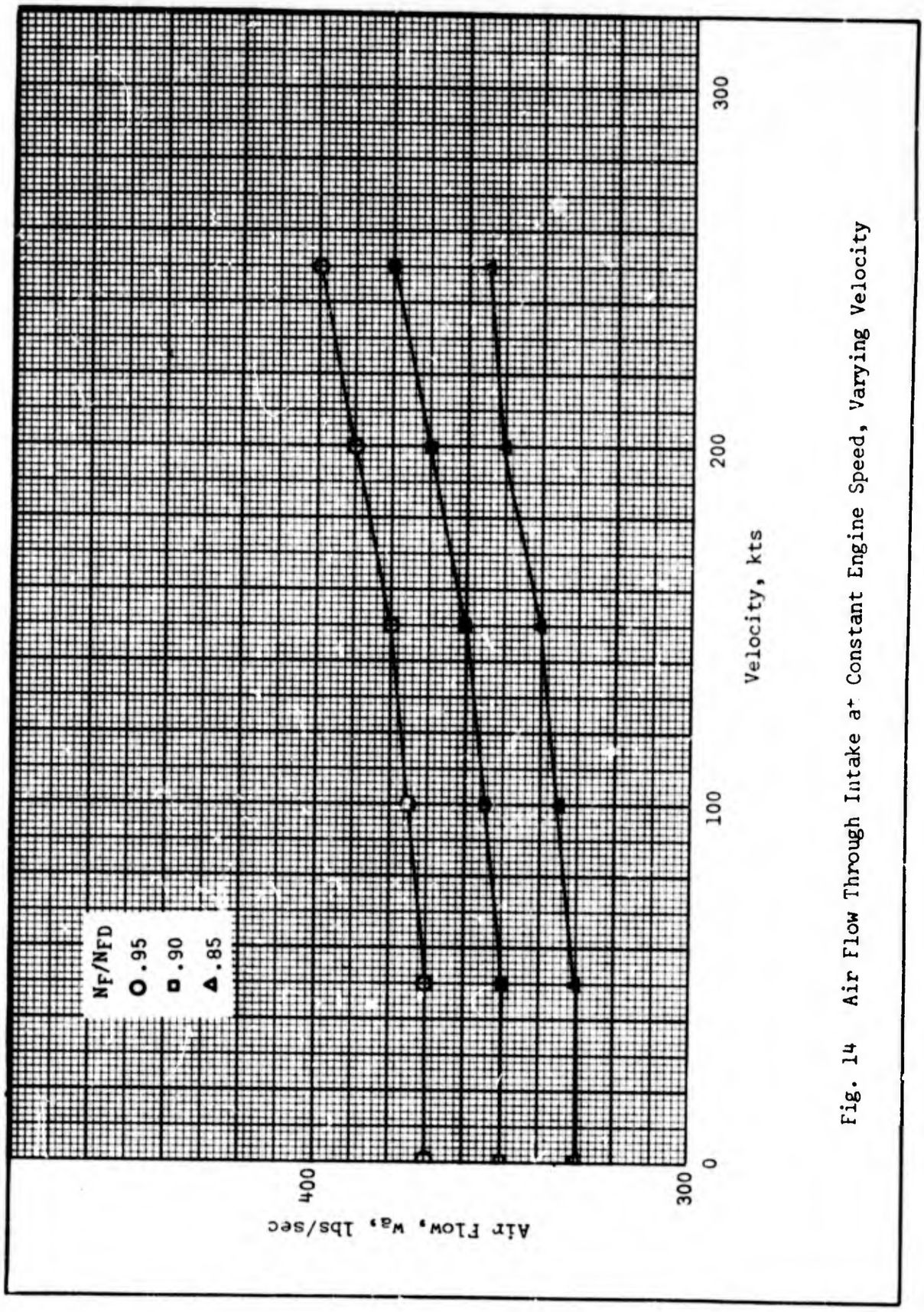

Fig. 14 Air Flow Through Intake at Constant Engine Speed, Varying Velocity

$\underline{X_w}$.

$$\frac{\partial x}{\partial w} = - \frac{\partial(F_w \sin\theta_0)}{\partial w} - \frac{\partial(F_u \cos\theta_0)}{\partial w} - \frac{\partial(F_I \sin\theta_0)}{\partial w} + \frac{\partial(L_{WB}\sin\alpha)}{\partial w} -$$

$$\frac{\partial(D_{WB}\cos\alpha)}{\partial w} + \frac{\partial(L_T \sin\alpha_t)}{\partial w} + \frac{\partial(T_1+T_2)}{\partial w} \cos(\delta_j+\theta_{0T})$$

$$\frac{\partial F_w \sin\theta_0}{\partial w} = \sin\theta_0 \frac{w_a}{g} \frac{\partial(w_{zx}^2 + w_{zz}^2)^{1/2}}{\partial w}$$

$$= - \frac{w_a}{g} \sin\theta_0 \cos\theta_0$$

where: $\frac{\partial w_{zz}}{\partial w} = - \cos\theta_0$

$$\frac{\partial F_u \cos\theta_0}{\partial w} = \frac{w_a}{g} \sin\theta_0 \cos\theta_0$$

therefore:

$$- \frac{\partial(F_w \sin\theta_0)}{\partial w} - \frac{\partial(F_u \cos\theta_0)}{\partial w} = 0$$

$$\frac{\partial F_I}{\partial w} = 0$$

$$\frac{\partial(L_{WB}\sin\alpha)}{\partial w} = \frac{\partial 1/2 \rho V^2 S C_{LWB}(w_o+w)/V}{\partial w}$$

$$= 1/2 \rho S \frac{\partial V(w_o+w)\, C_{LWB}}{\partial w}$$

$$= 1/2 \rho S \left\{ V(w_o+w) \frac{\partial C_{LWB}}{\partial w} + C_{LWB} \left[(w_o+w) \frac{\partial V}{\partial w} + V \frac{\partial(w_o+w)}{\partial w} \right] \right\}$$

but $\sin\alpha = (w_o+w)/V$ and at the small angles of attack where the airfoil is effective:

$$\alpha \simeq \frac{(w_o+w)}{V}$$

thus:

$$\frac{\partial C_{LWB}}{\partial w} = \frac{\partial C_{LWB}}{\partial \alpha}\frac{\partial \alpha}{\partial w} = \frac{1}{V}\frac{\partial C_{LWB}}{\partial \alpha} = \frac{1}{V}\, a_{WB}$$

therefore:

$$\frac{\partial L_{WB}\sin\alpha}{\partial w} = {}^1/_2\rho V S\,[a_{WB}\sin\alpha + C_{LWB}\,(1+\sin^2\alpha)]$$

$$\frac{\partial L_T \sin\alpha_t}{\partial w} = \frac{\partial\, {}^1/_2\rho V^2 S_T C_{LT}\sin\alpha_t}{\partial w}$$

$$= {}^1/_2\rho S_T\,[C_{LT}\,(V^2\frac{\partial \sin\alpha_t}{\partial w} + \sin\alpha_t\frac{\partial V^2}{\partial w}) + V^2\sin\alpha_t\frac{\partial C_{LT}}{\partial w}]$$

$$\frac{\partial \sin\alpha_t}{\partial w} = \cos\alpha_t\frac{\partial \alpha_t}{\partial w} = \cos\alpha_t\frac{\partial \alpha_t}{\partial \alpha}\frac{\partial \alpha}{\partial w}$$

$$= \frac{\cos\alpha_t\,(1 - \partial\epsilon/\partial\alpha)}{V}$$

$$\frac{\partial C_{LT}}{\partial w} = \frac{\partial C_{LT}}{\partial\, \alpha_t}\frac{\partial \alpha_t}{\partial w}\frac{\partial \alpha}{\partial w} = \frac{a_T\,(1 - \partial\epsilon/\partial\alpha)}{V}$$

$$\frac{\partial (L_T\sin\alpha_t)}{\partial w} = {}^1/_2\rho V S_T[(1 - \partial\epsilon/\partial\alpha)(\cos\alpha_t\, C_{LT} + \sin\alpha_t\, a_T) + 2C_{LT}\sin\alpha_t\sin\alpha]$$

$$\frac{\partial(D_{WB}\cos\alpha)}{\partial w} = \frac{\partial\left(\frac{1}{2}\rho V^2 S C_D \frac{u_o}{V}\right)}{\partial w} = \frac{1}{2}\rho S \frac{\partial(VC_D u_o)}{\partial w}$$

$$= \frac{1}{2}\rho S u_o \left(C_D \frac{\partial V}{\partial w} + V \frac{\partial C_D}{\partial w}\right)$$

$$= \frac{1}{2}\rho S u_o \left[C_D \sin\alpha + a_D\right] = \frac{1}{2}\rho V S \cos\alpha \left[C_D \sin\alpha + a_D\right]$$

$$\frac{\partial(T_1+T_2)\cos(\delta_j+\theta_{0T})}{\partial w} = \cos(\delta_j+\theta_{0T}) \frac{\partial(T_1+T_2)}{\partial V} \frac{\partial V}{\partial w}$$

$$= \cos(\delta_j+\theta_{0T}) \sin\alpha \frac{\partial(T_1+T_2)}{\partial V}$$

Finally:

$$\frac{\partial X}{\partial w} = \frac{1}{2}\rho V S \left[C_{LWB}\left(1 + \sin^2\alpha\right) + a_{WB}\sin\alpha\right] -$$

$$\frac{1}{2}\rho V S \cos\alpha \left[a_D + C_D \sin\alpha\right] +$$

$$\frac{1}{2}\rho V S_T \left[(1 - \partial\varepsilon/\partial\alpha)(C_{LT}\cos\alpha_t + a_T \sin\alpha_t) +\right.$$

$$\left. 2C_{LT}\sin\alpha_t \sin\alpha\right] + \frac{\partial(T_1+T_2)}{\partial V}\sin\alpha\cos(\delta_j+\theta_{0T})$$

Z Derivatives

Z_u

$$\frac{\partial Z}{\partial u} = \frac{\partial F_I \cos\theta_0}{\partial u} + \frac{\partial F_w \cos\theta_0}{\partial u} - \frac{\partial F_u \sin\theta_0}{\partial u} - \frac{\partial L_{WB}\cos\alpha}{\partial u} -$$

$$\frac{\partial L_T \cos\alpha_t}{\partial u} - \frac{\partial D_{WB}\sin\alpha}{\partial u} - \frac{\partial(F_{R_1}+F_{R_2})}{\partial u} - \frac{\partial(T_1+T_2)\sin(\delta_j+\theta_{0T})}{\partial u}$$

F_R is a control force and:

$$\frac{\partial(F_{R_1}+F_{R_2})}{\partial u} = 0$$

As previously derived:

$$\frac{\partial F_w}{\partial u} = +\,(w_a/g)\,\sin\theta_0 \quad \text{and} \quad \frac{\partial F_u}{\partial u} = (w_a/g)\,\cos\theta_0$$

therefore:

$$\frac{\partial(F_w\cos\theta_0)}{\partial u} - \frac{\partial(F_u\sin\theta_0)}{\partial u} = 0$$

The derivations of the remaining terms are very similar to those of X_u therefore only final expressions are given.

$$\frac{\partial(L_{WB}\cos\alpha)}{\partial u} = {}^1/_2\rho VSC_{LWB}\,(1 + \cos^2\alpha)$$

$$\frac{\partial(D_{WB}\sin\alpha)}{\partial u} = {}^1/_2\rho VSC_D\,\sin\alpha\,\cos\alpha$$

$$\frac{\partial(L_T\cos\alpha_t)}{\partial u} = {}^1/_2\rho VS_TC_{LT}\,[2\,\cos\alpha\,\cos\alpha_t + (1 - \partial\varepsilon/\partial\alpha)\,\sin\alpha_t\,\sin\alpha\,\cos\alpha]$$

$$\frac{\partial(T_1+T_2)\,\sin(\delta_j+\theta_{0T})}{\partial u} = \frac{\partial(T_1+T_2)}{\partial V}\,\cos\alpha\,\sin(\delta_j+\theta_{0T})$$

finally:

$$\frac{\partial Z}{\partial u} = -{}^1/_2\rho VSC_{LWB}\,(1 + \cos^2\alpha) - {}^1/_2\rho VS_TC_{LT}\,[\cos\alpha_t\,\cos\alpha + (1 - \partial\varepsilon/\partial\alpha)\,\sin\alpha_t\,\sin\alpha\,\cos\alpha] - {}^1/_2\rho VSC_D\,\sin\alpha\,\cos\alpha - \frac{\partial(T_1+T_2)}{\partial V}\,\cos\alpha\,\sin(\delta_j+\theta_{0T})$$

$$Z_u = \frac{1}{m}\frac{\partial Z}{\partial u}$$

$\underline{Z_w}$. The derivation of Z_w is very similar to X_w so only final results are given:

$$\frac{\partial Z}{\partial w} = \frac{\partial(F_I\cos\theta_0)}{\partial w} - \frac{\partial(F_w\cos\theta_0)}{\partial w} - \frac{\partial(F_w\sin\theta_0)}{\partial w} - \frac{\partial(L_{WB}\cos\alpha)}{\partial w} -$$

$$\frac{\partial(L_T\cos\alpha_t)}{\partial w} - \frac{\partial(D_{WB}\sin\alpha)}{\partial w} - \frac{\partial(F_{R_1}+F_{R_2})}{\partial w} -$$

$$\frac{\partial(T_1+T_2)\sin(\delta_j+\theta_{0T})}{\partial w}$$

where: $$-\frac{\partial(F_w\cos\theta_0)}{\partial w} - \frac{\partial(F_u\sin\theta_0)}{\partial w} = -\frac{w_a}{g}$$

$$\frac{\partial(L_{WB}\cos\alpha)}{\partial w} = {}^1/_2\rho VS\cos\alpha\,[C_{LWB}\sin\alpha + a_{WB}]$$

$$\frac{\partial(D_{WB}\sin\alpha)}{\partial w} = {}^1/_2\rho VS\,[\sin a_D + C_D\,(1+\sin^2\alpha)]$$

$$\frac{\partial(L_T\cos\alpha_t)}{\partial w} = {}^1/_2\rho VS_T\,[(1-\partial\varepsilon/\partial\alpha)(\cos\alpha_t\, a_T - C_{LT}\sin\alpha_t) +$$

$$2C_{LT}\cos\alpha_t\sin\alpha]$$

$$\frac{\partial(T_1+T_2)\sin(\delta_j+\theta_{0T})}{\partial w} = \frac{\partial(T_1+T_2)}{\partial V}\sin\alpha\sin(\delta_j+\theta_{0T})$$

finally:

$$\frac{\partial Z}{\partial w} = -\frac{w_a}{g} - {}^1/_2\rho VS\cos\alpha\,(C_{LWB}\sin\alpha + a_{WB}) -$$

$${}^1/_2\rho VS_T\,[(1 - \partial\epsilon/\partial\alpha)(\cos\alpha_t\, a_T - C_{LT}\sin\alpha_t) +$$

$$2C_{LT}\cos\alpha_t\sin\alpha] - {}^1/_2\rho VS\,[\sin\alpha\, a_D + C_D\,(1 + \sin^2\alpha)] -$$

$$[\partial(T_1+T_2)/\partial V]\sin\alpha\sin(\delta_j+\theta_{0T})$$

$$Z_w = \frac{1}{m}\frac{\partial Z}{\partial w}$$

$\underline{Z_q}$. Z_q is very often neglected but was included here because of the uncertainty of the magnitude of its affect. Only the tail contribution caused by the change of α_t was included. The derivation is conventional (Ref 6:154,155). The change in the angle of attack of the tail is:

$$\Delta\alpha_t = (h_t-h)\,q/u_o$$

$$\Delta Z = -{}^1/_2\rho V^2 S_T\, a_T\cos\alpha_t\,(h_T-h)\,q/u_o$$

$$\frac{\partial Z}{\partial q} = -[{}^1/_2\rho S_T\, a_T\,(h_T-h)/u_o]\frac{\partial(V^2\cos\alpha_t q)}{\partial q}$$

$\partial V^2/\partial q$ is assumed negligible.

$$\frac{\partial\cos\alpha_t}{\partial q} = -\sin\alpha_t\partial\alpha_t/\partial q = -\sin\alpha_t\,(h_T-h)/u_o$$

$$\frac{\partial Z}{\partial q} = -[{}^1/_2\rho V^2 S_T\, a_T\,(h_T-h)/u_o][\cos\alpha_t - \sin\alpha_t\,(h_T-h)q/u_o]$$

Allowing only small q perturbation and realizing that $\sin\alpha_t$ is necessarily small:

$$\frac{\partial Z}{\partial q} = - {}^1/_2 \rho V S_T \, a_T \, (h_T - h) \cos\alpha_t / \cos\alpha$$

$$Z_q = \frac{1}{m} \frac{\partial Z}{\partial q}$$

$\underline{Z_{\dot{w}}}$. $Z_{\dot{w}}$ is also often neglected but is included here. Only the tail contribution caused by the lag of the downwash is included. The derivation is somewhat different from Etkin's (Ref 4:165). The lag in the downwash caused by w is:

$$\Delta\varepsilon = - \frac{\partial \varepsilon}{\partial \alpha} \dot{\alpha} \frac{(h_T - h)}{u_o}$$

To get the change in the angle of attack of the tail, the change of the downwash must be multiplied by the effectiveness of the tail to respond to changes in angle of attack of the aircraft.

Thus:

$$-\Delta\alpha_t = - (1 - \partial\varepsilon/\partial\alpha) \, \partial\varepsilon/\partial\alpha \, \dot{\alpha} \frac{(h_T - h)}{u_o}$$

and

$$\Delta Z = - {}^1/_2 \rho V^2 S_T \, a_T \cos\alpha_t \, (1 - \frac{\partial \varepsilon}{\partial \alpha}) \frac{\partial \varepsilon}{\partial \alpha} \dot{\alpha} \frac{(h_T - h)}{u_o}$$

$$\frac{\partial Z}{\partial \dot{w}} = - {}^1/_2 \rho S_T \, a_T \, (h_T - h) \, (1 - \frac{\partial \varepsilon}{\partial \alpha}) \frac{\partial \varepsilon}{\partial \alpha} \frac{\cos\alpha_t}{\cos\alpha}$$

M Derivatives

In the solution of the performance equations many small terms were neglected and they must, for consistency, be neglected in the derivatives. They include all terms with Z_e, Z_{WB}, D_T and Z_T reducing the moment equation to:

$$M = F_w \cos\theta_0 (\ell_N+h) - F_u \sin\theta_0 (\ell_N+h) + L_{WB} \cos\alpha (h-h_{nWB}) -$$

$$L_T \cos\alpha_t (h_T-h) + (h-h_{nWB}) D_{WB} \sin\alpha + M_o + [T_1(h-h_{T_1}) +$$

$$T_2(h-h_{T_2})]\sin(\delta_j+\theta_{0T}) + F_{R_2}(h_{R_2}+h) - F_{R_1}(h_{R_1}-h) -$$

$$F_I \cos\theta_0 (\ell_N+h)$$

All derivatives of F_R and F_I are zero. It will be noticed that the resulting M equation consists only of terms of the Z equation and moment arms. As may be expected then, the M derivatives are simply the Z derivatives multiplied times moment arms.

$\underline{M_u}$.

$$\frac{\partial M}{\partial u} = (\ell_N+h) (\cos\theta_0 \frac{\partial F_w}{\partial u} - \sin\theta_0 \frac{\partial F_u}{\partial u}) + \frac{\partial M_o}{\partial u} +$$

$$(h-h_{nWB}) \frac{\partial L_{WB}\cos\alpha}{\partial u} - (h_T-h) \frac{\partial L_T \cos\alpha_t}{\partial u} +$$

$$(h-h_{nWB}) \frac{\partial D_{WB}\sin\alpha}{\partial u} + \sin(\delta_j+\theta_{0T}) [(h-h_{T_1}) \frac{\partial T_2}{\partial u} +$$

$$(h-h_{T_2}) \frac{\partial T_2}{\partial u}]$$

All of the above terms may be found from Z_u except $\partial M_o/\partial u$

$$\frac{\partial M_o}{\partial u} = \frac{\partial(^1/_2 \rho V^2 S \bar{c} C_{Ma.c.})}{\partial u} = \rho V S C_{Ma.c.} \cos\alpha \bar{c}$$

$$\frac{\partial M}{\partial u} = {}^1/_2\rho VSC_{LWB}\ (h-h_{nWB})\ (1 + \cos^2\alpha) +$$

$${}^1/_2\rho VS_TC_{LT}\ (h-h_T)\ [2\ \cos\alpha_t\ \cos\alpha +$$

$$(1 - \partial\epsilon/\partial\alpha)\ \sin\alpha_t\ \sin\alpha\ \cos\alpha +$$

$${}^1/_2\rho VSC_D\ \sin\alpha\ \cos\alpha\ (h-h_{nWB}) +$$

$$\sin(\delta_j+\theta_{0T})\ \cos\alpha\ [(h-h_{T_1})\ \frac{\partial T_1}{\partial V} + (h-h_{T_2})\ \frac{\partial T_2}{\partial V}\ ] +$$

$$\rho VSC_{Ma.c.}\ \cos\alpha\ \bar{c}$$

$$M_u = \frac{1}{I_{yy}}\ \frac{\partial M}{\partial u}$$

$\underline{M_w}$. In similar method to M_u and using the Z_w derivative:

$$\frac{\partial M}{\partial w} = (\ell_N+h)\ \frac{w_a}{g} + \rho VS\bar{c}\sin\alpha\ C_{Ma.c.} +$$

$${}^1/_2\rho VS\ \cos\alpha\ (h-h_{nWB})(C_{LWB}\ \sin\alpha + a_{WB}) -$$

$${}^1/_2\rho VS_T\ (h_T-h)\ [(1 - \partial\epsilon/\partial\alpha)(\cos\alpha_t\ a_T - C_{LT}\ \sin\alpha_t) +$$

$$2C_{LT}\ \cos\alpha_t\ \sin\alpha] + \sin\alpha\ \sin(\delta_j+\theta_{0T})$$

$$[\ \frac{\partial T_1}{\partial V}\ (h-h_{T_1}) + \frac{\partial T_2}{\partial V}\ (h-h_{T_2})] +$$

$${}^1/_2\rho VS\ (h-h_{nWB})\ [\sin\alpha\ a_D + C_D\ (1 + \sin^2\alpha)]$$

$$M_w = \frac{1}{I_{yy}}\ \frac{\partial M}{\partial w}$$

M_q and $M_{\dot{w}}$. For both M_q and $M_{\dot{w}}$ only the tail contribution are considered.

$$\frac{\partial M}{\partial q} = (h_T - h) \frac{\partial Z}{\partial q}$$

$$\frac{\partial M}{\partial \dot{w}} = (h_T - h) \frac{\partial Z}{\partial \dot{w}}$$

$$M_q = \frac{1}{I_{yy}} \frac{\partial M}{\partial q}$$

$$M_{\dot{w}} = \frac{1}{I_{yy}} \frac{\partial M}{\partial \dot{w}}$$

All of the variables in the derivatives have already been used explicitly in the performance solution except $\partial T_1/\partial V$ and $\partial T_2/\partial V$. The variation of thrust with velocity was used implicitly and is found from the slopes of the curves in Fig. 9. The dimensional derivatives X_u, etc., are now used to solve the equations of motion.

Hawker Siddeley Derivatives

The stability derivatives of an accelerating transition were taken from Reference 2 and used for comparison with those calculated. The Hawker Siddeley derivatives were given for velocities from 50 to 220 knots and hence, comparison at very low speeds was impossible. It was necessary to make two conversions to the derivatives. First, the given nondimensional derivatives were dimensionalized using the nondimensionalizing factors given (Ref 2:7). Second, the derivatives were given for a wind axis system centered at the wing-body aerodynamic center and were converted to a body axis system also centered at the aerodynamic center. The derivatives used for comparison with the Hawker Siddeley derivatives were calculated for the body axis at the aerodynamic center rather than converting those calculated at the center of mass.

The conversion equations were derived by a method similar to Babister (Ref 7:696-698). For this derivation, X', u' and Z', w' are the forces and velocities aligned with the wind axes and X, u and Z, w the forces and velocities aligned with the body axes. The lateral axis of each system coincide. The angle between the X and X' and the Z and Z' axes is α.

Thus: $X = X' \cos\alpha - Z' \sin\alpha$

$Z = Z' \cos\alpha - X' \sin\alpha$

$M = M'$

$u' = u \cos\alpha + w \sin\alpha$

$w' = w \cos\alpha + u \sin\alpha$

$V' = V$

$$mX_u = \frac{\partial X}{\partial u} = \frac{\partial X}{\partial u'}\frac{\partial u'}{\partial u} + \frac{\partial X}{\partial w'}\frac{\partial w'}{\partial w}$$

$$= \left(\frac{\partial X'}{\partial u'}\frac{\partial u'}{\partial u} + \frac{\partial X'}{\partial w'}\frac{\partial w'}{\partial u}\right)\cos\alpha - \left(\frac{\partial Z'}{\partial u'}\frac{\partial u'}{\partial u} + \frac{\partial Z'}{\partial w'}\frac{\partial w'}{\partial u}\right)\sin\alpha$$

$$X_u = X'_u \cos^2\alpha - (X'_{w'} + Z'_{u'}) \sin\alpha \cos\alpha + Z'_{w'} \sin^2\alpha$$

Similarly:

$$X_w = X'_{w'} \cos^2\alpha + (X'_{u'} - Z'_{w'}) \sin\alpha \cos\alpha - Z'_{u'} \sin^2\alpha$$

$$Z_u = Z'_{u'} \cos^2\alpha + (X'_{u'} - Z'_{w'}) \sin\alpha \cos\alpha - X'_{w'} \sin^2\alpha$$

$$Z_w = Z'_{w'} \cos^2\alpha + (Z'_{u'} + X'_{w'}) \sin\alpha \cos\alpha + X'_{u'} \sin^2\alpha$$

$$Z_{\dot{w}} = Z'_{\dot{w}'} \cos\alpha$$

$$Z_q = Z'_{q'} \cos\alpha$$

$$M_u = M'_{u'} \cos\alpha - M'_{w'} \sin\alpha$$

$$M_w = M'_{w'} \cos\alpha + M'_{u'} \sin\alpha$$

$$M_{\dot{w}} = M'_{\dot{w}'} \cos\alpha$$

$$M_q = M'_{q'}$$

The change of the axis system produces significant changes in many of the derivatives; principally X_u, X_w, Z_u, and M_u. Table I is a summary of the calculations and presents a comparison of the values before and after the axis shift.

Table I

Comparison of The Hawker Siddeley Derivatives, Wind and Body Axes

V	α	sinα	cosα	$\sin^2\alpha$	$X'_{u'}$	$X'_{w'}$	$Z'_{u'}$	$Z'_{w'}$	$M'_{u'}$
50	4°	.0695	1	.00483	-.032	-.015	-.04	-.17	.0026
75	6 1/2°	.113	1	.0128	-.043	-.025	-.08	-.27	.0040
100	7	.122	1	.0149	-.050	-.032	-.13	-.36	.0054
125	6.2	.108	1	.0117	-.056	-.026	-.16	-.41	.0059
150	5.5	.096	1	.0092	-.061	-.002	-.19	-.49	.0036
175	4.8	.0835	1	.00697	-.065	.021	-.20	-.52	.0026
200	3.5°	.061	1	.00372	-.072	.029	-.20	-.62	.0012

V	$M'_{w'}$	$M'_{\dot{w}'}$	$M'_{q'}$	X_u	X_w	Z_u	Z_w	M_u	M_w
50	.003	-.00051	-.96	-.029	-.0054	-.03	-.173	.0024	.0032
75	.0055	-.00057	-.23	-.036	.00164	-.055	-.282	.0034	.0060
100	.0075	-.00067	-.31	-.036	.00774	-.0922	-.379	.0045	.0080
125	.0050	-.0009	-.42	-.0407	.01305	-.122	-.483	.0054	.0056
150	-.001	-.0012	-.58	-.047	.039	-.149	-.508	.0037	-.0007
175	-.0055	-.00132	-.68	-.053	.059	-.162	-.535	.0031	-.0053
200	-.0075	-.00132	-.72	-.063	.061	-.166	-.630	.0017	-.0074

V. Equations of Motion

The equations of motion are derived for the body axis system used for the stability derivatives. Only those derivatives for which expressions were found in Section IV are retained and the equations are linearized.

Stick Fixed Equations

A simplified derivation is presented here as the equations are standard and complete derivations may be found in any stability and control text (Refs 4 and 6).

X Equation.

$$X_o + \Delta X - mg(\sin\theta_0 + \theta \cos\theta_0) = m\dot{u} + mq\, w_o$$

Subtracting steady reference values:

$$\Delta X - mg\theta \cos\theta_0 = m\dot{u} + mq\, w_o$$

Assuming small perturbations of u and w only and neglecting higher order terms:

$$\Delta X = \frac{\partial X}{\partial u} u + \frac{\partial X}{\partial w} w$$

Dividing by m:

$$X_u u + X_w w - g\theta \cos\theta_0 = \dot{u} + qw_o$$

$$(X_u - s)\, u + X_w w - (g \cos\theta_0 + w_o s)\theta = 0$$

Z Equation.

$$Z_o + \Delta Z + mg(\cos\theta_0 - \theta \sin\theta_0) = m(\dot{w} - u_o q)$$

Subtracting reference values:

$$\Delta Z - mg\ \theta \sin\theta_0 = m(\dot{w} - u_o q)$$

Assuming small perturbations of u, w, $\dot{w}$, and q only and once more neglecting higher order terms:

$$\frac{1}{m} \Delta Z = Z_u\ u + Z_w\ w\ Z_{\dot{w}}\ \dot{w} + Z_q\ q$$

$$Z_u\ u + Z_w\ w + Z_{\dot{w}}\ \dot{w} - \dot{w} + Z_q\ q + u_o q - g\theta \sin\theta_0 = 0$$

$$Z_u\ u + (Z_w + Z_{\dot{w}}\ s - s)\ w + (Z_q\ s + u_o\ s - g \sin\theta_0)\theta = 0$$

M Equation. Besides the linear, uncoupling and perturbation assumptions of the X and Z equations, the assumption of negligible spinning rotor inertia is made in the moment equation.

$$M_o + \Delta M = I_{yy}\ \dot{q}$$

M_o must be zero, therefore:

$$\Delta M = I_{yy}\ \dot{q}$$

As in the Z equation perturbations:

$$\frac{1}{I_{yy}} \Delta M = M_u\ u + M_w\ w + M_{\dot{w}}\ \dot{w} + M_q\ q$$

$$M_u\ u + (M_w + M_{\dot{w}}\ s)\ w + (M_q - s)s\theta = 0$$

The resultant stability determinant is:

$$\begin{vmatrix} (X_u - s)u + & X_w\, w & - & (g\cos\theta_0 + w_o s)\theta \\ Z_u\, u & + [Z_w + (Z_{\dot{w}} - 1)s]\, w + & [(Z_q + u_o)s - g\sin\theta_0]\theta & \\ M_u\, u & + & (M_w + M_{\dot{w}} s)\, w & + & (M_q - s)\, s\, \theta \end{vmatrix} = 0$$

A reduction of the determinant forms the usual characteristic quartic:

$$A\, s^4 + B\, s^3 + C\, s^2 + D\, s + E = 0$$

where assuming $\cos\theta_0 \approx 1$:

$$A = 1 - Z_{\dot{w}}$$

$$B = - X_u + Z_{\dot{w}} (X_u + M_q) - Z_w - M_q - M_{\dot{w}} (Z_q + u_o)$$

$$C = - X_u [M_q (Z_{\dot{w}} - 1) - Z_w - M_{\dot{w}} (Z_q + u_o)] + Z_w M_q - M_w (Z_q + u_o) - Z_u (X_w - w_o M_{\dot{w}}) - w_o M_u (Z_{\dot{w}} - 1)$$

$$D = - X_u [Z_w M_q - M_w (Z_q + u_o)] + X_w [Z_u M_q - M_u (Z_q + u_o)] + g [Z_u M_{\dot{w}} - M_u (Z_{\dot{w}} - 1)] + w_o (Z_u M_w - M_u Z_w)$$

$$E = g (Z_u M_w - M_u Z_w)$$

The solution of the stability quartic is the final calculation of the computer programs in Appendices B and C.

VI. Results, Conclusions, and Recommendations

The most notable result of the stability calculations was that the P-1127 was unstable in some form throughout most of the transition. Although the stability varied between the accelerating and nonaccelerating transitions, there was fairly good agreement between the derivatives. There was very good agreement with the Hawker Siddeley derivatives in most cases but very poor agreement in two derivatives, X_w and M_w, in certain velocity regimes. A discussion of the performance, each derivative and the overall stability through the transition follows.

Performance

The performance of the accelerating transition was compared to that given in Reference 2. The nozzle deflection variation with speed and the final velocity at end of transition agreed very well as may be seen from Fig. 15. This agreement was to be expected as the variation and final speed are primarily dependent on the inertial properties of the airplane which were given in Reference 2.

The maximum angle of attack and the minimum climb angle were at approximately 100 kts for both the given and calculated values. However, the given maximum values of α and θ were about 7.0° and -1.5° respectively and the calculated values only 4.8° and 1°. The given and calculated angles at the completion of transition agreed somewhat better; the given α was 2.5° and the calculated α 2.0°, the given θ was 5 and the calculated was 4.0°. It is believed that the disparity in values at and below 100 kts is due to the fact that the lift loss due to jet interference was not considered. The jet interference lift

loss presented by Captain David Archino in AFIT Thesis GAM/AE/68-2 would indicate that the maximum lift loss would be in this velocity area. The difference in the angles of attack would appear to be small but this difference is significant in the derivative calculations. $\sin\alpha$ is important in both the derivative calculations and the conversion of the derivatives from one axis system to another. The maximum difference of α amounts to a change of $\sin\alpha$ of 31.6%. The slope of the drag curve also changes considerably and affects the value of X_w. A comparison of the values of α and θ is presented in Figs. 17 and 18.

There was no data with which to compare the performance of the nonaccelerating transition. It was learned in correspondence with Edwards AFB that the P-1127 stalled at about 130 kts and flew with angle of attack of 8° at 140 kts when the nozzles were fully to the rear. It is, therefore, felt that steady flight as calculated at about 160 kts with angle of attack of 6° is reasonably accurate. The variation of nozzle angle with speed is shown in Fig. 16. It must be noted that the variation is very much different from that of the accelerating transition.

Stability Derivatives

In the general discussion of all the derivatives, there are several possible reasons for error and variation between the different transitions. As has already been pointed out, a small error in angle of attack can cause a considerable error in the derivatives. It is also possible to have compressibility effects in the accelerating transition as the Mach number at the completion of the transition is about .31. One of the basic assumptions in the accelerating transition

was that the acceleration affect on the derivatives was negligible. In the comparison of the accelerating to nonaccelerating transition, there are two inherent differences which will cause variation in the derivatives. First immediately after hover, the nonaccelerating airfoils are assumed to be fully effective; whereas, the nonaccelerating airfoils are not effective until about 30 kts. In both cases there must certainly be some error. Certainly the angle of attack at which the accelerating airfoil is effective is very approximate. Also, in comparing the two transitions, although the airplane attitude is the same to the Earth axis, at no time are the velocity and angle of attack the same. To accurately compare the transitions, it would be necessary to solve the nonaccelerating transition for exactly the same flight conditions as the accelerating transition. Even with all the factors involved, the comparison of the given calculated derivatives and the accelerating and nonaccelerating derivatives is interesting. In most cases the derivatives are not greatly different.

$\underline{X}_u$. The comparison of the calculated X_u to that given by Hawker Siddeley shows very good agreement until the end of the transition as is shown in Fig. 19. The error of 16% at 200 kts is greatest and may be caused by compressibility.

The accelerating X_u increases in value until about 30 kts, when the wing becomes effective. As the affect of the induced drag increases the value of X_u decreases. The nonaccelerating X_u has a smaller value at the hover and immediately begins decreasing because the induced drag is assumed to be immediately present. The angle of attack during the accelerating transition never reaches the 6° of the

nonaccelerating transition, hence the accelerating X_u remains higher than the nonaccelerating. The X_u derivatives are presented in Fig. 27.

X_w. The agreement of the calculated X_w with that given is good from 50 kts to 125 kts. However after 125 kts, the two values diverge and the agreement is very poor. There are several possible reasons for this. First, if only the wing lift contribution were considered, X_w would agree well. However when the drag contribution is added (primarily the slope of the drag curve), X_w is reduced by about 50%. Added to this reduction is another 50% caused by the tail lift which acts opposite to the wing lift because of the negative value of the tail incidence and the still present downwash. It is very possible that the slope of the drag curve could be incorrect because of the approximate solution in Appendix A. This error in the slope of the curve would not affect C_D greatly but would very significantly affect X_w. The tail downwash was an approximation and cannot be considered very accurate. The comparison of the X_w values are shown in Fig. 20.

With reference to Fig. 28, the affect of assuming the nonaccelerating wing to be fully effective at a constant angle of attack of 6° and the accelerating wing becoming effective at about 30 kts may be seen to be similar to X_u. Once again there is some agreement in the values and the variation with velocity. These derivatives cannot be considered very accurate but the affect on the stability is slight as will be discussed later.

Z_u. This derivative decreases continually with speed as would be expected. Z_u is highly dependent on C_{LWB} and C_{LT}. The greatest difference between calculated and given values occurs around 100 kts which is also where the maximum tail downwash and minimum tail

effectiveness with angle of attack are assumed. As will be seen later in the M_w discussion, it is quite possible that the assumed maximum ϵ_0 is too small and this would cause Z_u to be too negative as is indicated in Fig. 21.

The Z_u values of the nonaccelerating transition are very close to those of the accelerating. The larger value for the accelerating transition and the small difference in slope is once more due to the difference in angle of attack and assumed effectiveness. Z_u for the hover is usually considered to be zero but the small negative value is caused by the thrust contribution. The accelerating and nonaccelerating values of Z_u are shown in Fig. 29.

$\underline{Z_w}$. The agreement of the calculated derivative is very good in this case. Little can be said about the comparison in Fig. 22.

The important points to be noted in Fig. 30 for the accelerating and nonaccelerating transitions are the nonzero hover value, the constantly decreasing Z_w with speed and the difference at low speed. The nonzero value at hover is once more a thrust contribution. The slope of the wing-body lift curve is the primary factor in the determination of value of Z_w and hence, when the wings of both transitions are effective, the values are very nearly the same.

$\underline{Z_{\dot{w}}}$. Hawker Siddeley gave no values for $Z_{\dot{w}}$ so no comparison could be made. Fig. 31 shows the comparison of the accelerating and nonaccelerating transitions. There is a large difference in the values of $Z_{\dot{w}}$ mostly because of the difference in the assumed tail downwash. The now usual difference is seen at low speed due to airfoil effectiveness. Between 50 and 110 kts the values are very nearly the same. Above 110 kts however, the accelerating tail downwash begins

decreasing and the nonaccelerating tail downwash remains constant until 150 kts. The accelerating Z_w begins decreasing before the nonaccelerating but both derivatives once more converge at the completion of transition.

Z_q. There are no comparison Hawker Siddeley values but the two transitions' values are shown in Fig. 32. The only difference in the derivatives is at low speed once more due to the airfoil effectiveness.

M_u. The derivatives of Fig. 23 are for the body axis centered at the wing-body aerodynamic center, hence there is no contribution from the wing-body lift. One would normally expect M_u to be negative because of the horizontal tail contribution to the derivative. However, for this VTOL configuration M_u remains positive at all times in the transition. When the tail is not effective, below 30 kts, the derivative is positive because of the thrust and drag contribution. As may be seen from Fig. 9, the increase of the cold jet thrust with speed is much larger than that of the hot jet causing a positive contribution to M_u. The P-1127 has a fairly high wing, therefore, the increase in drag with velocity causes a positive contribution. When the tail becomes effective at about 30 kts there is an abrupt rise in M_u. It should be remembered from Fig. 6 that, for the accelerating transition the zero-lift downwash and the $\partial\varepsilon/\partial\alpha$ were considered zero until the nozzle angle reached 60°. At a velocity of 30 kts, the angle of attack is -5°; the nozzle angle is 55°; the zero-lift downwash is 58% of its maximum value and the $\partial\varepsilon/\partial\alpha$ is 0.58. The tail lift vector is then directed down so that any increase speed causes a positive moment. As the speed increases the angle of attack is increasing more rapidly than the downwash thus M_u decreases until about 60 kts.

However, as the speed increases past 60 kts, the angle of attack does not increase as rapidly as the downwash and the tail ceases to respond to changes in the aircraft angle of attack thus M_u rapidly increases to a maximum value at 110 kts. The fact that the given maximum value is greater than that calculated would indicate that the maximum zero-lift downwash may indeed be greater than 10°. At the completion of the transition, the calculated tail incidence is negative which accounts for the fact that the calculated M_u levels off.

The values of M_u with the axes centered at the center of mass are in general smaller than those for the axes at the aerodynamic center. These smaller values are caused by the wing-body lift vector to the rear of the center of mass. In the comparison of the two transitions in Fig. 33, it is most important to remember that the angle of attack of the nonaccelerating transition is always a positive 6°. Because of this positive angle of attack, the wing-body lift keeps M_u low for the nonaccelerating transition. M_u becomes negative at very low speed because the zero-lift downwash is small but increases rapidly as the downwash approaches a maximum value.

M_w. This derivative is the most important derivative in the study of the longitudinal stability. As in non-VTOL aircraft, the value of M_w is primarily determined by the effectiveness of the tail to respond to changes in the aircraft angle of attack. The comparison of the calculated and given M_w is shown in Fig. 24. These derivatives show the P-1127 to be more unstable than it actually is because the wing-body contribution (not included) has a stabilizing influence. The calculated M_w is less than or equal to that given for all speeds. The lesser value of the calculated M_w from 50 to 110 kts is especially

interesting. This smaller value could be caused mostly by only one parameter, $\partial\varepsilon/\partial\alpha$. It would appear from Fig. 24 that the calculated effectiveness of the tail to angle of attack change is greater than it should be. This means that the estimated $\partial\varepsilon/\partial\alpha$ is not large enough. The linear variation assumption of $\partial\varepsilon/\partial\alpha$ with nozzle angle was obviously an over simplification and the $\partial\varepsilon/\partial\alpha$ must approach one more rapidly than estimated. Although not attempted, a second degree variation might prove more accurate. The estimation of ε_0 was also very approximate and would affect mostly the maximum value of M_w.

Fig. 34 shows the correct static stability derivatives for the two transitions. It may be seen that in either case the vehicle is very nearly neutrally stable or unstable for a good portion of the transition. The values of M_w are very nearly the same for most speeds, illustrating the dependence of the derivative on the treatment of the downwash rather than on aircraft flight attitude. The importance of the static stability derivative is illustrated by the fact that the dynamic stick fixed stability of the airplane follows very nearly the static stability.

$\underline{M_{\dot{w}}}$. The comparison of the calculated derivative with that given by Hawker Siddeley is shown in Fig. 25. The agreement here is not very good. $M_{\dot{w}}$ is primarily dependent on the value of $\partial\varepsilon/\partial\alpha$ which was allowed to become one at $\delta_j = 30^\circ$ or V = 110 kts. Allowing $\partial\varepsilon/\partial\alpha$ to become one makes $M_{\dot{w}}$ zero. As in M_w this apparently was an over simplification but it was the only estimate available. Only the tail contribution to the derivative was considered but it is believed that any wing or body contribution would not appreciably change the agreement.

Because of the disagreement with the Hawker Siddeley derivatives, very little faith is put in the accuracy of the derivatives calculated for the two transitions as shown in Fig. 35. The one important thing to note about $M_{\dot{w}}$ is that it is stabilizing or neutral in all cases. As in the case of X_w, $M_{\dot{w}}$ does not affect the stability much, and hence need not be estimated accurately.

M_q. The equation for M_q is the conventional tail contribution to the derivative. The agreement with the Hawker Siddeley derivative shown in Fig. 26 is very good.

The calculated derivative for the two transitions is believed to be quite reliable. For both transitions M_q is zero at the hover. This zero approximation is definitely not correct because there will be a negative contribution from the air trapped in the intake duct and a negative contribution from the momentum vector on the intake. Both of the above contributions would be small, however.

Stability of the Accelerating Transition

The stability of the accelerating transition may be separated into two velocity areas; the stability below 30 kts airspeed when the angle of attack is such that the airfoils are ineffective and the stability above 30 kts. The stability roots at less than and more than 30 kts airspeed are shown in Figs. 37 and 38 respectively. The negative half of the imaginary axis has not been shown in either figure.

The stability at airspeed less than 30 kts is characterized by three unstable roots, two oscillatory and one real. The one negative real root is unimportant. In hovering flight, the airplane is very

nearly neutrally stable. The unstable real root causes a time to double amplitude of 6.5 sec which is well within the ability of a pilot to hold. The instability is accentuated by the second oscillatory unstable mode which has a time to double amplitude of 8 sec. I. A. Fisher has indicated that the P-1127 is easily controlled in hovering flight (Ref 8). As the airspeed increased to 30 kts the one positive real root increases causing a greater instability. At about 30 kts the calculated roots would indicate a time to double amplitude of 1.65 sec. If this root is really this large, the pilot would be working exceedingly hard to control the airplane. However, the motion is nonoscillatory which should help pilot ease of control. It is interesting to note that Fisher has made the same division in speed regimes, above and below 30 kts, when discussing the stability. However, he indicates that below 30 kts the airplane is manuevered quite easily which puts some doubt on the validity of the calculated root (Ref 8:4).

At 30 kts the calculated stability of the airplane changes instantaneously because of the assumed instantaneous effectiveness of the airfoils. Undoubtedly, the change occurs somewhat gradually as the angle of attack increases. However, at 30 kts the angle of attack is changing about 3 degrees per second. The wing will probably pass through the nonlinear portion of the lift curve in this 3 degrees or less. To the pilot then, this transition will seem almost instantaneous and the instantaneous assumption of the calculation should be quite valid. It should also be noted that although the stability changes are very large, the controls necessary for trim do not change radically.

It may be seen from Fig. 38 that the airplane becomes increasingly unstable as the airspeed increases to about 110 kts. As previously noted in the discussion of M_w, the static stability follows the same trend. The stability is at its worst at 110 kts when the time to double amplitude is 2.5 sec. The period of the oscillation is 21.8 sec so the oscillation will double its amplitude in only 11.5% of the period. This instability would make the airplane difficult but not impossible to fly. The pilot would be moving the controls continually to keep up with the airplane. Fisher has noted that the P-1127 is difficult to fly accurately from 30 - 100 kts and that the pilot does indeed have many control reversals (Ref 8:4).

As the airplane accelerates past 110 kts, it rapidly approaches stable flight becoming completely stable at about 135 kts. After the airplane becomes stable the roots produce the normal short period and phugoid modes. At the completion of the transition the phugoid mode has a period of about 55 sec with a time to half amplitude of 23 sec. The short period mode has a period of about 2 secs and a time to half amplitude of 0.7 sec.

Stability of the Nonaccelerating Transition

The stability roots for the nonaccelerating transition vary considerably as the speed increases. For this reason the discussion of the stability has been divided into four speed areas, 0 - 25 kts, 25 - 90 kts, 90 - 125 kts and 125+ kts. The presentation of the roots of the characteristic equation for the four areas is in Figs. 39-42.

The stability in hovering flight is almost identical to that of the accelerating transition the only difference being the thrust and

intake air contributions. As the airspeed is increased the airplane becomes increasingly unstable to about 25 kts. Unlike the accelerating transition, the airfoils are effective hence the airplane does not become as unstable as in the accelerating case. The time to double amplitude at 25 kts is 2.5 sec.

At about 25 kts the dynamic pressure is large enough to cause the aerodynamic contributions to reverse the trend and the airplane becomes more stable as the speed increases. The roots appear to be converging to the expected phugoid and short period modes. However as the airspeed approaches 90 kts the tail downwash is rapidly increasing and the static stability is decreasing.

The most unstable flight in the nonaccelerating transition occurs from 90 - 125 kts. As may be seen from a comparison of Figs. 6 and 7 the nozzle remains rotated down for a longer span of airspeed in the nonaccelerating transition. This causes a maximum downwash over a longer period and more importantly, causes a larger downwash at a higher airspeed. From Fig. 34, it may be seen that the airplane in a nonaccelerating transition is more statically unstable over a longer span of airspeed than in an accelerating transition. The dynamic stability produces the same result. The maximum instability at 125 kts results in a time to double amplitude of about 1.5 sec. Unfortunately, the P-1127 is seldom flown at steady airspeed in this unstable regime so there are no comparative values to validate the results. However, it is interesting to note that the airplane is flown by the accelerating transition because of the increased stability which has been indicated by the calculated results.

The stability of the nonaccelerating P-1127 steadily increases after 125 kts and becomes completely stable at about 160 kts. At the completion of the transition at about 165 kts, the conventional phugoid and short period modes have been produced with times to half amplitude and periods almost identical to those at the completion of the accelerating transition.

Primary Conclusions

The validity of the results has been generally supported by the agreement of the derivatives and the stability with that of the actual airplane. It is felt that the assumption that the airfoils of the nonaccelerating transition are immediately effective causes little error because of the small difference in the stability at low speeds of the nonaccelerating and accelerating transitions. As previously stated the assumption of instantaneous boundary layer attachment should cause little error because of the rapid rate of angle of attack change. A probable error in the estimation of the airfoil effectiveness is the angle of attack at which the boundary layer attaches. This angle was estimated from experimental airfoil section data in which the stall was measured as the airfoil went from unstalled to stalled flight. However, the accelerating airfoil is flying from a stalled to an unstalled flight condition. In general the difference in the direction of the transition causes the stalled airfoil to unstall at a higher angle of attack than the angle at which the unstalled airfoil stalls. Once again because of the rapid acceleration, this error is believed to be small.

The greatest error in the study is obviously in the linear downwash assumption. The value of the maximum downwash appears to be reasonably close to the actual value. However, it is believed that the zero-lift downwash is greater at lower speeds than that estimated. It is also doubtful that $\partial\varepsilon/\partial\alpha$ actually reaches a value of one. When more wind tunnel tests have been performed, a suitable parameter based on nozzle angle, V_∞/V_j, wing planform, and tail distance and height may be found. The only reasonably accurate method of obtaining downwash information now is by powered-model wind tunnel tests.

The lift loss and wing moment from jet interference should not be neglected. This lift loss occurs in the speed area of the critical stability and may contribute appreciably to the stability derivatives.

Because of the disagreement of the X_w and $M_{\dot{w}}$ derivatives, the affect of X_w, $M_{\dot{w}}$ and $Z_{\dot{w}}$ on the stability was investigated. Completely neglecting the derivatives separately and collectively had negligible affect on the stability in hovering flight. Neglecting only X_w had a negligible affect throughout the transition. The difference in the time to double amplitude at 110 kts was less than .01 sec. $Z_{\dot{w}}$ and $M_{\dot{w}}$ are interdependent and were considered to be zero together. Neglecting $Z_{\dot{w}}$ and $M_{\dot{w}}$ reduced the stability at all speeds. The greatest difference was at the completion of the transition when the time to half amplitude of the short period was increased by .09 sec. At 125 kts the time to double amplitude was decreased by only .06 sec. Assuming the worst possibility and neglecting all three derivatives collectively also resulted in reduced stability at all speeds. In the area of critical stability at about 100 kts, the time to double amplitude was reduced

by .08 sec. At the completion of the transition the times to half amplitude for the phugoid and the short period modes were increased by 1.3 sec and .11 sec respectively. It was concluded from this error analysis that $X_{\dot{w}}$, $Z_{\dot{w}}$ and $M_{\dot{w}}$ need not be accurately estimated. This conclusion further indicated the validity of the calculated stability.

Recommendations

The study of the longitudinal stability should be continued with a concentration on the transition of the airfoils from stalled to unstalled flight and a better estimation of the downwash characteristics. The lift loss and wing moment from the jet interference should be included.

The lateral stability of the vectored thrust VTOL needs to be more fully understood. I. A. Fisher has indicated that the P-1127 is laterally unstable at low speeds (Ref 8:4).

The programs of Appendices B and C with slight modifications could be used to obtain optimum design configurations for a vectored thrust VTOL. The variation of such parameters as the intake height, center of mass position, and engine position should provide very interesting changes in the stability.

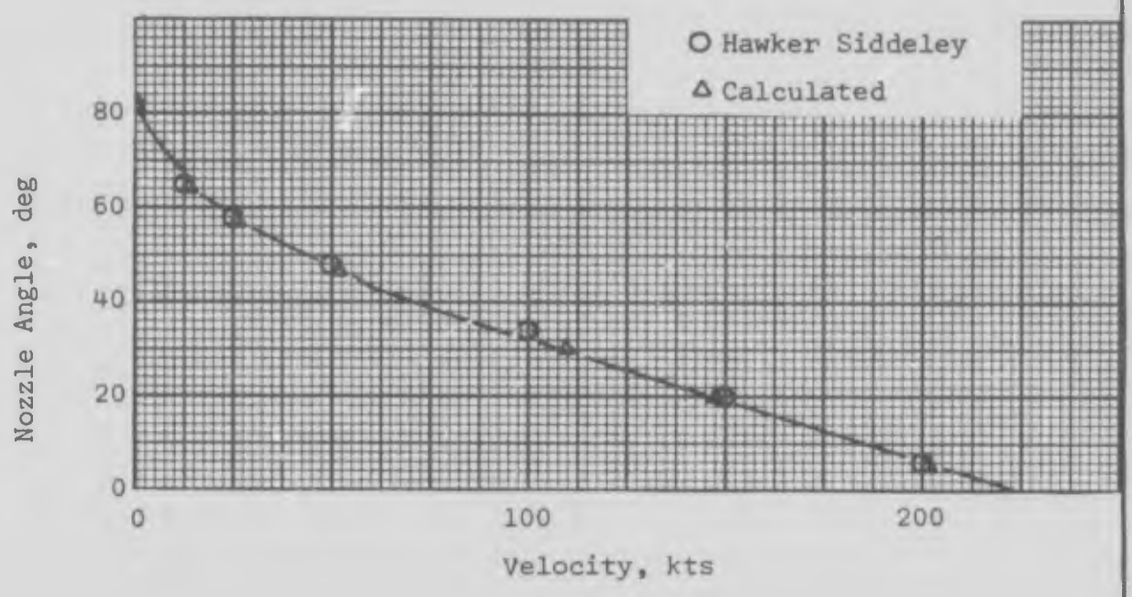

Fig. 15 Nozzle Angle (Accelerating Transition)

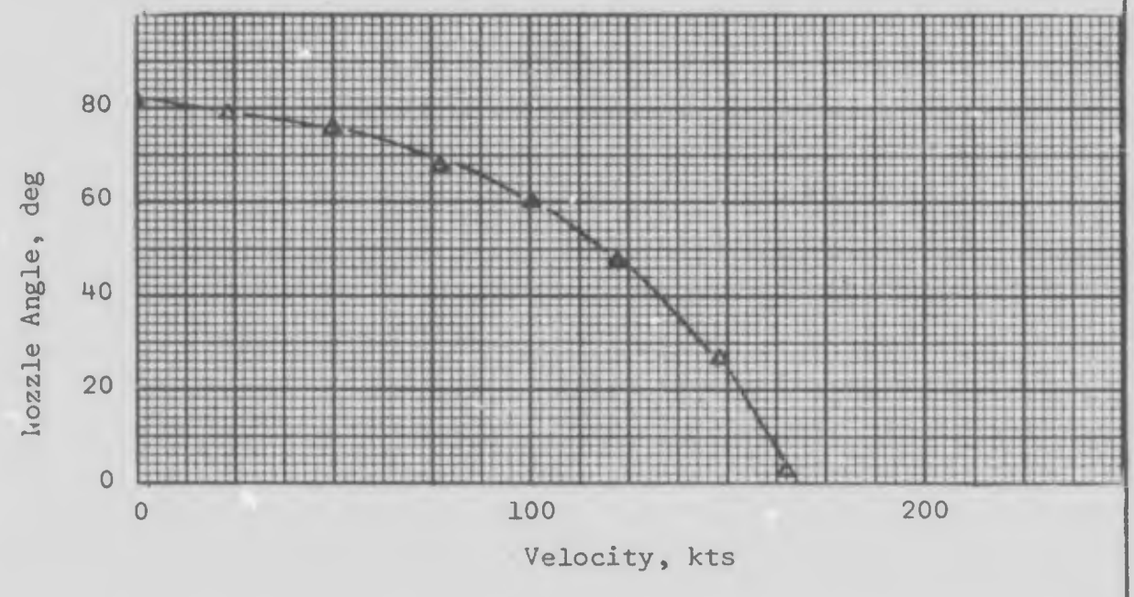

Fig. 16 Nozzle Angle (Nonaccelerating Transition)

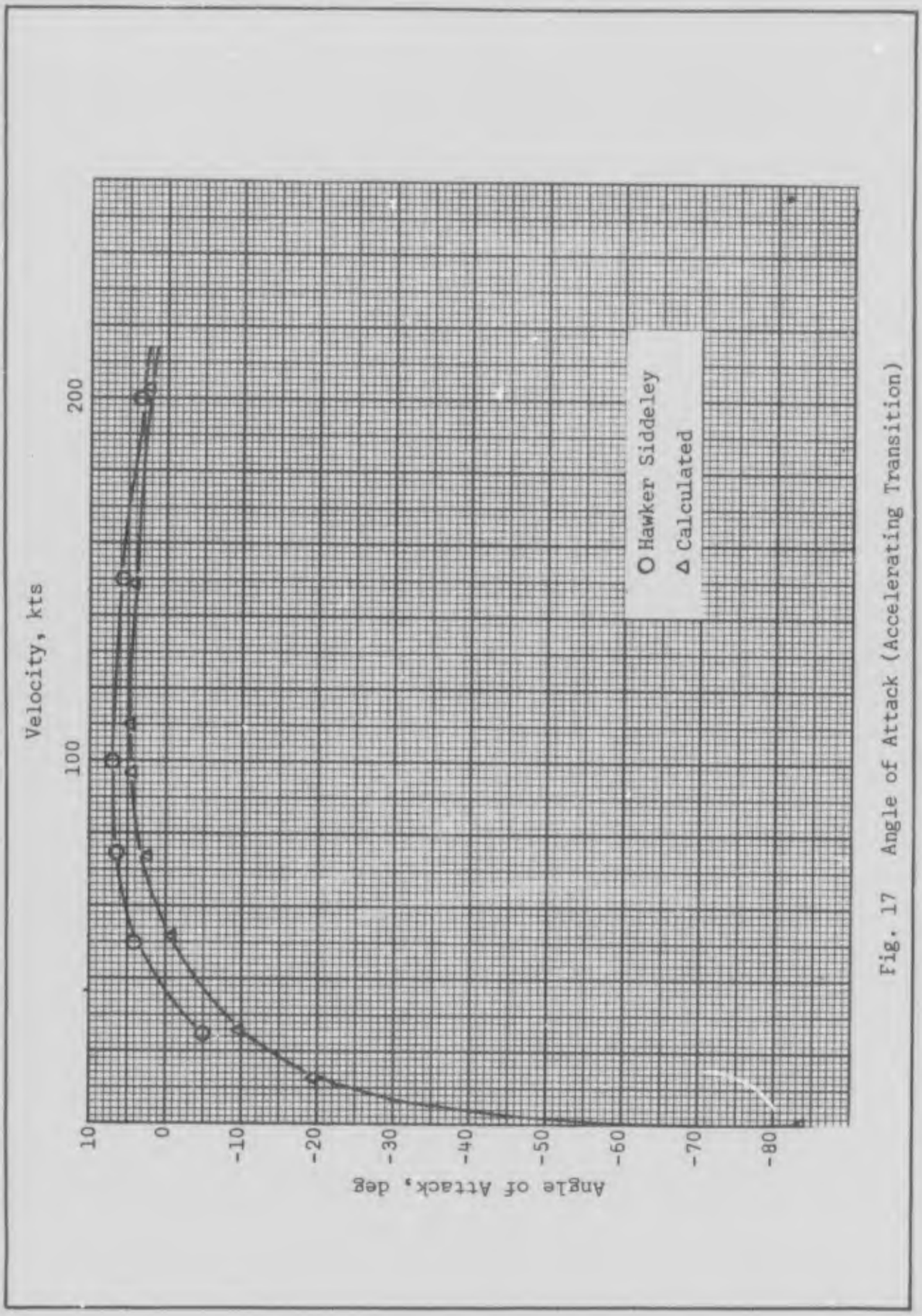

Fig. 17 Angle of Attack (Accelerating Transition)

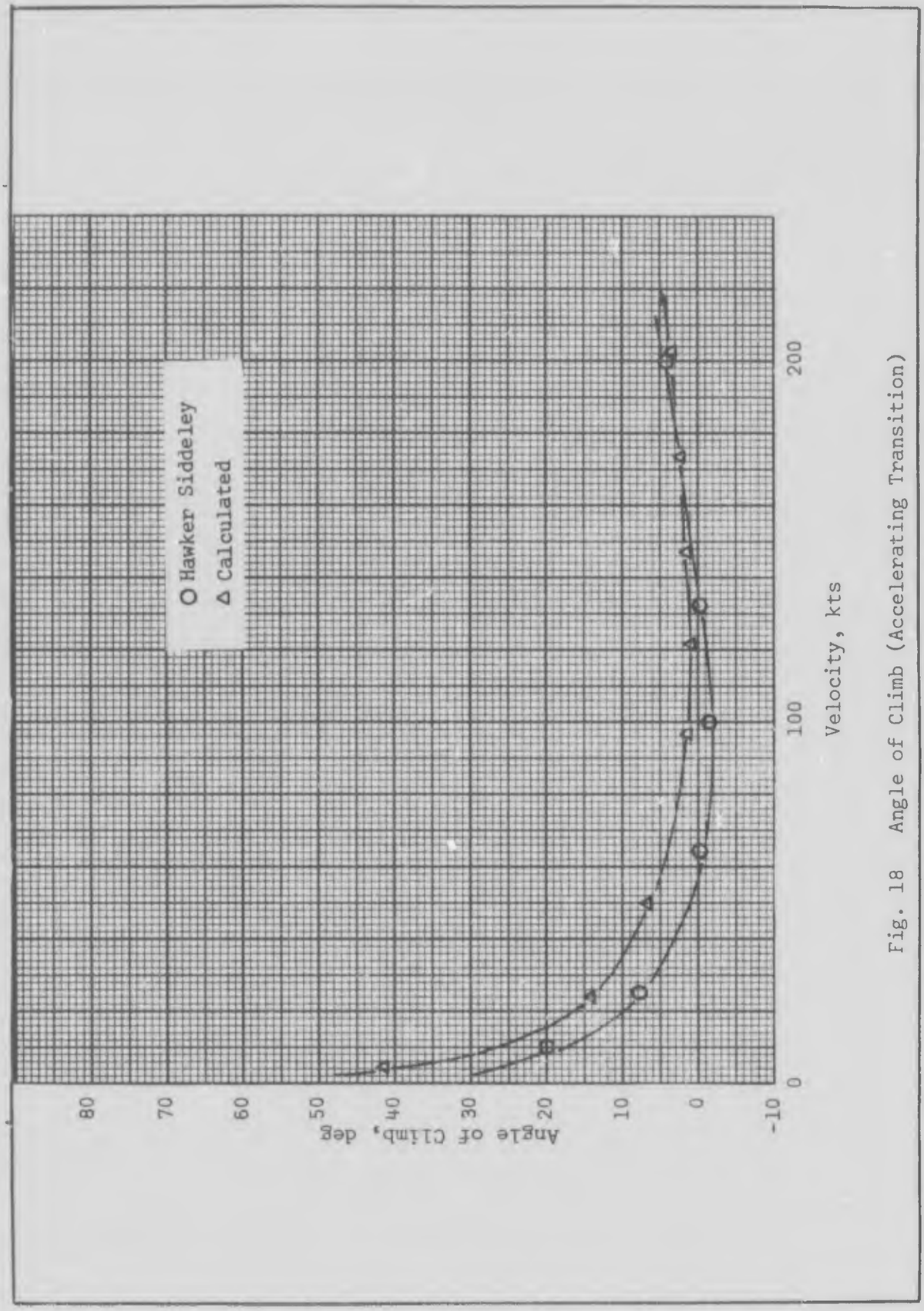

Fig. 18 Angle of Climb (Accelerating Transition)

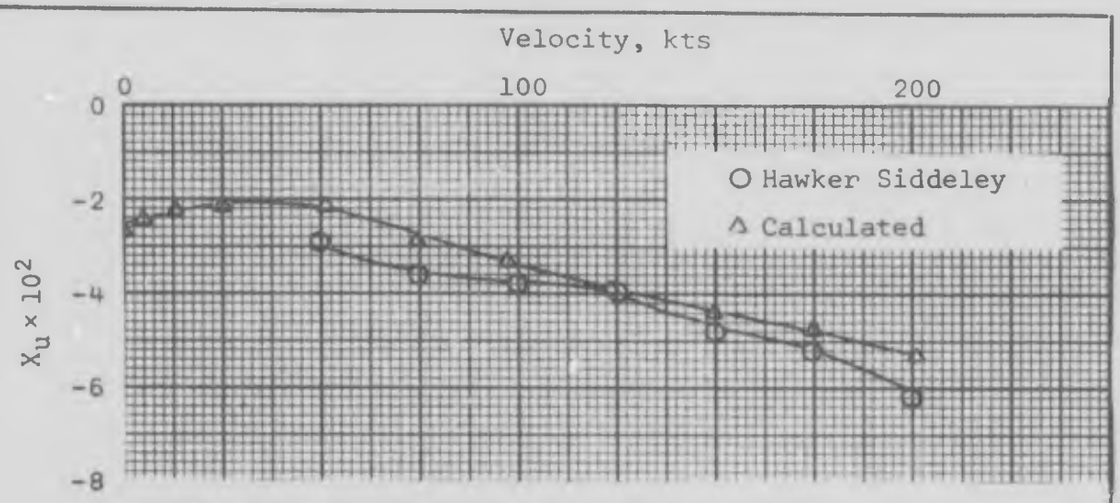

Fig. 19 X_u Comparison with Hawker Siddeley Derivative

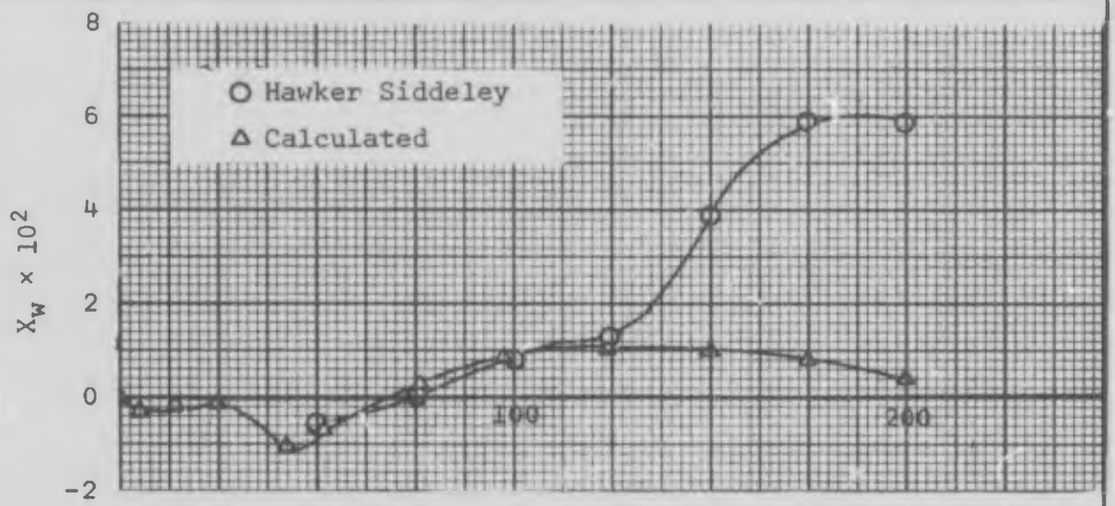

Fig. 20. X_w Comparison with Hawker-Siddeley Derivative

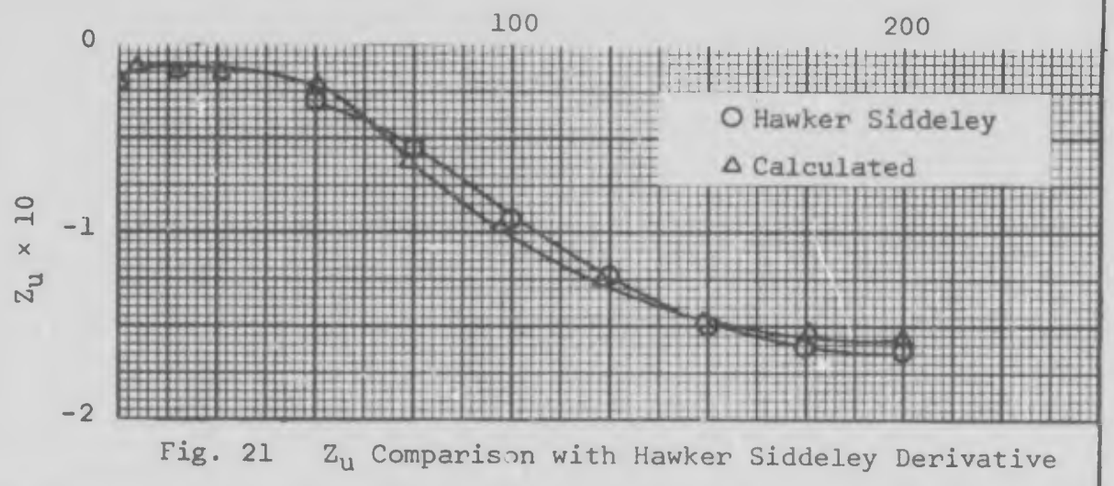

Fig. 21 Z_u Comparison with Hawker Siddeley Derivative

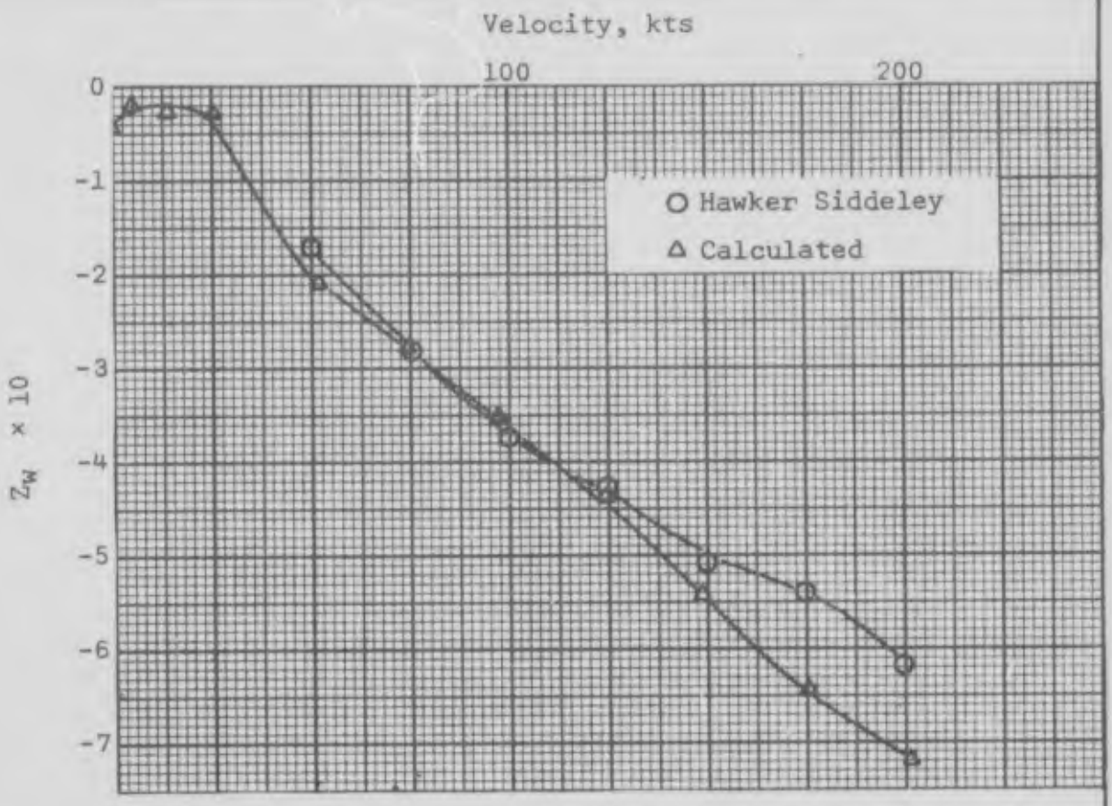

Fig. 22 Z_w Comparison with Hawker Siddeley Derivative

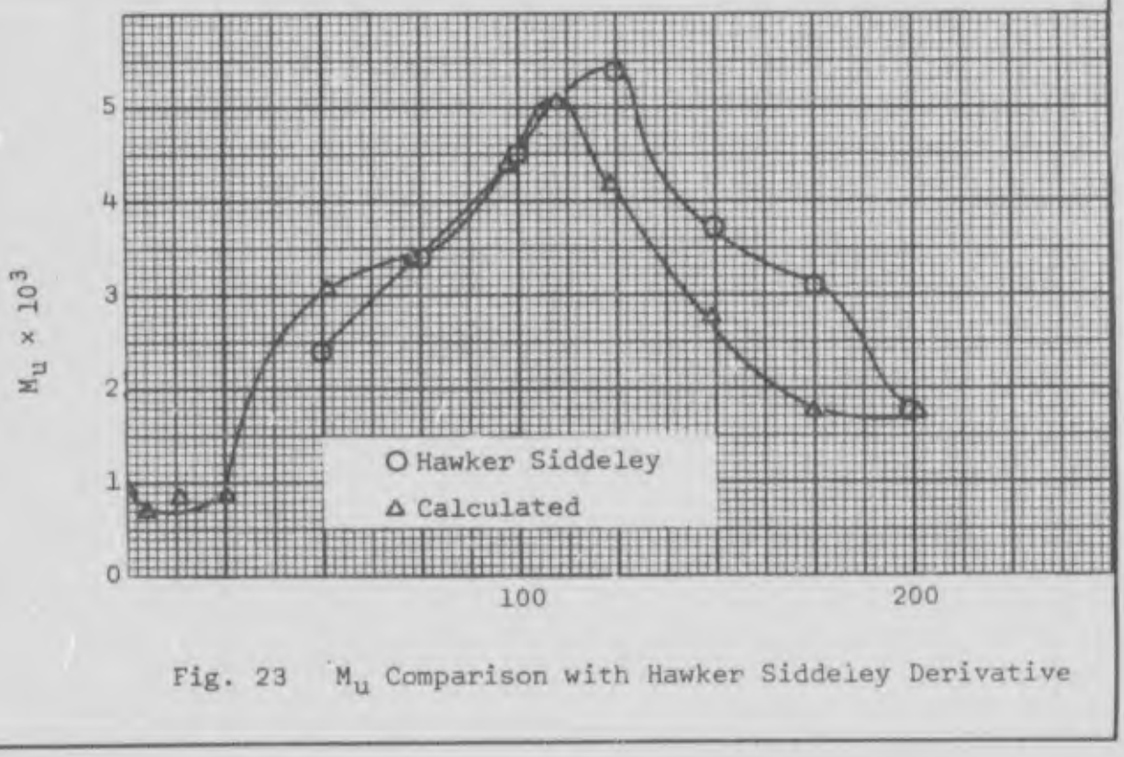

Fig. 23 M_u Comparison with Hawker Siddeley Derivative

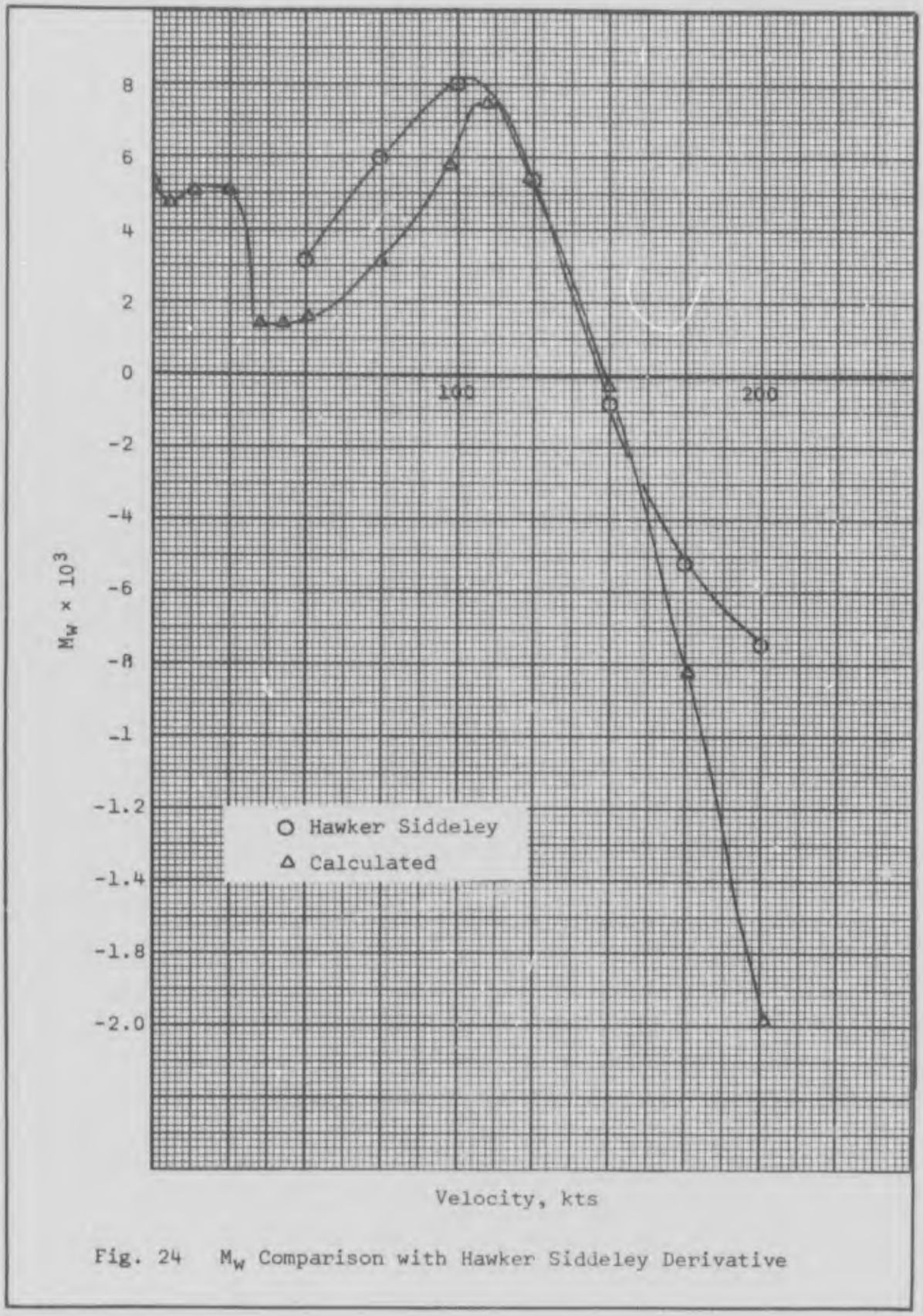

Fig. 24 M_w Comparison with Hawker Siddeley Derivative

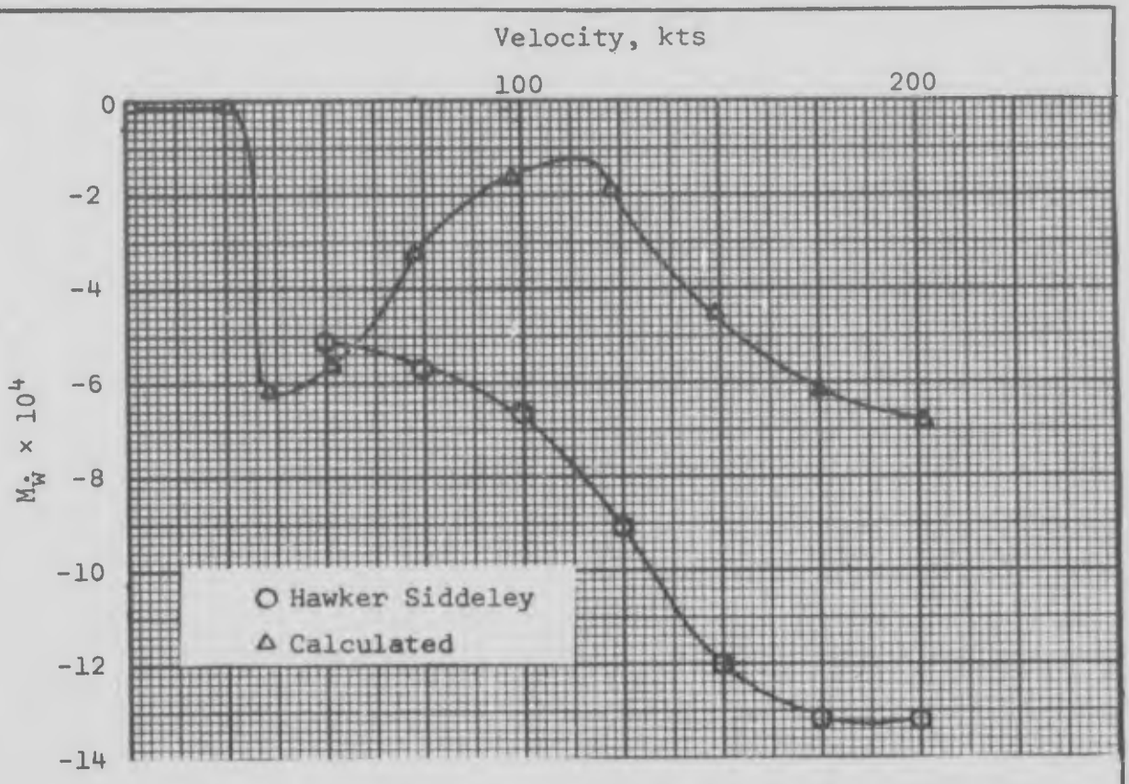

Fig. 25 $M_{\dot{w}}$ Comparison with Hawker Siddeley Derivative

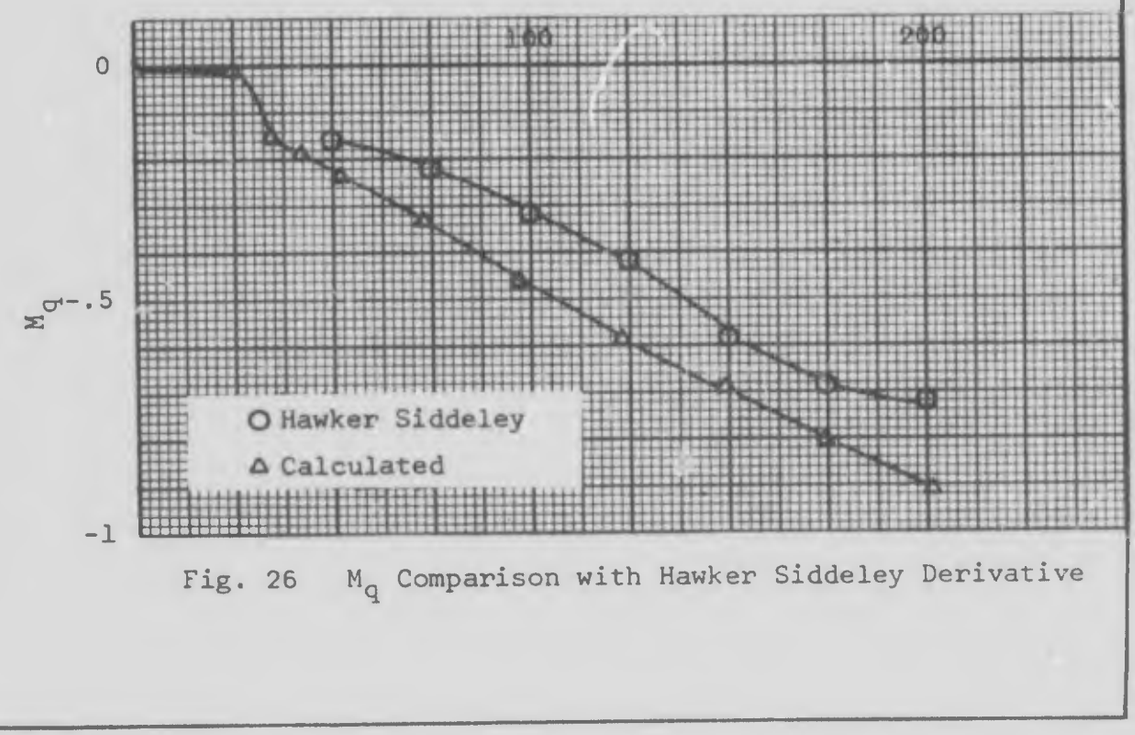

Fig. 26 M_q Comparison with Hawker Siddeley Derivative

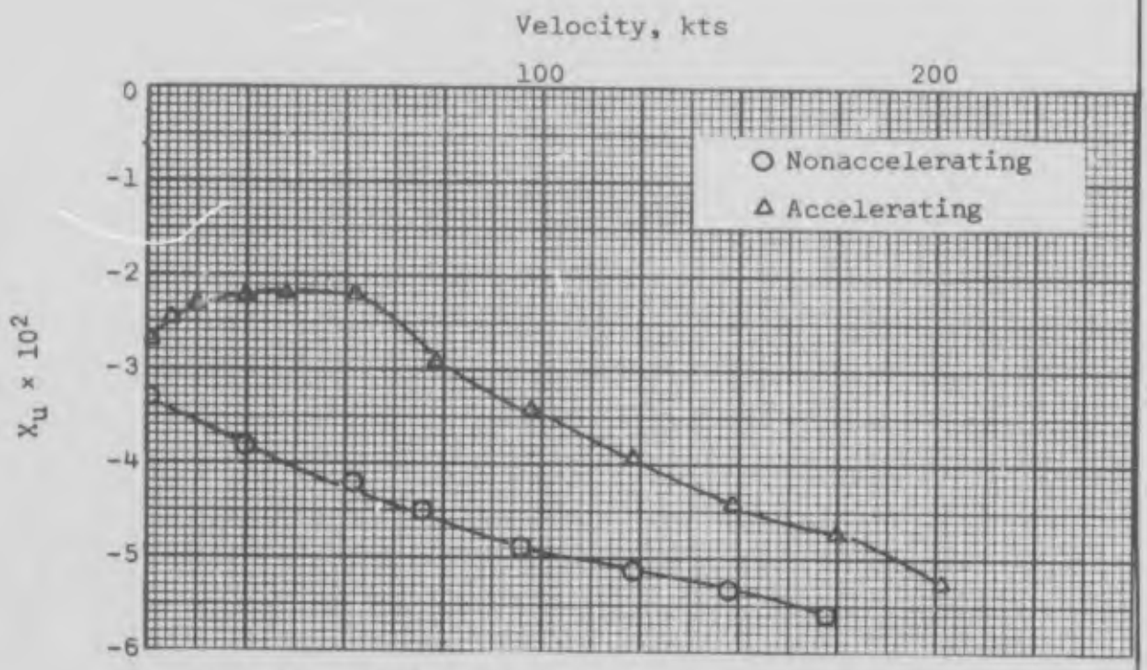

Fig. 27 X_u for Moment Reference at the Center of Mass

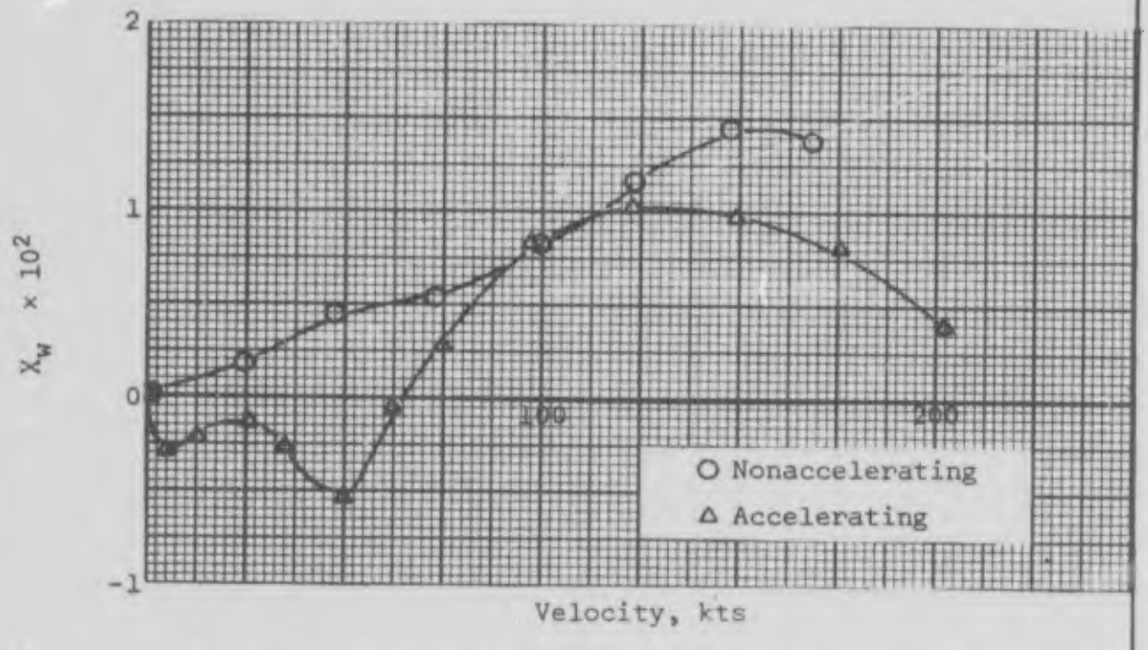

Fig. 28 X_w for Moment Reference at the Center of Mass

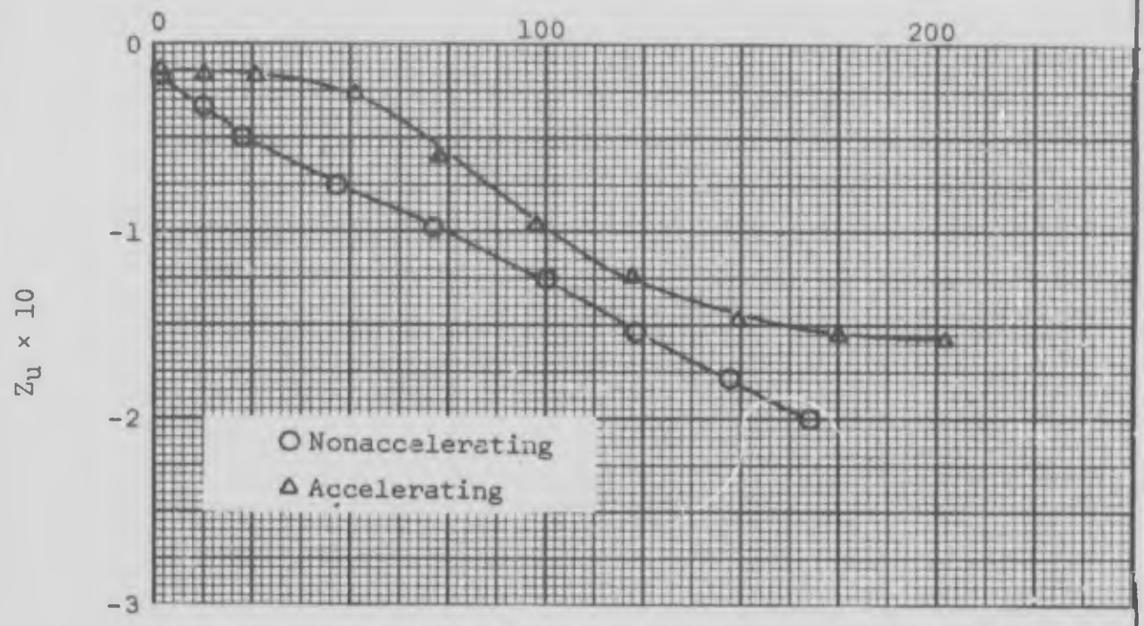

Fig. 29 Z_u with Moment Reference at the Center of Mass

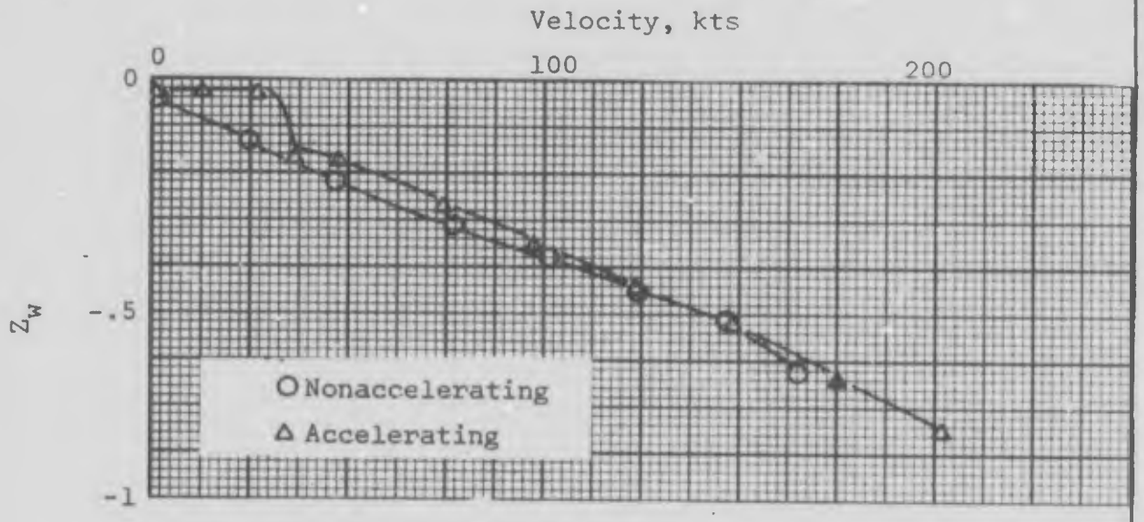

Fig. 30 Z_w with Moment Reference at the Center of Mass

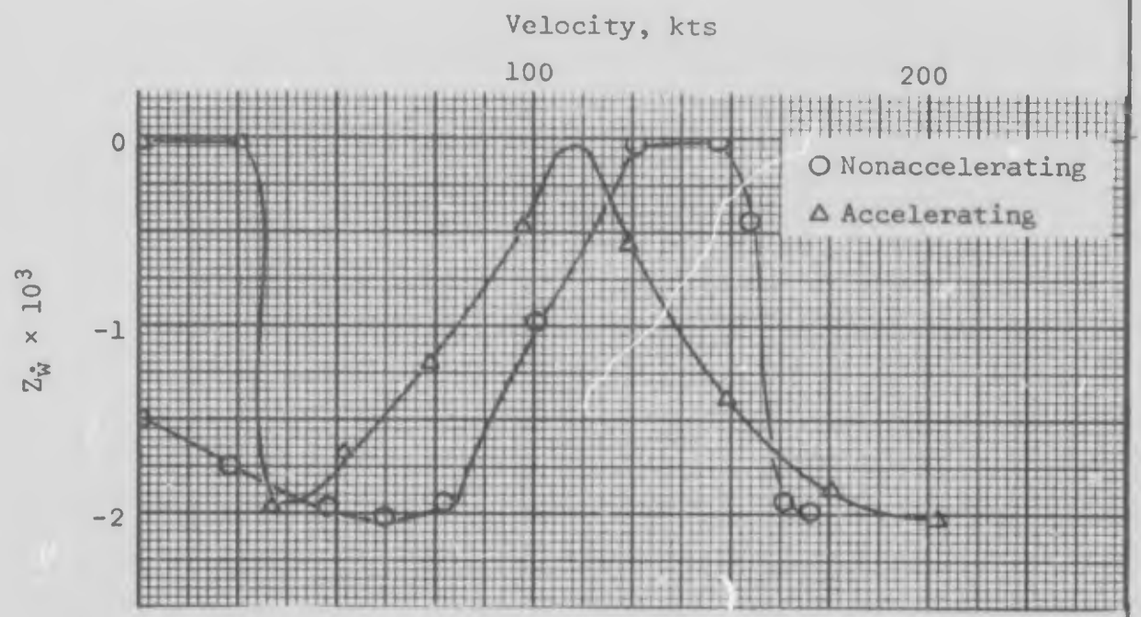

Fig. 31 $Z_{\dot{w}}$ with Moment Reference at the Center of Mass

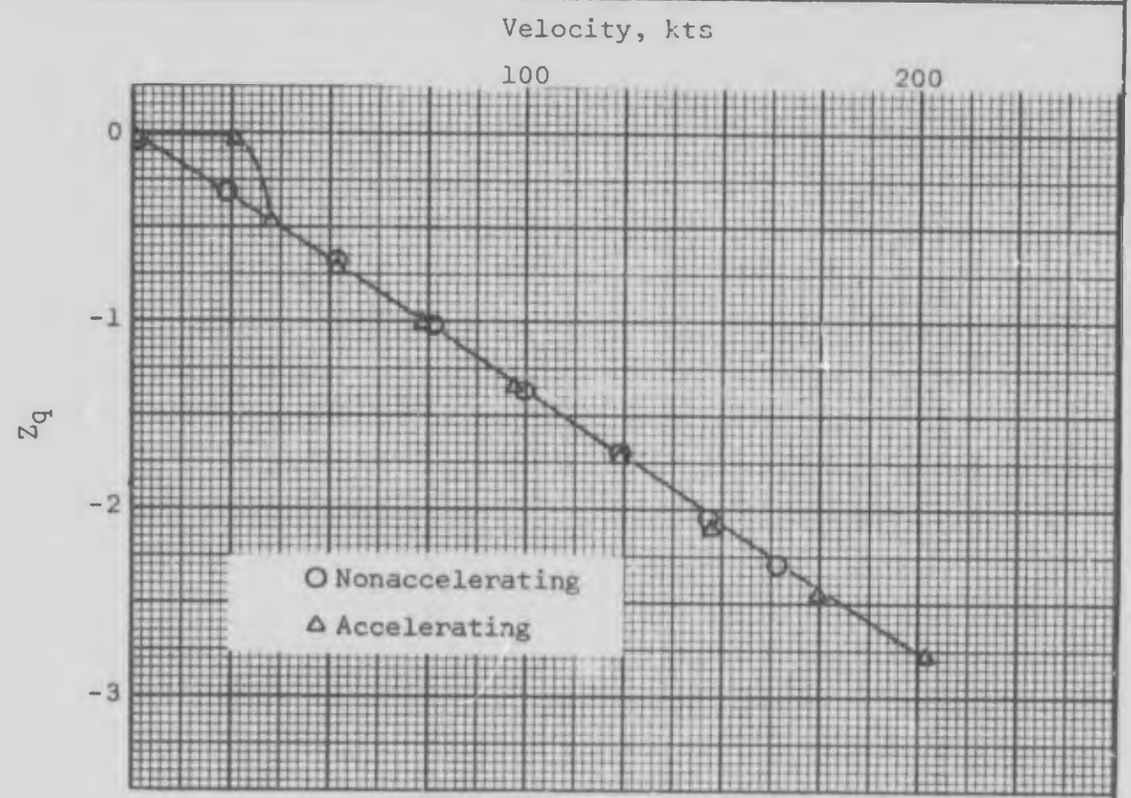

Fig. 32 Z_q with Moment Reference at the Center of Mass

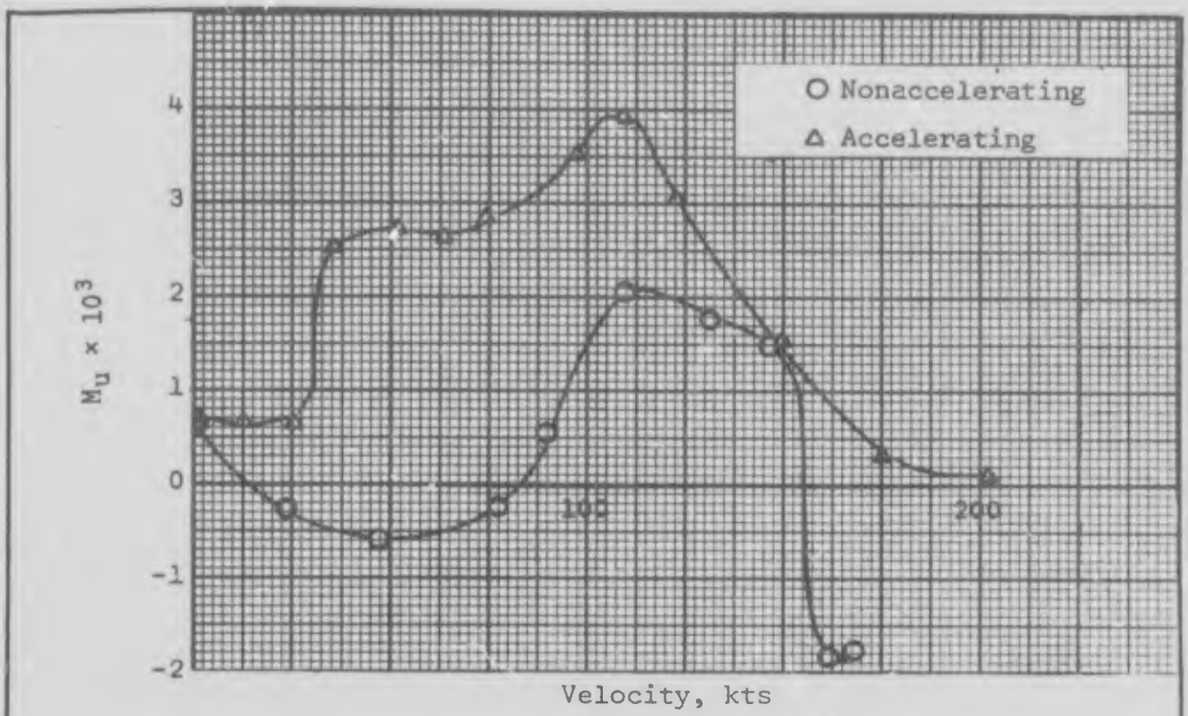

Fig. 33 M_u with Moment Reference at the Center of Mass

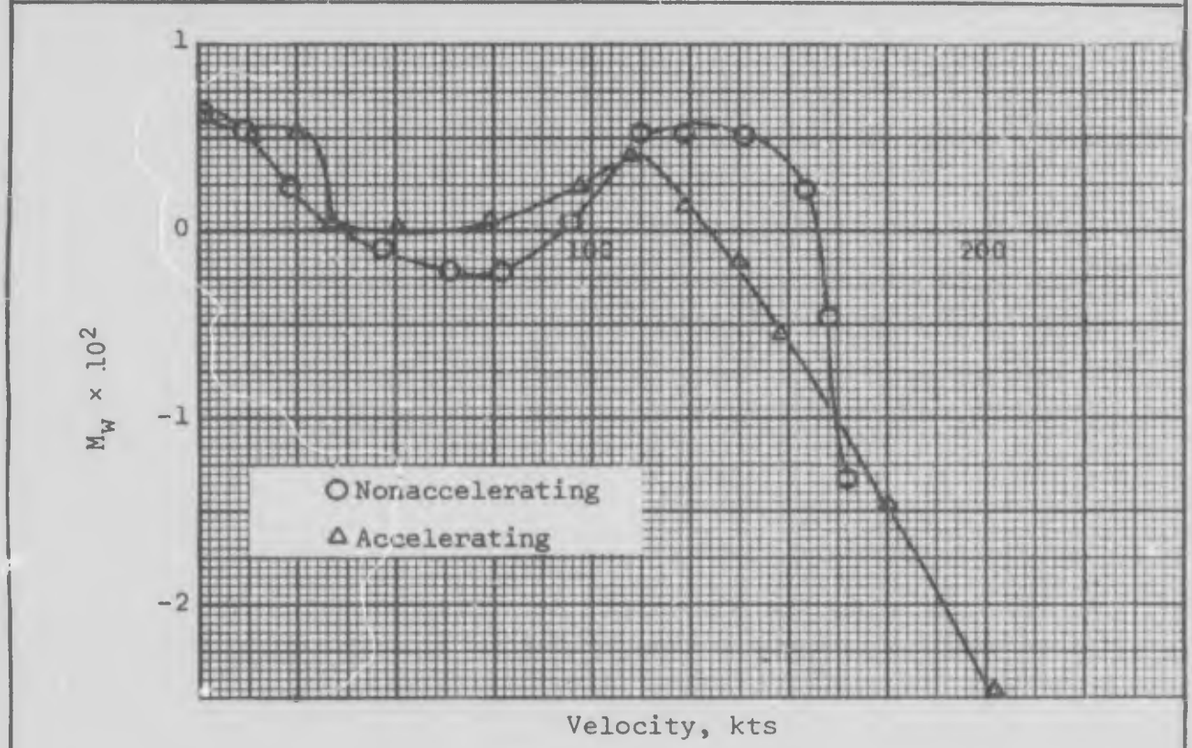

Fig. 34 M_w with Moment Reference at the Center of Mass

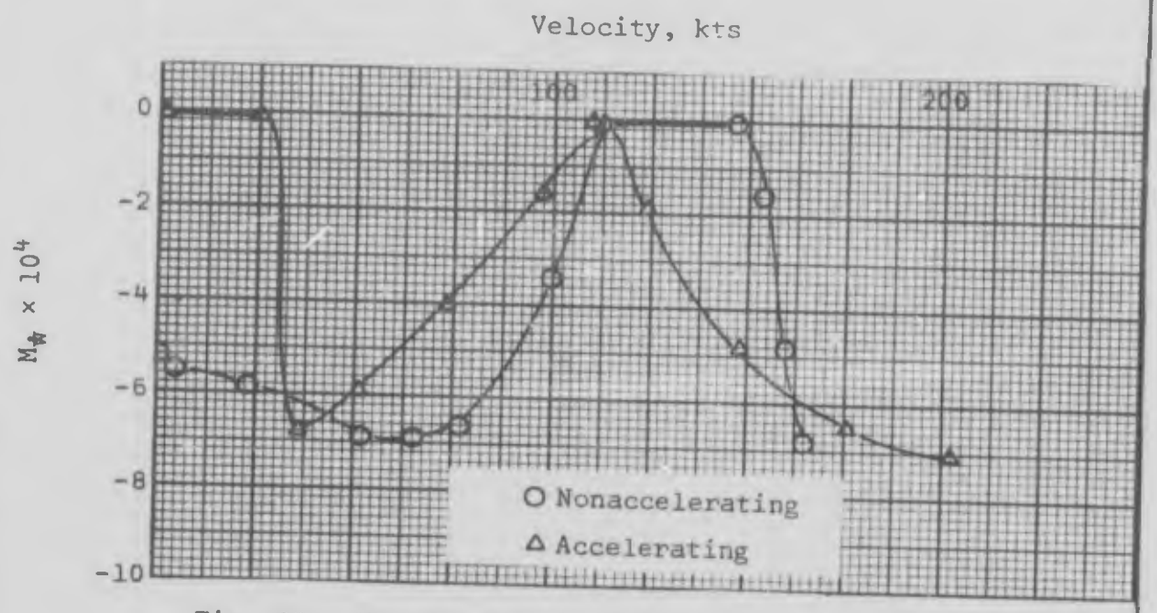

Fig. 35 $M_{\dot{w}}$ with Moment Reference at the Center of Mass

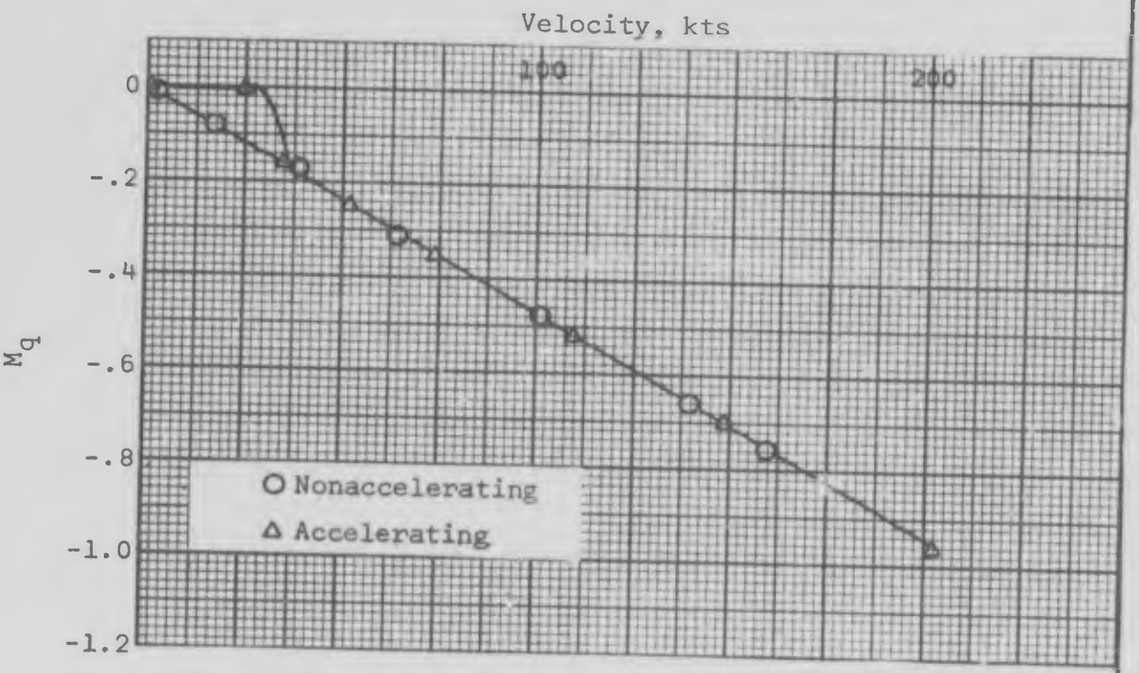

Fig. 36 M_q with Moment Reference at the Center of Mass

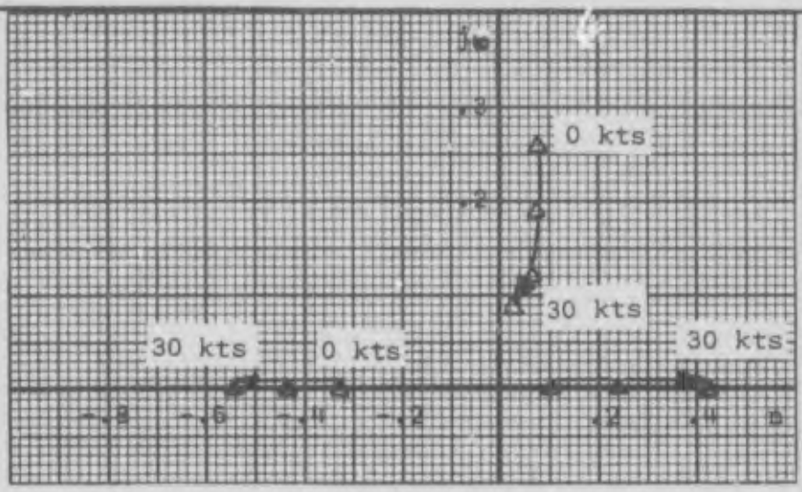

Fig. 37 Stability Roots for the Accelerating Transition (0-30 kts)

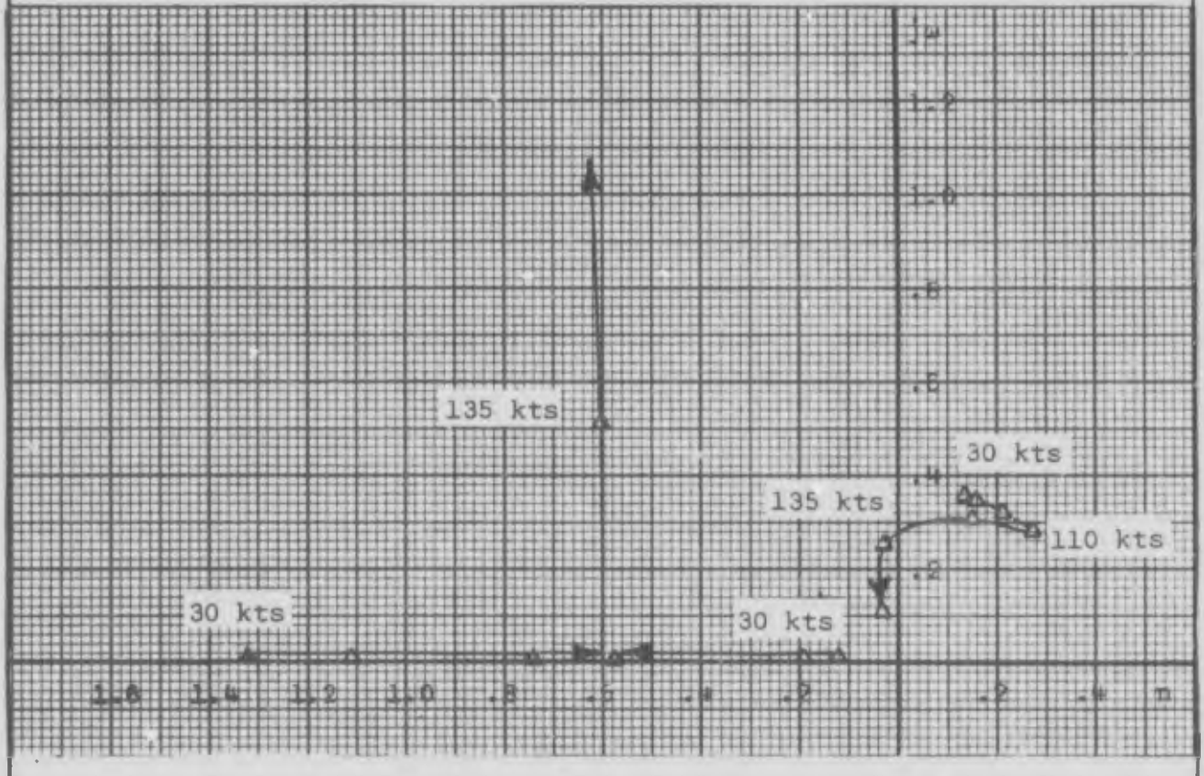

Fig. 38 Stability Roots for the Accelerating Transition (30 kts)

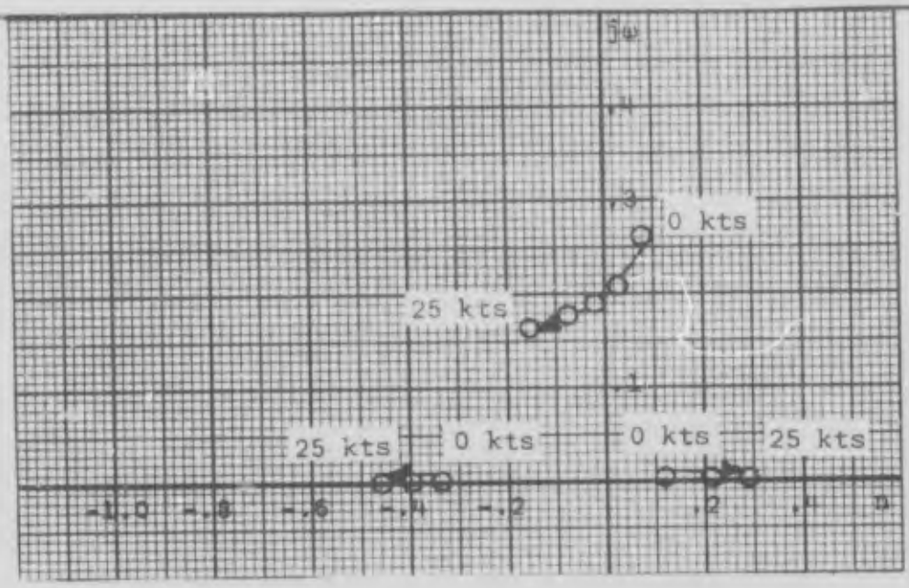

Fig. 39 Stability Roots for the Nonaccelerating Transition (0-25 kts)

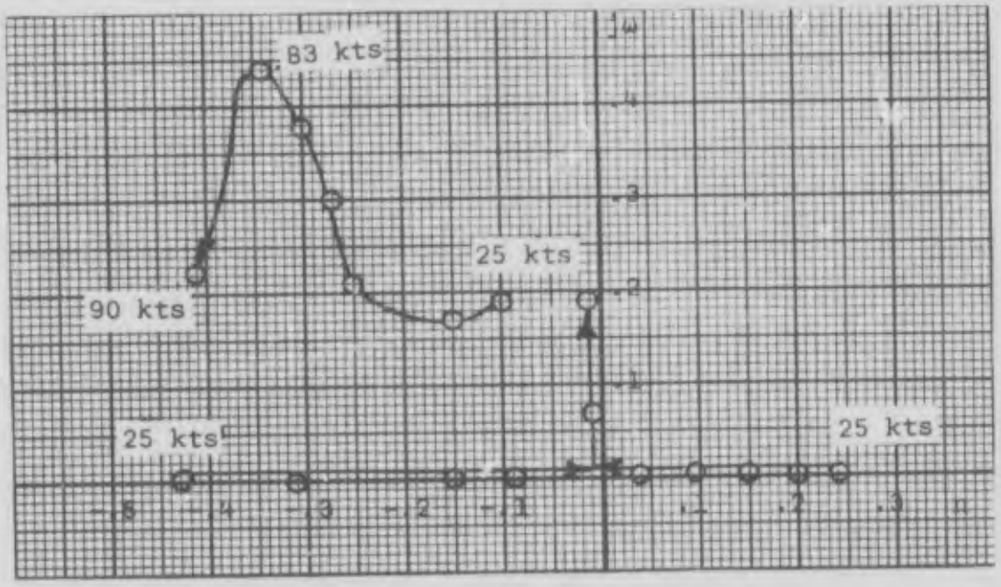

Fig. 40 Stability Roots for the Nonaccelerating Transition (25-90 kts

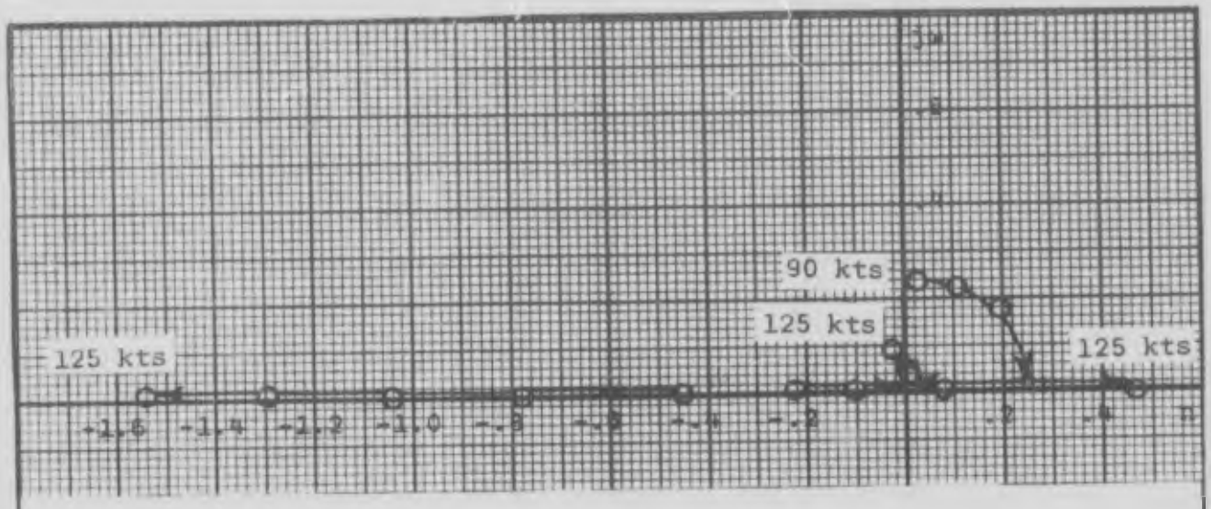

Fig. 41 Stability Roots for the Nonaccelerating Transition (90-125 kts)

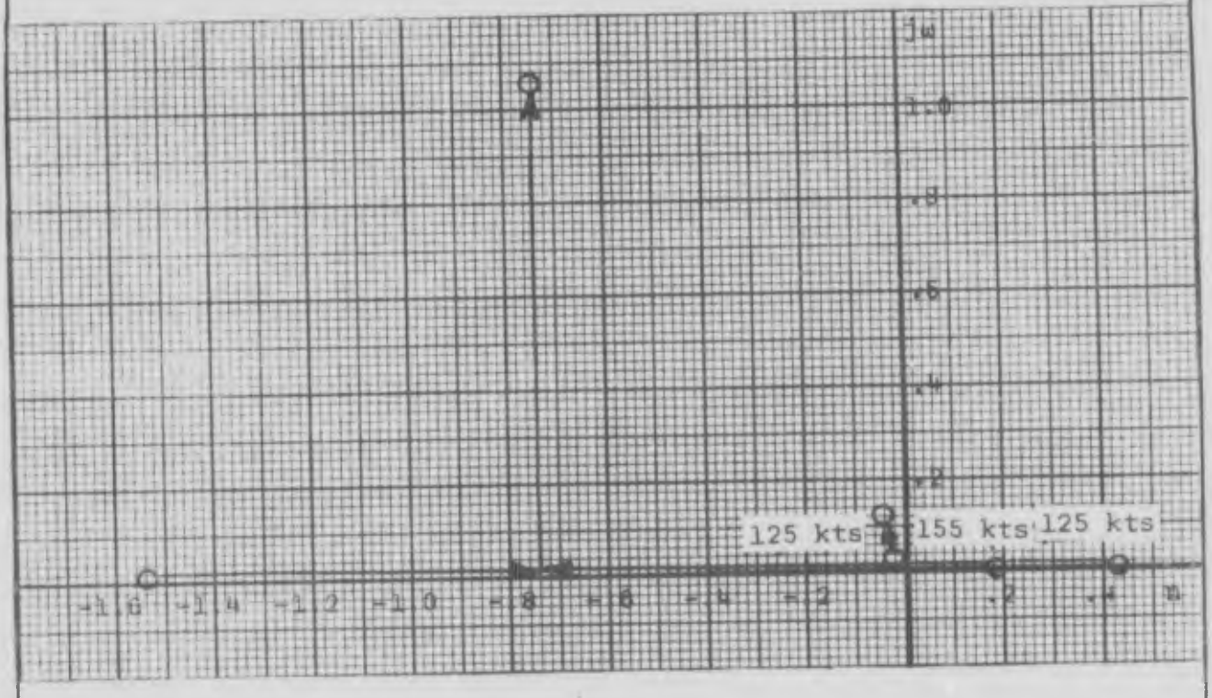

Fig. 42 Stability Roots for the Nonaccelerating Transition (125+ kts)

Bibliography

1. Kestrel Evaluation Squadron. Kestrel Evaluation Trials. West Raynham, Fakenham, Norfolk, United Kingdom, March 1966.

2. Hawker Siddeley Aviation Limited. Equations of Motion of the Hawker P-1127 During VTOL Manoeuvres. P.O.N. No. 614. Kingston-Upon-Thames, United Kingdom, October 1962.

3. Abbott, Ira H., Albert E. von Doenhoff, and Louis S. Stivers, Jr. Summary of Airfoil Data. NACA Report 824. Washington: National Advisory Committee for Aeronautics, 1945.

4. Etkin, Bernard. Dynamics of Flight. New York: John Wiley and Sons, Inc., 1959.

5. Vogler, Raymond D. and Richard E. Kuhn. Longitudinal and Lateral Stability Characteristics of Two Four-Jet VTOL Models in the Transition Range. NASA Technical Memorandum X-1092. Washington: National Aeronautics and Space Administration, May 1965.

6. Seckel, Edward. Stability and Control of Airplanes and Helicopters. New York: Academic Press Inc., 1964.

7. Babister, A.W. Aircraft Stability and Control. New York: Pergamon Press, 1961.

8. Fisher, I.A. Testing the Kestrel. Agard Report 518. Paris: Advisory Group for Aerospace Research and Development, North Atlantic Treaty Organization, October 1965.

9. Air Force Flight Dynamics Laboratory. USAF Stability and Control Datcom. Wright-Patterson AFB, Ohio, November 1965.

Appendix A

Calculation of the Aerodynamic Coefficients

The aerodynamic coefficients were calculated using the USAF Stability and Control Datcom and the values compared with the 65-009 airfoil of Reference 3 where possible. The P-1127 airfoils were known from Fig. 2 and it was known that the airfoils were symmetrical. Although the wing was not of constant thickness, to eliminate the need for integration an average thickness of 8% was used for the entire wing.

Datcom Reference

Lift Coefficient of the Wing-Body with Flaps Up

$$c_{l\alpha} = 6.28 + 4.7(t/c)[1+.00375\phi_{TE}] \text{ (per rad)} \qquad 4.1.1.2\text{-a}$$

$$= 6.60$$

$c_{l\alpha}$ of 65-009 = 6.50

$$a_{WB} = (C_{L\alpha})_{WB} = [K_N+K_{W(B)}+K_{B(W)}] (C_{L\alpha})_e \frac{S_e}{S_w} \qquad 4.3.1.2\text{-a}$$

$$\frac{S_e}{S_w} = .71$$

$(C_{L\alpha})_e$ is obtained from Fig. 4.1.3.2-11 using the entering parameter $(A_e/K)[\beta^2 + \tan^2\Lambda_{c/2}]^{1/2}$. Where:

$$K = c_{l\alpha}/2\pi = 1.05$$

$$\beta = \sqrt{1-M^2} \doteq 1 \quad \text{(low speed)}$$

$$A_e = b_e^2/S_e = 2.44$$

b_e is defined by: (see Fig. 43)

$$b_e^2 (\tan^{-1}\Lambda_0 - \tan^{-1}\Lambda_{TE}) + 4b_e c_t - 4S_e = 0$$

$$b_e = 2.15\times10^2 \text{ in} = 17.95 \text{ ft}$$

$$\tan\Lambda_{c/2} = \tan\Lambda_0 - 4/A\ [1/2(1-\lambda)/(1+\lambda)] \qquad 2.2.2\text{-}1$$

$\tan\Lambda_{c/2} = .534$ thus:

$$A_e/K\ [\beta^2 + \tan^2\Lambda_{c/2}]^{1/2} = 2.74$$

$$(C_{L\alpha})_e/A_e = 1.15$$

$$(C_{L\alpha})_e = 1.15\ (2.44) = 2.81$$

$$K_N = (C_{L\alpha})_N\ S_{Nref}/(C_{L\alpha})_e\ S_e \qquad 4.3.1.2\text{-}4$$

S_{Nref} is defined as flat plate body area as seen from the nose of the aircraft.

$$S_{Nref} = 29.8 \text{ ft}^2$$

$$(C_{L\alpha})_N = 2(k_2-k_1)\ S_o/V_B^{2/3} \quad \text{(per radian)} \qquad 4.2.1.1\text{-a}$$

$$V_B \doteq 96(\pi d^2)/4 + 78(d/2)^2/4 = 9.4\times10^5 \text{ in}^3$$

$$k_2-k_1 = 0.6 \qquad 4.2.1.1\text{-}6a$$

$$(C_{L\alpha})_N = 2(0.6)\ (29.8)\ (144)/(9.4\times10^5)^{2/3} = 0.54$$

$$K_N = .54(29.8)/(2.81)(132.1) = .0432$$

$$d/b = .27$$

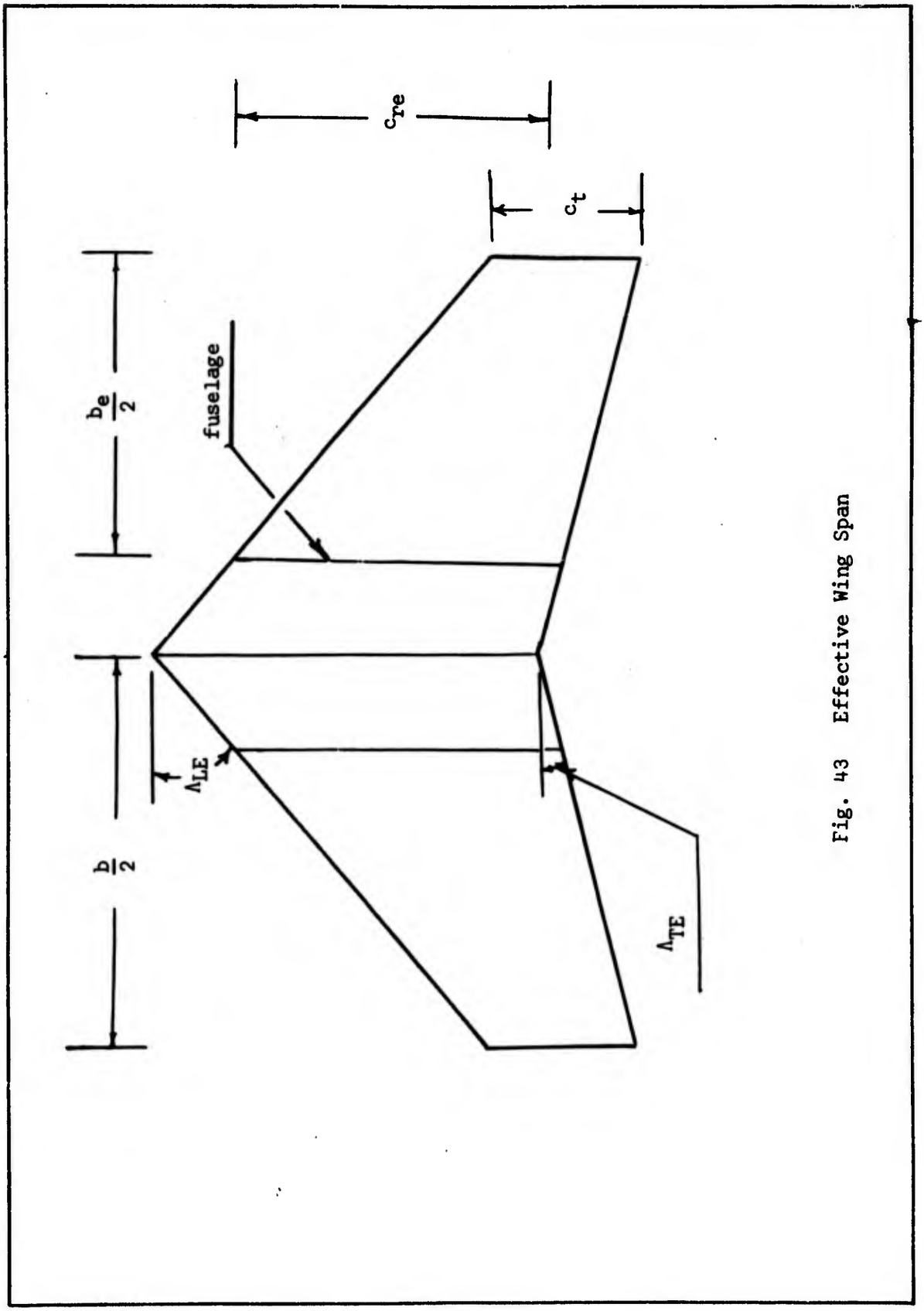

Fig. 43 Effective Wing Span

$K_{W(B)} = 1.24$ 4.3.1.2-10

$K_{B(W)} = .40$ 4.3.1.2-10

$(C_{L\alpha})_{WB} = (.0432+1.24+.40)(2.81)(132.1/186) = 3.35$

$a_{WB} = 3.35$

$C_{LMAX} = (C_{LMAX})\ \text{base} + \Delta C_{LMAX}$ 4.1.3.4c

(C_{LMAX}) base and C_{LMAX} are taken from graphs 4.1.3.4-16b and 4.1.3.4-17a respectively. The entering parameter for (C_{LMAX}) base is:

$(C_1+1)\ A/\beta\ \cos\Lambda_{LE}$ 4.1.3.4-16b

$\lambda = c_t/c_r = 56/140 = .4$

$C_1 = 0.4$ 4.1.3.4-17b

Entering parameter for C_{LMAX} is:

$(C_2+1)\ A\ \tan\Lambda_{LE}$ 4.1.3.4-17a

$C_2 = 1.1$ 4.1.3.4-17b

$(C_1+1)\ A/\beta\ \cos\Lambda_{LE} = (1.4)(2.797)(.765) = 2.99$

$(C_2+1)\ A\ \tan\Lambda_{LE} = (2.1)(2.797)(0.84) = 4.95$

$\Delta y = 1.35$ 2.2.1-8

$(C_{LMAX})_{\text{base}} = .81$ 4.1.3.4-16b

$\Delta C_{LMAX} = .05$

$C_{LMAX} = 0.86$ (wing only)

$\alpha C_{LMAX} = (\alpha C_{LMAX})_{base} + \Delta\alpha C_{LMAX}$ 4.1.3.4-d

$(\alpha C_{LMAX})_{base} = 22°$ 4.1.3.4-18a

$\Delta\alpha C_{LMAX} \doteq 0$ 4.1.3.4-18b

$\alpha C_{lmax} = 22°$ (wing only)

$\frac{(C_{LMAX})_{WB}}{(C_{LMAX})_W} \doteq 0.9$ and $\frac{(\alpha C_{LMAX})_{WB}}{(\alpha C_{LMAX})_W} \doteq .7$ 4.3.1.4-5

$(C_{LMAX})_{WB} \doteq .78, (\alpha C_{LMAX})_{WB} = 15.4°$

Lift with Flaps Down 50°

$$(C_{L\alpha})_\delta = \left[\left(\frac{c'}{c-1}\right) \frac{S_{Wf}}{S_W} + 1 \right] (C_{L\alpha})_{\delta=0}$$ 6.1.4.2.1

$\frac{c'}{c} = \frac{24}{25} = .96$ (measured from Fig. 44)

$\frac{S_{Wf}}{2} = b_f c_i - \frac{1}{2} b_f x_3 + \frac{1}{2} b_f x_4 = 43$

$c_i = c_r - b_i (\tan\Lambda_{LE} - \tan\Lambda_{TE})$

$x_3 = b_f \tan\Lambda_{LE}$

$S_{Wf} = 86 \text{ ft}^2$

$$(C_{L\alpha})_\delta = \left[-.04 \left(\frac{86}{186} + 1\right) \right] (C_{L\alpha})_{\delta=0°}$$

$$= (.9815)(C_{L\alpha})_{\delta=0} = 3.30$$

$\Delta C_{LMAX} = \Delta c_{lMAX} \left(\frac{S_{Wf}}{S_W}\right) K$ 6.1.4.3a

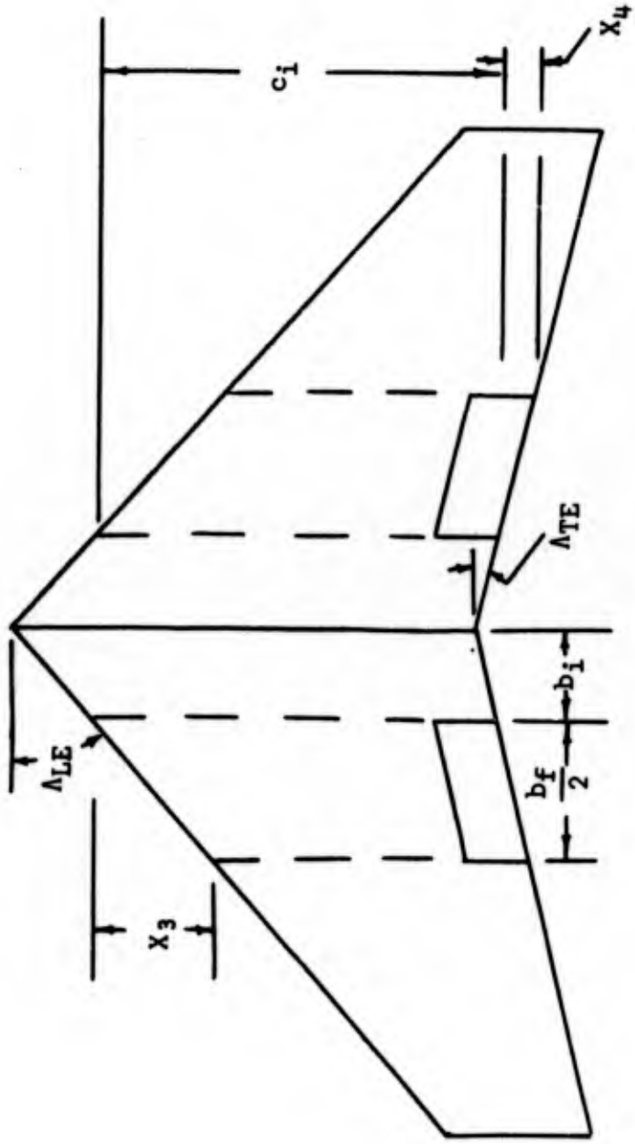

Fig. 44 Calculation of S_{WF}

$$\Delta c_{lMAX} = k_1 k_2 k_3 \, (\Delta c_{lMAX})_{base} \qquad 6.1.1.3\text{-}3$$

$$\Delta(c_{lMAX})_{base} = .82$$

$$\frac{c_f}{c_W} = \frac{17.6}{98} = .18$$

$$k_1 = .89 \qquad 6.1.1.3\text{-}6b$$

$$k_2 = .95 \qquad 6.1.1.3\text{-}7a$$

$$k_3 = 1.0 \qquad 6.1.1.3\text{-}7b$$

$$\Delta c_{lMAX} = .89(.95)(1.0)(.82) = .695$$

$$K = (1\text{-}.08 \cos^2 \Lambda_{c/4}) \cos^{3/4} \Lambda_{c/4} \qquad 6.1.4.3\text{-}1$$

$$\Lambda_{c/4} = 34^\circ \quad \text{(from Hawker Siddeley)}$$

$$K = .812$$

$$\Delta C_{LMAX} = .695(.463)(.812) = .262$$

$$C_{LMAX} = .78 + .262 = 1.042$$

Using 65-009 airfoil with flaps down 60°, $\Delta c_{lMAX} = .80$ and $\Delta C_{LMAX} = .301$, so values appear reasonable.

$$\Delta \alpha_{0cl} = -11^\circ$$

$$\Delta \alpha_{0CL} = -11(.463)(.812) = -4.1^\circ$$

For a summary of wing lift curve see Fig. 45.

Drag

$$(C_D)_{WB} = (C_{DO})_{WB} + (C_{Di})_W + [C_D(\alpha)]_B \frac{S_B}{S_W} \qquad 4.3.3.2\text{-a}$$

$$(C_{DO})_{WB} = C_{DOW} + (C_{DO})_B \frac{S_B}{S_E} \qquad 4.3.3.1\text{-a}$$

$$(C_{DOW}) = C_{Df} = 2C_f [1 + 2t/c + 100(t/c)^4] \doteq 2.32\ C_f$$

C_f is friction coefficient based on Reynolds number which is:

$$R_e = \frac{\rho V \bar{c}}{\mu}$$

$$(C_{DO})_B = 1.02\ C_f \left[1 + \frac{1.5}{(\ell_B/d)^{3/2}} + \frac{7}{(\ell_B/d)^3} \right] \frac{S_S}{S_B} + C_{Db} \qquad 4.2.3.1\text{-a}$$

$$\frac{S_S}{S_B} = \frac{495.2}{29.8} = 16.1$$

$$\frac{\ell_B}{d} = \frac{509.92}{74} = 6.89$$

$$C_{Db} \doteq 0$$

$$C_{DOB} = 1.13\ C_f$$

Where C_f is based on body Reynolds number.

Both turbulent and laminar flow were investigated. It is quite possible that laminar flow may exist on the wing at speeds below 50 ft/sec. However, at this low speed, drag is a minor force so only turbulent drag coefficients were used for simplicity. Table A-1 is a summary of the calculation of the zero-lift drag coefficient without flaps.

TABLE A-1

Summary of C_{DO} Calculations

V ft/sec	R_e Wing $\times 10^{-6}$	R_e Body $\times 10^{-6}$	C_f Wing $\times 10^3$	C_f Body $\times 10^3$	C_{DO} Wing $\times 10^3$	C_{DO} Body $\times 10^3$	$C_{DO} \frac{S_B}{S_W} \times 10^3$	$C_{DO} \times 10^3$
10	.554	2.7	5.4	3.7	12.5	4.18	.945	13.45
20	1.11	5.4	4.3	3.3	10.0	3.73	.84	10.84
30	1.66	8.1	4.1	3.1	9.5	3.51	.79	10.29
40	2.22	10.8	3.9	3.0	9.05	3.40	.78	9.83
50	2.77	13.5	3.7	2.9	8.57	3.28	.74	9.31
60	3.32	16.2	3.6	2.8	8.35	3.17	.715	9.07
70	3.88	18.9	3.5	2.7	8.10	3.05	.69	8.79
80	4.33	21.6	3.4	2.7	7.88	3.05	.69	8.57
90	4.98	24.3	3.4	2.65	7.88	3.00	.68	8.56
100	5.54	27.0	3.3	2.6	7.65	2.94	.66	8.31
125	6.92	33.8	3.2	2.5	7.42	2.83	.64	8.06
150	8.3	40.5	3.1	2.45	7.19	2.77	.625	7.82
200	11.1	54.0	3.0	2.35	6.95	2.66	.60	7.55
300	16.1	81.0	2.6	2.25	6.02	2.55	.575	6.59

$$(C_{Di})_W = \frac{C_L^2}{\pi A}(1 + \delta_1\delta_2) + k\Delta \qquad 4.1.5.2\text{-d}$$

$$\delta_1 \doteq .003 \qquad 4.1.5.2\text{-11}$$

$$\delta_2 = 1.37 \qquad 4.1.5.2\text{-12}$$

$$(1 + \delta_1\delta_2) = 1 + .0041 = 1.0041 \doteq 1$$

$$J = .3(C_1+1)\, A/\beta \cos\Lambda_{LE} \{(C_1+1)(C_2+1) - [(C_2+1)\, A \tan\Lambda_{LE}/7]^3\} = 2.52$$

$$K = 1 \qquad 4.1.5.2\text{-13}$$

Δ is based on J and

$$\frac{\tan\alpha}{\tan\alpha_{MAX}} = \frac{\tan\alpha}{\tan 15.4^\circ} = \frac{\tan\alpha}{.275} \qquad 4.1.5.2\text{-14}$$

$$\pi A = 8.78$$

Table A-2 is a summary of the induced drag coefficient calculation without flaps.

At most speeds and angles of attack, a sufficient approximation for $(C_{DO})_{WB}$ is .010.

$$[C_D(\alpha)]_B = \alpha^2 + 0.49\, f^2 \frac{C_{de}}{S_b}\alpha^4$$

$$C_{de} = 1.2 \qquad 4.2.1.2\text{-9b}$$

$$f = \frac{\ell_B}{d} = 6.89$$

$$\{[C_D\alpha]_B \frac{S_B}{S_W}\}_{MAX} = .012$$

TABLE A-2

Induced Drag Calculation W/O Flaps

α_{WB} deg	α_{WB} rad	C_{LW}	$\frac{C_L^2}{\pi A}$	$\tan\alpha$	$\frac{\tan\alpha}{\tan\alpha_{MAX}}$	Δ	C_{Di} Wing	$C_{Di}+C_{DO}$
0	0	0	0	0	0	0	0	.01
2	.0349	.117	.00156	.03492	.1265	0	.00156	.01156
4	.0698	.232	.00612	.06993	.254	0	.00612	.0162
6	.1046	.350	.01395	.10510	.382	0	.01395	.02395
8	.1398	.467	.0248	.14054	.510	.015	.0398	.0498
10	.1747	.585	.0390	.17633	.640	.025	.0640	.0740
12	.2096	.700	.0558	.21256	.772	.035	.0908	.1008
14	.245	.82	.0767	.24933	.905	.06	.1367	.1467
15.4	.267	.89	.0906	.27545	1.00	.075	.1656	.1756

$[C_D(\alpha)]_B$ is an order of magnitude smaller than $[C_D(\alpha)]_W$ and is safely neglected.

Drag with 50° Flap Deflection

$$\Delta C_{DMIN} = \Delta C_{df} K_b + K' \frac{(C_{Lf})^2}{\pi A} \qquad 6.1.7p$$

$$\Delta C_{df} = .091 \qquad 6.1.7\text{-}19$$

$$\frac{b_f}{b} = \frac{59.55}{133.36} = .45$$

$$K_b = .6 \qquad 6.1.4.1\text{-}2b$$

$$K' = 0.8 \qquad 6.1.7\text{-}21$$

$$\Delta C_L = .262$$

$$\Delta C_{DMIN} = \frac{.054 + 0.8(.262)^2}{(3.14)(2.797)}$$

$$= .054 + .00625 = .060$$

$$(C_{DO})_{ave} = .060 + .010 = .070$$

$$C_{Di} = \frac{C_L^2}{\pi A}(1 + \delta_1\delta_2) + K\Delta \doteq \frac{C_L^2}{\pi A} + \Delta$$

See Table A-3 for induced drag coefficient calculations with flaps.

$C_{Ma.c.}$ for 50° Flap Deflection

From Reference 7, 65-009 $C_{mc/4}$ is obtained.

$$C_{Mc/4} = C_{mc/4} \frac{S_{Wf}}{S_W} K$$

K is obtained as in 6.1.4.3-1.

TABLE A-3

Induced Drag With Flaps Calculation

α_W deg	α_W rad	C_L	$\frac{C_L^2}{\pi A}$	$\tan\alpha$	$\frac{\tan\alpha}{\tan\alpha_{MAX}}$	Δ	C_{Di}	$C_{Di}+C_{DO}$
0	0	0	0	0	0	0	0	.070
2	.0349	.115	.0015	.03492	.107	0	.0015	.0715
4	.0698	.237	.0064	.06993	.214	0	.0064	.0764
6	.1046	.345	.0136	.10510	.324	0	.0136	.0836
8	.1398	.461	.0242	.14054	.432	.01	.0342	.1042
10	.1747	.576	.0878	.17633	.545	.015	.0528	.1228
12	.2096	.690	.0543	.21256	.655	.025	.0793	.1493
14	.245	.810	.0747	.24933	.765	.040	.1107	.1807
16	.279	.921	.097	.28675	.883	.055	.152	.222
18	.314	1.03	.121	.32492	1.00	.075	.196	.266

TABLE A-4

$C_{Mc/4}$ Calculation With Flaps

α_W	$C_{mc/4}$	$C_{Mc/4}$
0	-.15	-.0565
3	-.175	-.066
7	-.2	-.0753
11	-.2	-.0753
13	-.2	-.0753
15	-.2	-.0753
17	-.2	-.0753
19	-.2	-.0753

In all wing-body calculations the angle of attack of the wing has been used as a reference. The wing has a constant incidence of 1.75°; thus, to represent the lift, drag and moment in terms of aircraft angle of attack all values must be shifted 1.75°. For a summary of all wing-body values with reference to aircraft angle of attack see Fig. 45.

Horizontal Tail Lift

$$c_{l\alpha} = 6.28 + 4.7(.07)\,[1+.00375\phi_{TE}] \qquad 4.1.1.2\text{-}9$$

$$= 6.28 + .33 = 6.61$$

$A = 3.26$ (Ref 2)

$$\tan\Lambda_{c/2} = \tan\Lambda_{LE} - 4/A\,[1/2(1-\lambda)/(1+\lambda)] \qquad 2.2.2\text{-}1$$

$$A/K\,[\beta^2 + \tan^2\Lambda_{c/2}] = 3.52$$

$$C_{L\alpha}/A = 1.00 \qquad C_{L\alpha} = 3.26 \qquad 4.1.3.2\text{-}11$$

Travel of the tail is restricted within the linear variation of lift with angle of attack, hence C_{LMAX} calculation is not necessary. See Fig. 47 for tail lift coefficient summary.

Wing-Body Aerodynamic Center

$$\frac{x_{a.c.}}{c_r} = \frac{\left(\frac{x_{a.c.}}{c_r}\right)_N C_{L\alpha N} \left(\frac{x_{a.c.}}{c_r}\right)_{W(B)} C_{L\alpha W(B)} \left(\frac{x_{a.c.}}{c_r}\right)_{B(W)} C_{L\alpha B(W)}}{\left(C_{L\alpha N} + C_{L\alpha W(B)} + C_{L\alpha B(W)}\right)}$$

$$4.3.2.1\text{-}a$$

$C_{L\alpha N} = .54$ (previously calculated)

$$\left(\frac{x_{a.c.}}{c_r}\right)_N = \frac{x_2}{c_r} + \left(\frac{d}{2c_r}\right)\tan\Lambda_{LE} \qquad 4.3.2.1\text{-}c$$

$$\left(\frac{x_2}{\ell_N}\right) = -.5 \qquad 4.3.2\text{-}1\text{-}10a$$

$x_2 \doteq -.5(144) = -72$ in

$$\left(\frac{x_{a.c.}}{c_r}\right)_N = -.292$$

$$\left(\frac{x_{a.c.}}{c_r}\right)_{W(B)} = \left(\frac{x_{a.c.}}{c_{re}}\right)\left(\frac{c_{re}}{c_r}\right) + \frac{d}{2c_r}\tan\Lambda_{LE} \qquad 4.3.2.1\text{-}d$$

$$\frac{x_{a.c.}}{c_{re}} \doteq -.5 \qquad 4.1.4.2\text{-}8$$

$\frac{\tan\Lambda_{LE}}{\beta} = .84$, and $A_e \tan\Lambda_{LE} = 2.05$

$$c_{re} = \frac{b_e}{2}\tan\Lambda_{LE} + c_t - \frac{b_e}{2}\tan\Lambda_{TE} = 121 \text{ in} \quad \text{(Fig. 43)}$$

$$\frac{c_{re}}{c_r} = \frac{121}{140} = .865$$

$$\frac{x_{a.c.}}{c_{rW(B)}} = .6545$$

$$\left(\frac{x_{a.c.}}{c_r}\right)_{B(W)} = \left(\frac{x_{a.c.}}{c_{re}}\right)_{B(W)} \frac{c_{re}}{c_r} + \left(\frac{d}{2}\right) \tan\Lambda_{LE}/c_r \qquad 4.3.2.1\text{-f}$$

$$\left(\frac{x_{a.c.}}{c_{re}}\right)_{B(W)} \pm .34 \qquad 4.3.2\text{-}1\text{-}11$$

$$\left(\frac{x_{a.c.}}{c_r}\right)_{B(W)} = .516$$

$$C_{L\alpha W(B)} = K_{W(B)} (C_{L\alpha})_e \frac{S_e}{S_W} = 2.49 \qquad 4.3.1.2a$$

$$C_{L\alpha B(W)} = .40(C_{L\alpha})_e \frac{S_e}{S_W} = .803$$

$$\left(\frac{x_{a.c.}}{c_r}\right) = .485$$

This corresponds to h_{nWB} 68 in = 5.65 ft; as a percentage of the mean aerodynamic chord this is .1775$\bar{c}$.

Tail Aerodynamic Center

$$\frac{x_{a.c.}}{c_r} = \left(\frac{x_{a.c.}}{c_{re}}\right) \frac{c_{re}}{c_r}$$

$$\lambda = \frac{21}{67} = .314$$

$$\frac{x_{a.c.}}{c_{re}} = .6 \qquad 4.1.4.2\text{-}8$$

$$\frac{c_{re}}{c_r} \pm .95 \quad \text{(from geometry Ref. 5)}$$

$$\frac{x_{a.c.}}{c_r} = .57$$

This corresponds to .282 of the geometric mean chord.

Tail Downwash in Conventional Flight

The downwash is investigated at $\alpha = 3^\circ$ because this is the approximate angle of attack at the completion of the accelerating transition.

$$\frac{(\alpha-\alpha_0)}{(C_{LMAX}-\alpha)} = \frac{9^\circ}{18^\circ} = .5$$

$$\frac{b_{eff}}{b} = 1 \qquad 4.4.1\text{-}30$$

$$\frac{A_{eff}}{A} = 1 \qquad 4.4.1\text{-}30$$

$$\frac{2\ell_T}{b} = \frac{16.663}{11.41} = 1.45$$

$$\left(\frac{\partial\varepsilon}{\partial\alpha}\right)_\alpha = .6 \qquad 4.4.1\text{-}31$$

$$\left(\frac{\partial\varepsilon}{\partial\alpha}\right)_v = .7 \qquad 4.4.1\text{-}31$$

$$a = h_H - \ell_{eff}\left(\frac{\alpha-0.41C_L}{\pi A_{eff}}\right) - \left(\frac{b_{eff}}{2}\right)\tan\Gamma - 6.2 \qquad 4.4.1\text{-}c$$

$$b_v = b_{eff} - (b_{eff} - b_{vru})\left(\frac{2l_{eff}}{b\xi_{ru}}\right)^{1/2} \qquad 4.4.1\text{-}e$$

$$b_{vru} = [0.78(0.10)(\lambda-0.4)\ 0.003\Lambda_{c/4}]\ b_{eff} = 18.3 \qquad 4.4.1\text{-}f$$

$$\xi_{ru} = \frac{0.56A}{C_L} = 31.3$$

$$b_v = 264.42 \text{ in}$$

$$\frac{b_H}{b_v} = .61$$

$$\frac{2a}{b_v} = .565$$

$$\frac{(\partial\varepsilon/\partial\alpha)}{(\partial\varepsilon/\partial\alpha)_v} = .7 \qquad \text{4.4.1-32b}$$

$$\left(\frac{\partial\varepsilon}{\partial\alpha}\right) = 0.42$$

The computation of ε_0 is not by Datcom method and is presented in the body of the report.

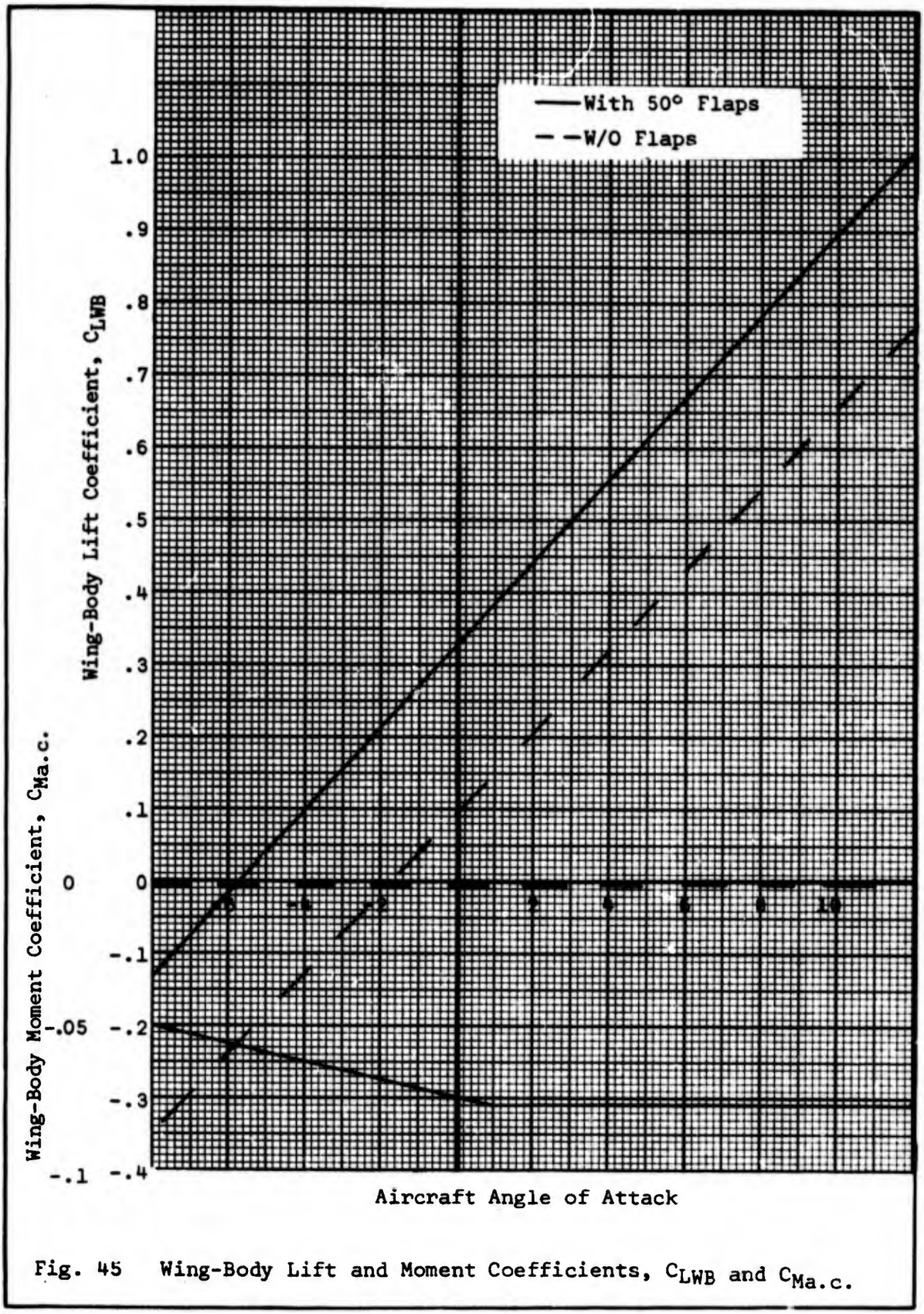

Fig. 45 Wing-Body Lift and Moment Coefficients, C_{LWB} and $C_{Ma.c.}$

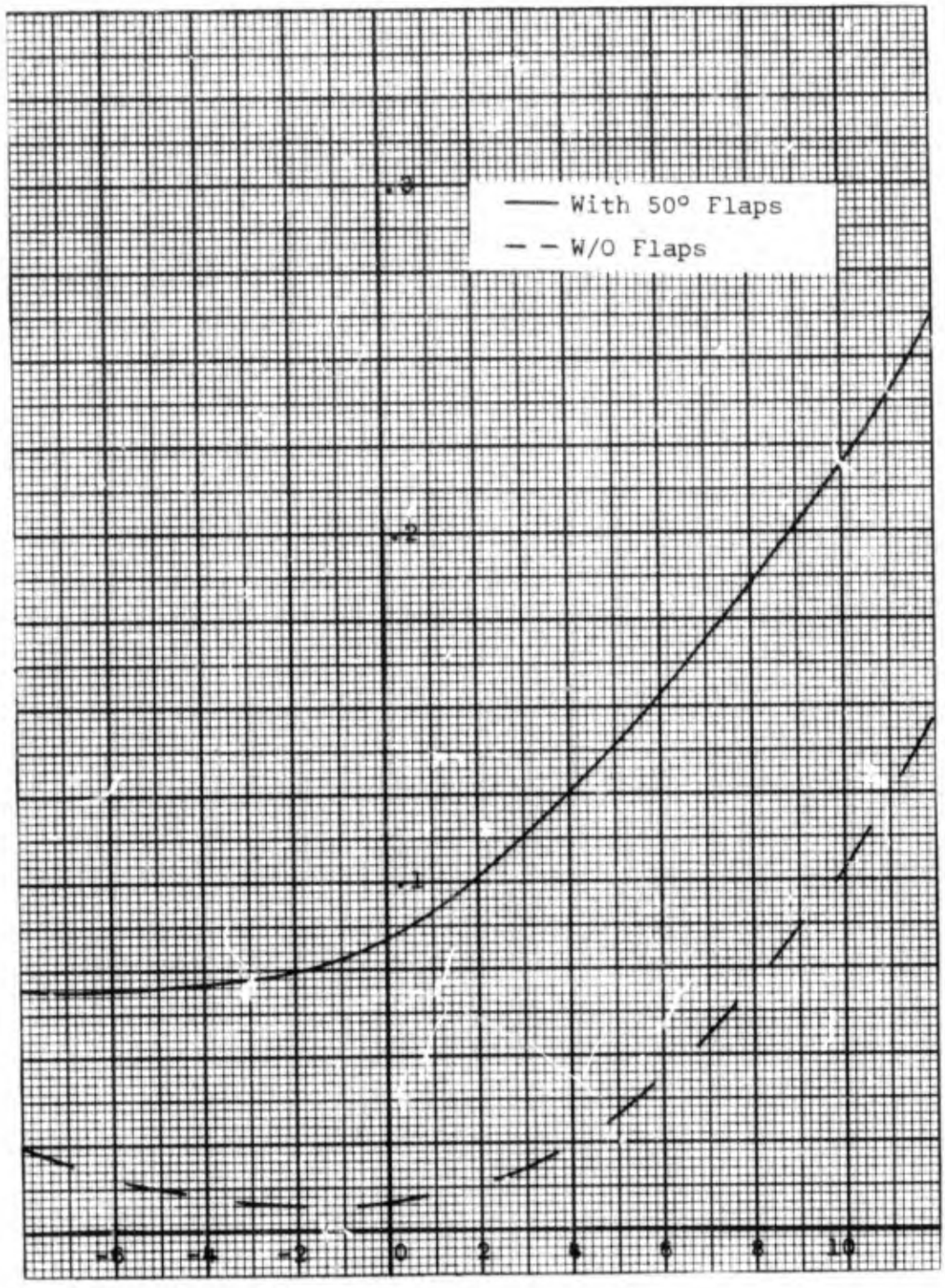

Fig. 46 Aircraft Drag Coefficient

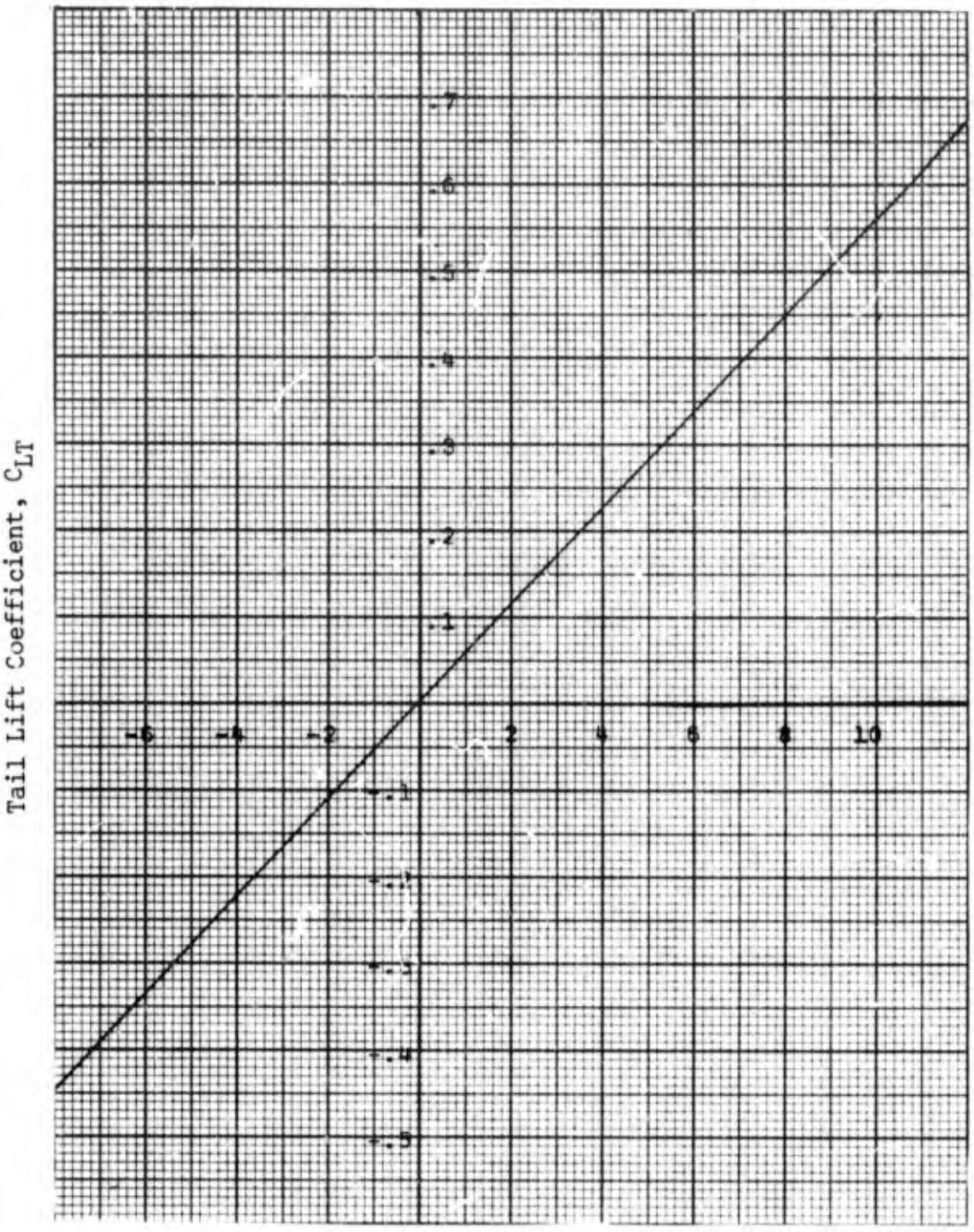

Fig. 47 Tail Lift Coefficient

Appendix B

Computer Program Solution of The Accelerating Transition

The program was written to be as generally applicable as possible. Of course, all the aerodynamic coefficients, distances and other variables are for the P-1127 only. The program could be used for other VTOL airplanes only with extensive changes. However, only small changes are needed to solve any P-1127 accelerating transition at constant attitude and engine speed. Specifically there are two areas of the program which need to be examined if the constant references are changed. First the variation of the tail downwash must be reviewed by estimating the parameter $(C_T V_\infty / V_j)/\sin\delta_j$. Second the variation of with velocity will change if other than 95% maximum engine speed is used. This change of thrust will also affect the reaction moment available. Most of this information was not available and hence has not been included in this report.

A presentation of the program is in the following pages. The program is mostly self explanatory, however, several variables need to be defined here for clarity.

RHO = 1/2 ρ

EPI = ϵ_0

ALPHAT = $(1 - \partial\epsilon/\partial\alpha)\ \alpha$

PEPIA = $\partial\epsilon/\partial\alpha$

```
C  SOLUTION OF THE APPROXIMATE EQUILIBRIUM EQUATIONS FOR THE P-1127 VECTORED
C  THRUST VTOL THROUGH TRANSITION
C  THE TRANSITION IS FOR AN ACCELERATING AIRPLANE. THE RPM IS HELD
C  CONSTANT AT 95 PERCENT WHILE THE EXHAUST NOZZLES ARE RETARDED AT A
C  CONSTANT RATE OF 3.5 DEG/SEC. THE AIRPLANE IS HELD AT A CONSTANT
C  REFERENCE ANGLE OF 6 DEG TO THE HORIZONTAL EARTH AXIS. THESE
C  PARAMETERS ARE AT THE DISCRETION OF THE PROGRAMMER BUT THE PROGRAM
C  FOR THE TOTAL THRUST AND THE ACCELERATION MUST BE CHANGED SLIGHTLY
C  IF OTHER THAN 95 PERCENT RPM AND 3.5 DEG/SEC ARE USED.
      REAL LN,MW,MI,MT,MO,ME,MA,MU,M,LS,MR,LWB,LTA
      REAL MTTU,MCLU,MCLTU,MWAU,MUP,MUPM,MCLW,MCLTW,MWAW,MTTW,MWP,MWPM,
     1MWDOT,MQ,MWDOTM,MQM,IYY,MUM,MWM,MRNF,M1,MD
      DIMENSION X(21), Y(21),C(5)
      DIMENSION COE(5),ROOTR(4),ROOTI(4)
      READ(5,10)DELJ,DDELJ,THEOT,THEO,THEC,ALPHA,EPIO,HR2
      READ(5,11)H,HNWB,LN,HT1,HT2,HT,CBAR,HR1,ZE
      READ(5,12)S,ST,AT,AWB,V,U,W,RHO,FIO,WEI
      READ(5,13)C7,C8,C9,C10,C11,C12,C13,C14,C15,C16
      READ(5,17)C1,C2,C3,C4,C5,C6,IYY,TL,H1,ZWB
      READ(5,18)X
      READ(5,18)Y
10    FORMAT(8F9.4)
11    FORMAT(8F9.4,1F8.4)
12    FORMAT(1F8.2,3F6.2,3F4.2,1F9.6,2F6.0)
13    FORMAT(1F8.2,8F8.4,1F8.0)
17    FORMAT(6F4.1,1F8.0,3F6.2)
18    FORMAT(8F10.5/8F10.5/5F10.5)
      WRITE(6,10)DELJ,DDELJ,THEOT,THEO,THEC,ALPHA,EPIO,HR2
      WRITE(6,11)H,HNWB,LN,HT1,HT2,HT,CBAR,HR1,ZE
      WRITE(6,12)S,ST,AT,AWB,V,U,W,RHO,FIO,WEI
      WRITE(6,13)C7,C8,C9,C10,C11,C12,C13,C14,C15,C16
      WRITE(6,17)C1,C2,C3,C4,C5,C6,IYY,TL,H1,ZWB
```

```
C DEFINITION OF VARIABLES
      N=21
      K=4
      LIST=1
      CALL PLSQ(X,Y,N,K,C,LIST,EMAX,ERMS,EMEQ)
 1    DELT=DELJ+THEOT
      DELTL=DELT+THEO
      Q=RHO*(V**2)
C RANGE OF APPLICABLE ALPHA IS DEFINED BY LINEAR RANGE OF CLWB
C  THE AIRFOILS OF THE AIRPLANE ARE ASSUMED TO BE STALLED UNTIL THE
C  AIRPLANE ANGLE OF ATTACK IS WITHIN THE LINEAR LIFT CURVE SLOPE OF
C  THE WING. THE AERODYNAMIC VARIABLES ARE ALLASSUMED TO BE ZERO WITH
C  THE EXCEPTION OF CD WHICH TAKES ON THE VALUE FOR PARASITE DRAG ONLY.
      IF(ALPHA.LE.0.2090.AND.ALPHA.GE.-0.1395)GO TO 2
      CLWB=0.
      CD=0.07
      CLT=0.
      CMO=0.
      EPI=0.
      ETA=0.
      ALPHAT=0.
      AWB=0.0
      AT=0.0
      AD=0.0
      GO TO 21
C AERODYNAMIC VARIABLES ARE SOLVED BY LINEAR VARIATION WITH ALPHA
 2    CLWB=ALPHA*AWB+0.331
      CMO=-0.0753
      AWB=3.30
      AT=3.26
      CD=C(1)*ALPHA**4+C(2)*ALPHA**3+C(3)*ALPHA**2+C(4)*ALPHA+C(5)
      AD=C(1)*4.*ALPHA**3+C(2)*3.*ALPHA**2+C(3)*2.*ALPHA+C(4)
```

```
C   THE ZERO LIFT DOWNWASH IS ZERO UNTIL THE NOZZLE ANGLE, DELJ, REACHES
C   60 DEG. IT THEN VARIES LINEARLY WITH NOZZLE ANGLE TO A VALUE OF
C   EPSILON MAXIMUM AT DELJ=30 DEGAND A VALUE OF ZERO AT DELJ= 0 DEG.
C   THE PARTIAL DERIVATIVE OF EPSILON WITH ALPHA IS ZERO FROM DELJ= 90 DEG
C   TO DELJ= 60 DEG, THEN VARIES LINEARLY WITH DELJ TO ONE AS DELJ GOES
C   TO 30 AND TO 0.39 AS DELJ GOES TO ZERO.
      IF(DELJ.GT.1.046)GO TO 22
      IF(DELJ.LE.1.046.AND.DELJ.GT.0.523)GO TO 23
      IF(DELJ.LE.0.523)GO TO 20
 22   EPI=0.0
      ALPHAT=0.C
      GO TO 21
 23   EPI=(0.5+0.5*((1.046-DELJ)/0.523))*EPIO
      ALPHAT=(0.5-((1.046-DELJ)/0.523)*0.5)*ALPHA
      GO TO 21
 20   EPI=(DELJ/0.523)*EPIO
      ALPHAT=(1.-(0.39+(0.61/0.523)*DELJ))*ALPHA
C THE DOWNWASH EFFECT OF THE THRUST ON THE NOSE IS ASSUMED TO VARY LINEARLY
C WITH THE NOZZLE ANGLE.IT IS DOUBTFUL THAT THIS ASSUMPTION IS VALID AT LOW
C NOZZLE ANGLES BUT THE EFFECT IS SMALL THEN
 21   FI=(DELJ/1.57)*FIO
C THE VARIATION OF THRUST WITH VELOCITY IS NOW BROUGHT .THE TURBINE THRUST IS
C LINEAR AND THE FAN THRUST VERY NEARLY SO.THE FAN THRUST HAS BEEN LINEARIZED
C IN SECTIONS
      IF(V.GT.100.)GO TO 30
      T1=6450.+C1*V
      T1V=C1
      WA=370.
      GO TO 33
 30   WA=370.+C6*(V-100.)
      IF(V.GT.200.) GO TO 31
      T1=7100.+C2*(V-100.)
      T1V=C2
      GO TO 33
```

```
 31    IF(V.GT.300.) GO TO 32
       T1=7520.+C3*(V-200.)
       T1V=C3
       GO TO 33
 32    T1=7900.+C4*(V-300.)
       T1V=C4
 33    T2=7500.+C5*V
       T2V=C5
C THE MOMENT EQUATION IS NEXT SOLVED TO OBTAIN TAIL INCIDENCE AND REACTION
C MOMENT.BOTH ARE SOLVED USING THEIR RELATIONSHIP TO CONTROL STICK MOVEMENT
       FW=(WA*W)/32.2
       FU=(WA*U)/32.2
       MW=Q*S*(H-HNWB)*CLWB
       MI=LN*COS(THEO)*(FW-FI)
       MT=(T1*(H-HT1)+T2*(H-HT2))*SIN(DELT)
       MO=CMO*Q*S*CBAR
       ME=Q*ST*AT*(HT-H)*EPI
       MA=Q*ST*AT*(HT-H)*ALPHAT
C ME AND MA ARE NOT COMBINED AS THE VARIATION OF EPI AND ALPHAT IS DOUBTFUL
       MU=FU*ZE
       MD=Q*S*CD*ZWB*COS(THEC)
       M=MW+MI+MT+MO+ME-MA+MU+MD
       TC=Q*ST*AT*(HT-H)
       IF(ALPHA.GT.0.2090.OR.ALPHA.LT.-0.2090)GO TO 50
       IF(Q.EQ.0.C)GO TO 50
C VARIATION OF REACTION MOMENT AND TAIL INCIDENCE WITH STICK MOVEMENT IS NOT
C ALWAYS LINEAR. HERE THE VARIATION HAS BEEN LINEARIZED BY SEGMENTS OF THE CURVE
       LS=(M- 1.4*C7 -2.*TC*C8)/(C8*TC+C7)
       IF(LS.LT.-2.) GO TO 34
       IF(LS.GT.0.) GO TO 40
       MR=-(LS+1.4)*C7
       ETA=(LS+2.)*C8
       GO TO 60
```

```
34    LS=(M-1.4*C7-2.*TC*C11)/(C11*TC+C7)
      IF(LS.LT.-5.) GO TO 35
      MR=-(LS+1.4)*C7
      ETA=(LS+2.)*C11
      GO TO 60
35    LS=(M+16200.+TC*(0.0786-5.*C12))/(TC*C12)
      MR= 16200.
      ETA=(LS+5.)*C12-0.0786
      GO TO 60
40    LS=(M-1.4*C7-0.0611*TC)/(C9*TC+C7)
      IF(LS.GT.1.) GO TO 41
      MR=-(LS+1.4)*C7
      ETA=C9*LS+0.0611
      GO TO 60
41    LS=(M-12000.+C16-0.0611*TC)/(C9*TC+C16)
      IF(LS.GT.1.6) GO TO 42
      MR=-12000.-C16*(LS-1.)
      ETA=C9*LS+0.0611
      GO TO 60
42    LS=(M-19000.-0.1133*TC+1.6*C10*TC)/(C10*TC)
      MR=-19000.
      ETA=C10*(LS-1.6)+0.1133
      GO TO 60
50    M=MI+MT
      MR=-M
      GO TO 60
60    IF(DELJ.LT.0.349)GO TO 61
      GO TO 62
61    MR=MR*(DELJ/0.349)
      ETA=(M+MR)/TC
62    IF(MR.LT.0.00)GO TO 80
      FR=(MR*COS(THEC))/(HR2-H)*COS(DELJ)
      GO TO 81
80    FR=-(MR*COS(THEC))/(HR1-H)*COS(DELJ)
81    LWB=Q*S*CLWB*COS(THEC)
      LTA=Q*ST*AT*(ALPHAT+ETA-EPI)*COS(THEC)
```

```
      TW=(T1+T2)*SIN(DELTL)
      WDOT=(32.2*(WEI-LWB-LTA-FR-TW-FW+FI))/WEI
      DU=Q*S*( CD*COS(THEC)+CLWB*SIN(THEC))
      TU=(T1+T2)*COS(DELTL)
      DT=Q*ST*AT*(ALPHAT+ETA-EPI)*SIN(THEC)
      UDOT=(32.2*(TU-DU-DT-FU))/WEI
      DELJ=DELJ*57.3
      THEC=THEC*57.3
      ALPHA=ALPHA*57.3
      ETA=ETA*57.3
      WRITE(6,200)
  200 FORMAT(101HO DELJ     ALPHA     ETA      THEC      FU        FW        FI
     1     V         U         W        MR        T1        T2)
      WRITE(6,100)DELJ,ALPHA,ETA,THEC,FU,FW,FI,V,U,W,MR,T1,T2
  100 FORMAT(1HO,10F8.2,3F8.0)
      DELJ=DELJ/57.3
      THEC=THEC/57.3
      ALPHA=ALPHA/57.3
      ETA=ETA/57.3
      TTV=T1V+T2V
      SR=RHO*S*V
      STR=RHO*ST*V
      CA=COS(ALPHA)
      SA=SIN(ALPHA)
      CO=COS(THEO)
      CC=COS(THEC)
      SO=SIN(THEO)
      SC=SIN(THEC)
      ALPHT=ALPHAT+ETA-EPI
      SAT=SIN(ALPHT)
      CAT=COS(ALPHT)
```

```
C THE COMPUTATION OF THE STABILITY DERIVATIVES BASED ON THEFORCES AND
C MOMENTS OF THE PREVIOUSLY COMPUTED TRIM POINTS FOLLOWS) IN THE CASE OF
C THE ACCELERATING TRANSITION, THE FORCES AND MOMENTS ARE ASSUMED TO
C BE THOSE THAT WOULD BE ON THE VEHICLE IN UNACCELERATED FLIGHT AT THE SAME
C POINT)

C  COMPUTATION OF DIMENSIONAL DERIVATIVE XU
      PEPIA=1.-(ALPHAT/ALPHA)
 820  CLT=AT*(ALPHAT+ETA-EPI)
      WAXU=WA/32.2
      CLXU=SR*CLWB*SA*CA
      CDXU=SR*CD*(1.+CA**2)
      CLTXU=STR*CLT*(2.*SAT *CA-(1.-PEPIA)*CAT*SA)
      TTVXU=TTV*CA*COS(DELT)
      XU=CLXU+CLTXU-CDXU-WAXU+TTVXU
      XUM=(XU*32.2)/WEI
C THE XW DIMENSIONAL DERIVATIVE
      CLXW=SR*(CLWB*(1.+SA**2)+AWB*SA)
      CDXW=SR*CA*(AD+CD*SA)
      CLTXW=STR*((1.-PEPIA)*(CLT*CAT+AT*SAT)+2.*CLT*SAT*SA)
      TTVXW=TTV*SA*COS(DELT)
      XW=CLXW+CLTXW-CDXW+TTVXW
      XWM=(XW*32.2)/WEI
C THE ZU DIMENSIONAL DERIVATIVE
      CLZU=(1.+CA**2)*SR*CLWB
      CLTZU=STR*CLT*(2.*CAT*CA+(1.-PEPIA)*SAT*SA*CA)
      CDZU=SR*CD*SA*CA
      TTVZU=TTV*CA*SIN(DELT)
      ZU=-CLZU-CDZU-TTVZU-CLTZU
      ZUM=(ZU*32.2)/WEI
```

```
C THE ZW DIMENSIONAL DERIVATIVE
      WAZW=WA/32.2
      CLZW=SR*CA*(CLWB*SA+AWB)
      CLTZW=STR*((1.-PEPIA)*(CAT*AT-CLT*SAT)+2.*CLT*CAT*SA)
      CDZW=SR*(SA*AD+CD*(1.+SA**2))
      TTVZW=TTV*SA*SIN(DELT)
      ZW=-WAZW-CLZW-CLTZW-CDZW-TTVZW
      ZWM=(ZW*32.2)/WEI
C THE ZQ AND ZWDOT DIMENSIONAL DERIVATIVES ( TAIL CONTRIBUTIONS ONLY)
      ZQ=STR*AT*(H-HT)
      ZQM=(ZQ*32.2)/WEI
      ZWDOT=RHO*ST*AT*(1.-PEPIA)*(H-HT)*(PEPIA)
      ZWDOTM=(ZWDOT*32.2)/WEI
C THE MU DIMENSIONAL DERIVATIVE WITH DRAG, HEIGHT OF THE HORIZONTAL TAIL,
C AND HEIGHT OF THE WING CONSIDERED NEGLIGBLE IN ALL M DERIVATIVES
      MCLU=CLZU*(H1-HNWB)
      MCLTU=CLTZU*(H1-HT)
      MTTU=CA*SIN(DELT)*(T1V*(H1-HT1)+T2V*(H1-HT2))
      CMOU=2.*SR*CMO*CBAR
      CDMXU=ZWB*CDXU
      MUP=MCLU+MCLTU+MTTU+CMOU+CDMXU
      MUPM=MUP/IYY
C THE MW DIMENSIONAL DERIVATIVE
      MCLW=CLZW*(H1-HNWB)
      MCLTW=CLTZW*(H1-HT)
      MWAW=(LN*WA)/32.2
      MTTV=SA*SIN(DELT)*(T1V*(H1-HT1)+T2V*(H1-HT2))
      CDMW=CDZW*(H1-HNWB)
      CDMXW=ZWB*CDXW
      MWP=MCLW+MCLTW+MWAW+MTTV+CDMW+CDMXW
      MWPM=MWP/IYY
```

```
C THE MC AND MWDOT DERIVATIVES ( TAIL CONTRIBUTIONS ONLY)
      MC=ZC*(HT-H1)
      MCM=MC/IYY
      MWDOT=ZWDOT*(HT-H1)
      MWDOTM=MWDOT/IYY
      WRITE(6,910)
  910 FORMAT(97H0     XUM        XWM         ZUM         ZWM        ZWDOTM        Z
     1QM       MUPM        MWPM        MWDOTM      MQM)
      WRITE(6,900)XUM,XWM,ZUM,ZWM,ZWDOTM,ZQM,MUPM,MWPM,MWDOTM,MQM
  900 FORMAT(1H0,10F10.5)
      WO=V*SIN(ALPHA)
      UO=V*COS(ALPHA)
      A=ZWDOTM-1.
      B=XUM-ZWDOTM*(XUM+MQM)+ZWM+MQM+MWDOTM*(ZQM+UO)
      C=XUM*(MQM*(ZWDOTM-1.)-ZWM-MWDOTM*(ZQM+UO))-ZWM*MQM+MWPM*(ZQM+UO)+
     1ZUM*(XWM-WO*MWDOTM)+WO*MUPM*(ZWDOTM-1.)
      D=XUM*(ZWM*MQM-MWPM*(ZQM+UO))-XWM*(ZUM*MQM-MUPM*(ZQM+UO))-32.2*(ZU
     1M*MWDOTM-MUPM*(ZWDOTM-1.))-WO*(ZUM*MWPM-MUPM*ZWM)
      E=32.2*(MUPM*ZWM-ZUM*MWPM)
      NX=4
      COE(1)=A
      COE(2)=B
      COE(3)=C
      COE(4)=D
      COE(5)=E
      CALL SMULR(COE,NX,ROOTR,ROOTI)
      WRITE(6,950)
  950 FORMAT(75H0    R1         R2         R3         R4         R5         R6
     1         R7         R8)
      WRITE(6,960)ROOTR,ROOTI
  960 FORMAT(1HC,8F10.5///)
```

```
      W=W+WDOT
      U=U+UDOT
      IF(U.LE.0.0)GO TO 71
      THEC=-ATAN(W/U)
      GO TO 72
 71   THEC=1.57
 72   ALPHA=THEO-THEC
      V=SQRT(U**2+W**2)
C  THE NEW VALUE OF DELJ IS NOW ASSIGNED AND THE CALCULATION REPEATED
C  UNTIL DELJ IS EQUAL TO OR LESS THAN ZERO.
      DELJ=DELJ-DDELJ
      IF(DELJ.LT.0.) GO TO 70
      GO TO 1
 70   STOP
      END
```

Appendix C

Computer Program for the Solution of The Nonaccelerating Transition

The computer program presented on the following pages for the P-1127 in a nonaccelerating transition is very simple to use. It should be suitable for any nonaccelerating transition at constant angle of attack and weight. Unlike the program for the accelerating transition this program has included the variation of engine speed and reaction moment. It is believed that the treatment of the downwash would be suitable for any possible transition. As in the accelerating program, several variables need to be defined for clarity.

RHO = $1/2\ \rho$

EPI = ϵ_0

ALPHAT = $(1 - \partial\epsilon/\partial\alpha)$

PEPIA = $\partial\epsilon/\partial\alpha$

```
COSOLUTION IS DESIGNED FOR CONSTANT ALPHA AND THEC. HENCE THEO IS CONSTANT
C THE TRANSITION IS STEADY FROM STEP TO STEP IN VELOCITY. THE MOMENT EQUATION
C IS SOLVED APPROXIMATELY BY USING THRUST AND NOZZLE ZNGLE FOR PREVIOUS STEP
C VELOCITY. THE REACTION MOMENT AND TAIL INCIDENCE ARE THEN SUBSTITUTED INTO
C THE X AND Z FORCE EQUATIOS TO SOLVE FOR THE ACTUAL THRUST AND NOZZLE ANGLE
C AT THE SPECIFIED SPEED. SOLUTION IS FOR LINEAR LIFT CURVE SLOPE RANGE ONLY.
      REAL LN, LS,M,MW,MI,MT,MO,ME,MA,MU,LWB,LTA,K,MR
      REAL MTTU,MCLU,MCLTU,MWAU,MUP,MUPM,MCLW,MCLTW,MWAW,MTTV,MWP,MWPM,
     1MWDOT,MQ,MWDOTM,MQM,IYY,MUM,MWM,MRNF,M1,MD
      DIMENSION X(21), Y(21),C(5)
      DIMENSION COE(5),ROOTR(4),ROOTI(4)
      READ(5,10)DELJ,DELV,THEOT,THEO,THEC,EPIO,ALPHA,HR2
      READ(5,11)H,HNWB,LN,HT1,HT2,HT,CBAR,HR1,ZE
      READ(5,12)S,ST,AT,AWB,V,U,W,RHO,FIO,WEI
      READ(5,13)C7,C8,C9,C10,C11,C12,C13,C14,C15,C16
      READ(5,14)C32,C33,C41,C42,C43,C44
      READ(5,15)C45,C51,C52,C53,C54,C60
      READ(5,16)C31,T1,K
      READ(5,17)C1,C2,C3,C4,C5,C6,IYY,TL,H1,ZWB
      READ(5,18)X
      READ(5,18)Y
10    FORMAT(8F9.4)
11    FORMAT(8F9.4,1F8.0)
12    FORMAT(1F8.2,3F6.2,3F4.2,1F9.6,2F6.0)
13    FORMAT(1F8.2,8F8.4,1F8.0)
14    FORMAT(6F10.6)
15    FORMAT(6F10.6)
16    FORMAT(1F10.6,2F10.3)
17    FORMAT(6F4.1,1F8.0,3F6.2)
18    FORMAT(8F10.5/8F10.5/5F10.5)
      WRITE(6,10)DELJ,DELV,THEOT,THEO,THEC,EPIO,ALPHA,HR2
      WRITE(6,11)H,HNWB,LN,HT1,HT2,HT,CBAR,HR1,ZE
      WRITE(6,12)S,ST,AT,AWB,V,U,W,RHO,FIO,WEI
      WRITE(6,13)C7,C8,C9,C10,C11,C12,C13,C14,C15,C16
```

```
      WRITE(6,14)C32,C33,C41,C42,C43,C44
      WRITE(6,15)C45,C51,C52,C53,C54,C60
      WRITE(6,16)C31,T1,K
      WRITE(6,17)C1,C2,C3,C4,C5,C6,IYY,TL,H1,ZWB
C   PLSQ IS A STANDARD 7094 COMPUTER PROGRAM OF THE SESCD FACILITY FOR
C   FITTING A POLYNOMIAL TO A CURVE BY THE METHOD OF LEAST SQUARES. N IS
C   THE NUMBER OF POINTS OF THE CURVE SELECTED. KK ISTHE DEGREE OF THE
C   POLYNOMIAL DESIRED WHICH IS A THE DISCRETION OF THE PROGRAMMER. X IS
C   THE ABCISSA, ALPHA, AND Y IS THE ORDINATE,CD. LIST= 1 CALLS FOR THE
C   ERROR ANALYSIS. EMAX, ERMS AND EMEQ.
      N=21
      KK=4
      LIST=1
      CALL PLSQ(X,Y,N,KK,C,LIST,EMAX,ERMS,EMEQ)
 1     Q=RHO*V**2
      CLWB=AWB*ALPHA+0.331
      CMC=-0.0753
      CD=C(1)*ALPHA**4+C(2)*ALPHA**3+C(3)*ALPHA**2+C(4)*ALPHA+C(5)
      AD=C(1)*4.*ALPHA**3+C(2)*3.*ALPHA**2+C(3)*2.*ALPHA+C(4)
      DELT=DELJ+THEOT
      DELTL=DELT+THEO
C   THE ZERO LIFT DOWNWASH ON THE TAIL IS ASSUMED TO INCREASE LINEARLY
C   WITH NOZZLE ANGLE TO A MAXIMUM VALUE AT DELJ = 60. THE ZERO LIFT
C   DOWNWASH IS THEN CONSTANT AT THE MAXIMUM VALUE FROM DELJ = 60 TO DELJ
C   =30, THEN DECREASES LINEARLY WITH DELJ UNTIL BOTH DELJ AND THE ZERO
C   LIFT DOWNWASH ARE ZERO. THE PARTIAL DERIVATIVE OF EPSILON WITH ALPHA
C   VARIES LINEARLY FROM ZERO TO ONE WITH DELJ FROM DELJ = 90 DEG TO DELJ
C   = 60 DEG, IS ONE FROM DELJ = 60 TO DELJ = 30 , THEN DECREASES LINEARLY
C   TO A VALUE OF 0.39 AT DELJ = 0.
      IF(DELJ.GT.1.046)GO TO 22
      IF(DELJ.LE.1.046.AND.DELJ.GT.0.523)GO TO 23
      IF(DELJ.LE.0.523)GO TO 20
```

```
   22   EPI=(1.57-DELJ)/0.523*EPIO
        ALPHAT=(DELJ-1.046)/0.523*ALPHA
        GO TO 21
   23   EPI=EPIO
        ALPHAT=0.0
        GO TO 21
C THE DOWNWASH AT THE TAIL IS ASSUMED CONSTANT UNTIL NOZZLE ANGLE HS 30 DEG
C THEN DECREASED LINEARLY TO ZERO AS THE NOZZLE ANGLE GOES TO ZERO. THE
C EFFECTIVE TAIL ANGLE LESS THE TAIL INCIDENCE IS ASSUMED TO INCREASE
C LINEARLY THROUGH THE SAME RANGE.
   20   EPI=(0.1+0.9*(DELJ/0.523))*EPIO
        ALPHAT=(1.-(0.39+(0.61/0.523)*DELJ))*ALPHA
C THE DOWNWASH EFFECT OF THE THRUST ON THE NOSE IS ASSUMED TO VARY LINEARLY
C WITH THE NOZZLE ANGLE. IT IS DOUBTFUL THAT THIS ASSUMPTION IS VALID AT LOW
C NOZZLE ANGLES BUT THE EFFECT THEN IS SMALL AT ANY RATE
   21   FI=(DELJ/1.57)*FIO
C THE RATIO OF THE FAN THRUST TO THE TURBINE THRUST IS NON-LINEAR. THE RATIO,K,
C VARIES WITH BOTH TOTAL THRUST AND SPEED. IN THIS SOLUTION THE CURVES HAVE
C BEEN LINEARLY APPROXIMATED. COMPUTER CURVE FITTING METHODS COULD BE USED
C IF GREATER ACCURACY IS DESIRED. IT IS BELIEVED THAT THE ERROR IS SMALL.
C   K=T2/T1 AND MUST BE ESTIMATED FORM  A GRAPH. K VARIES WITH BOTH
C   AIRPLANE VELOCITY AND TOTAL THRUST AND IS THEREFORE VERY DIFFICULT
C   TO PROGRAM AN ACCURATE ESTIMATION.
        IF(V.LE.80.)GO TO 300
        IF(V.LE.160.)GO TO 400
        IF(V.GT.160.)GO TO 500
  300   IF(T1*(1.+K).GE.14000.)GO TO 310
        IF(T1*(1.+K).GE.13000.)GO TO 320
        IF(T1*(1.+K).GE.12000.)GO TO 330
        IF(T1*(1.+K).LT.12000.)GO TO 340
  310   K=1.20-((15000.-T1*(1.+K))*C31)
        GO TO 600
  320   K=1.075-((14000.-T1*(1.+K))*C32)
        GO TO 600
```

```
330   K=0.985-((13000.-T1*(1.+K))*C33)
      GO TC 600
340   K=0.92
      GO TC 600
400   IF(T1*(1.+K).GE.15000.)GO TO 410
      IF(T1*(1.+K).GE.14000.)GO TO 420
      IF(T1*(1.+K).GE.13000.)GO TO 430
      IF(T1*(1.+K).GE.12000.)GO TO 440
      IF(T1*(1.+K).LT.12000.)GO TO 450
410   K=1.20-((15800.-T1*(1.+K))*C41)
      GO TC 600
420   K=1.090-((15000.-T1*(1.+K))*C42)
      GO TC 600
430   K=0.975-((14000.-T1*(1.+X))*C43)
      GO TO 600
440   K=0.895-((13000.-T1*(1.+K))*C44)
      GO TC 600
450   K=0.850-((12000.-T1*(1.+K))*C45)
      GO TC 600
500   IF(T1*(1.+K).GE.14000. )GO TO 510
      IF(T1*(1.+K).GE.13000.) GO TO 520
      IF(T1*(1.+K).GE.12000.) GO TO 530
      IF(T1*(1.+K).GE.11000.) GO TO 540
      IF(T1*(1.+K).LT.11000.) GO TO 550
510   K=0.91+((T1*(1.+K)-14000.)*C51)
      GO TC 600
520   K=0.91-((14000.-T1*(1.+K))*C52)
      GO TC 600
530   K=0.84-((13000.-T1*(1.+K))*C53)
      GO TC 600
540   K=0.80-((12000.-T1*(1.+K))*C54)
      GO TC 600
550   K=0.72
      GC TC 600
```

```
C  THE VARIATION OF INTAKE AIR FLOW HAS BEEN BEEN LINEARIZED. THIS
C  APPROXIMATION ISIS ACCURATE AS THE CURVE IS VERY NEARLY LINEAR.
 600  WA=315.+(T1*(1.+K))*C60
      FW=(WA*W)/32.2
      FU=(WA*U)/32.2
      MW=Q*S*(H-HNWB)*CLWB
      MI=LN*COS(THEO)*(FW-FI)
      MT=T1*((H-HT1)+K*(H-HT2))*SIN(DELT)
      MO=CMC*Q*S*CBAR
      ME=Q*ST*AT*(HT-H)*EPI
      MA=Q*ST*AT*(HT-H)*ALPHAT
C ME AND MA ARE NOT COMBINED BECAUSE THE VARIATION OF EPI AND ALPHAT IS IN DOUBT
      MU=FU*ZE
      MD=Q*S*CD*ZWB*COS(THEC)
      M1=MW+MI+MT+MO+ME-MA+MU+MD
      TC=Q*ST*AT*(HT-H)
C VARIATION OF REACTION MOMENT AND TAIL INCIDENCE WITH STICK MOVEMENT IS NOT
C ALWAYS LINEAR. HERE THE VARIATION HAS BEEN LINEARIZED BY SEGMENTS OF THE CURVE
      TT=T1*(1.+K)
C  THE VARIATION OF RPM IS LINEAR WITH BOTH TOTAL THRUST AND VELOCITY.
C  THE AMOUNT OF BLEED AND REACTION CONTROL MOMENT AVAILABLE IS DEPENDENT
C  ON THE ENGINE RPM.THE SOLUTION MUST BE ITERATED AS A CLOSED SOLUTION
C  IS NOT POSSIBLE. I IS INTRODUCED AND ALLOWED TO GO TO 100 BEFORE THE
C  PROGRAM IS STOPPED. THUS IF THE ITERATION IS NOT CONVERGING THE
C  PROGRAMMER IS WARNED BY A PREMATURE STOPPAGE.
      RPMX=0.95-((13950.-TT)*0.45)/13950.
      RPMV=RPMX-(0.08*V)/423.
      CB=1.0-2.14*(1.0-RPMV)
      M=M1
      I=1
 33   LS=(M- 1.4*C7 -2.*TC*C8)/(C8*TC+C7)
      IF(LS.LT.-2.) GO TO 34
      IF(LS.GT.0.) GO TO 40
```

```
      MR=-(LS+1.4)*C7
      MRNF=(CB*MR)/0.893
      LS=-(1.4+MRNF/C7)
      ETA=(LS+2.)*C8
      GO TO 60
34    LS=(M-1.4*C7-2.*TC*C11)/(C11*TC+C7)
      IF(LS.LT.-5.)GO TO 35
      MR=-(LS+1.4)*C7
      MRNF=(CB*MR)/0.893
      LS=-(1.4+MRNF/C7)
      ETA=(LS+2.)*C11
      GO TO 60
35    LS=(M+16200.+TC*(0.0786-5.*C12))/(TC*C12)
      MR= 16200.
      MRNF=(CB*MR)/0.893
      ETA=(LS+5.)*C12-0.0786
40    LS=(M-1.4*C7-0.0611*TC)/(C9*TC+C7)
      IF(LS.GT.1.) GO TO 41
      MR=-(LS+1.4)*C7
      MRNF=(CB*MR)/0.893
      LS=-(1.4+MRNF/C7)
      ETA=C9*LS+0.0611
      GO TO 60
41    LS=(M-12000.+C16-0.0611*TC)/(C9*TC+C16)
      IF(LS.GT.1.6) GO TO 42
      MR=-12000.-C16*(LS-1.)
      MRNF=(CB*MR)/0.893
      LS=1.-(MR+12000.)/C16
      ETA=C9*LS+0.0611
      GO TO 60
42    LS=(M-19000.-0.1133*TC+1.6*C10*TC)/(C10*TC)
      MR=-19000.
      MRNF=(CB*MR)/0.893
      ETA=C10*(LS-1.6)+0.1133
```

```
 60   ERRCR=M1+MRNF-TC*ETA
      IF(ERROR.LE.100.) GO TO 63
      M=M+ERROR/2.
      I=I+1
      IF(I.EQ.100) GO TO 70
      GO TO 33
 63   MR=MRNF
      IF(DELJ.LT.0.349) GO TO 55
      GO TO 59
 55   MR=MR*(DELJ/0.349)
      ETA=(M+MR)/TC
 59   LWB=Q*S*CLWB*COS(THEC)
      LTA=Q*ST*AT*COS(THEC)*(ALPHAT+ETA-EPI)
C  IF MR IS GREATER THAN ZERO, THE FORWARD REACTION CONTROL IS USED AND
C  FR MUST BE CALCULATED WITH HR2 INSTEAD OF HR1.
      IF(MR.GE.0.)GO TO 61
      FR=(-MR*COS(THEO))/(HR1-H) *COS(DELJ)
      GO TO 62
 61   FR=(MR*COS(THEO))/(HR2-H)*COS(DELJ)
C  THE X AND Z EQUATIONS ARE NOW SOLVED FOR THE TOTAL THRUST, TT, AND
C  THE NOZZLE ANGLE , DELJ.
 62   F1=LWB+LTA+FW-FI+FR-WEI
      DU=Q*S*((CD*COS(THEC))+CLWB*SIN(THEC))
      F2=DU+FU+FR*SIN(THEO)
      DELTL=ATAN(-(F1/F2))
      TT=-F1/SIN(DELTL)
      DELJ=(DELTL-THEO-THEOT)*57.3
      ETA=ETA*57.3
      WRITE(6,100)
100   FORMAT(77H    V    DELJ   ETA    T1*(1.+K)      FU        FI
     1DU        MR      ALPHA  )
      WRITE(6,200)V,DELJ,ETA,TT,FU,FI,DU,MR,ALPHA
200   FORMAT(1H ,3F8.2,1F10.0,4F8.1,1F6.2)
```

```
      DELJ=DELJ/57.3
      ETA=ETA/57.3
      IF(V.LE.100.)GO TO 700
      IF(V.LE.200.)GO TO 710
      IF(V.LE.300.)GO TO 720
      IF(V.GT.300.)GO TO 730
700   T1V=C1
      GO TO 800
710   T1V=C2
      GO TO 800
720   T1V=C3
      GO TO 800
730   T1V=C4
800   T2V=C5
      TTV=T1V+T2V
      SR=RHO*S*V
      STR=RHO*ST*V
      ALPHT=ALPHAT+ETA-EPI
      SAT=SIN(ALPHT)
      CAT=COS(ALPHT)
      CA=COS(ALPHA)
      SA=SIN(ALPHA)
      CO=COS(THEO)
      CC=COS(THEC)
      SO=SIN(THEO)
      SC=SIN(THEC)
C THE COMPUTATION OF THE STABILITY DERIVATIVES BASED ON THEFORCES AND
C MOMENTS OF THE PREVIOUSLY COMPUTED TRIM POINTS FOLLOWS) IN THE CASE OF
C THE ACCELERATING TRANSITION, THE FORCES AND MOMENTS ARE ASSUMED TO
C BE THOSE THAT WOULD BE ON THE VEHICLE IN UNACCELERATED FLIGHT AT THE SAME
C POINT)
C  COMPUTATION OF DIMENSIONAL DERIVATIVE XU
      PEPIA=1.-(ALPHAT/ALPHA)
      CLT=AT*(ALPHAT+ETA-EPI)
```

```
      WAXU=WA/32.2
      CLXU=SR*CLWB*SA*CA
      CDXU=SR*CD*(1.+CA**2)
      CLTXU=STR*CLT*(2.*SAT *CA-(1.-PEPIA)*CAT*SA)
      TTVXU=TTV*CA*COS(DELT)
      XU=CLXU+CLTXU-CDXU-WAXU+TTVXU
      XUM=(XU*32.2)/WEI
C THE XW DIMENSIONAL DERIVATIVE
      CLXW=SR*(CLWB*(1.+SA**2)+AWB*SA)
      CDXW=SR*CA*(AD+CD*SA)
      CLTXW=STR*((1.-PEPIA)*(CLT*CAT+AT*SAT)+2.*CLT*SAT*SA)
      TTVXW=TTV*SA*COS(DELT)
      XW=CLXW+CLTXW-CDXW+TTVXW
      XWM=(XW*32.2)/WEI
C THE ZU DIMENSIONAL DERIVATIVE
      CLZU=(1.+CA**2)*SR*CLWB
      CLTZU=STR*CLT*(2.*CAT*CA+(1.-PEPIA)*SAT*SA*CA)
      CDZU=SR*CD*SA*CA
      TTVZU=TTV*CA*SIN(DELT)
      ZU=-CLZU-CDZU-TTVZU-CLTZU
      ZUM=(ZU*32.2)/WEI
C THE ZW DIMENSIONAL DERIVATIVE
      WAZW=WA/32.2
      CLZW=SR*CA*(CLWB*SA+AWB)
      CLTZW=STR*((1.-PEPIA)*(CAT*AT-CLT*SAT)+2.*CLT*CAT*SA)
      CDZW=SR*(SA*AD+CD*(1.+SA**2))
      TTVZW=TTV*SA*SIN(DELT)
      ZW=-WAZW-CLZW-CLTZW-CDZW-TTVZW
      ZWM=(ZW*32.2)/WEI
C THE ZQ AND ZWDOT DIMENSIONAL DERIVATIVES ( TAIL CONTRIBUTIONS ONLY)
      ZQ=STR*AT*(H-HT)
      ZQM=(ZQ*32.2)/WEI
      ZWDOT=RHO*ST*AT*(1.-PEPIA)*(H-HT)*(PEPIA)
```

```
      ZWDOTM=(ZWDOT*32.2)/WEI
C THE MU DIMENSIONAL DERIVATIVE WITH DRAG, HEIGHT OF THE HORIZONTAL TAIL,
C AND HEIGHT OF THE WING CONSIDERED NEGLIGBLE IN ALL M DERIVATIVES
C  H1 HAS BEEN INTRODUCED AS THE DISTANCE FROM THE WING APEX TO THE
C  MOMENT REFERENCE CENTER USED FOR DERIVATIVE CALCULATION. IN THE CASE
C  OF THE HAWKER SIDDELEY DERIVATIVES USED FOR COMPARISON , H1 IS AT THE
C  WING BODY AERODYNAMIC CENTER. FOR THE CORRECT SOLUTION OF THE
C  EQUATIONS OF MOTION, HOWEVER, THE MOMENT REFERENCE CENTER MUST BE
C  AT THE CENTER OF MASS.
      MCLU=CLZU*(H1-HNWB)
      MCLTU=CLTZU*(H1-HT)
      MTTU=CA*SIN(DELT)*(T1V*(H1-HT1)+T2V*(H1-HT2))
      CMOU=2.*SR*CMO*CBAR
      CDMXU=ZWB*CDXU
      MUP=MCLU+MCLTU+MTTU+CMOU+CDMXU
      MUPM=MUP/IYY
C THE MW DIMENSIONAL DERIVATIVE
      MCLW=CLZW*(H1-HNWB)
      MCLTW=CLTZW*(H1-HT)
      MWAW=(LN*WA)/32.2
      MTTV=SA*SIN(DELT)*(T1V*(H1-HT1)+T2V*(H1-HT2))
      CDMW=CDZW*(H1-HNWB)
      CDMXW=ZWB*CDXW
      MWP=MCLW+MCLTW+MWAW+MTTV+CDMW+CDMXW
      MWPM=MWP/IYY
C THE MQ AND MWDOT DERIVATIVES ( TAIL CONTRIBUTIONS ONLY)
      MQ=ZQ*(HT-H1)
      MQM=MQ/IYY
      MWDOT=ZWDOT*(HT-H1)
      MWDOTM=MWDOT/IYY
      WRITE(6,910)
 910  FORMAT(97HO     XUM        XWM        ZUM        ZWM        ZWDOTM     Z
     1QM      MUPM       MWPM       MWDOTM      MQM)
      WRITE(6,900)XUM,XWM,ZUM,ZWM,ZWDOTM,ZQM,MUPM,MWPM,MWDOTM,MQM
 900  FORMAT(1HO,10F10.5)
```

```
      WO=V*SIN(ALPHA)
      UO=V*COS(ALPHA)
      A=ZWDOTM-1.
      B=XUM-ZWDOTM*(XUM+MQM)+ZWM+MQM+MWDOTM*(ZQM+UO)
      C=XUM*(MQM*(ZWDOTM-1.)-ZWM-MWDOTM*(ZQM+UO))-ZWM*MQM+MWPM*(ZQM+UO)+
     1ZUM*(XWM-WC*MWDOTM)+WO*MUPM*(ZWDOTM-1.)
      D=XUM*(ZWM*MQM-MWPM*(ZQM+UO))-XWM*(ZUM*MQM-MUPM*(ZQM+UO))-32.2*(ZU
     1M*MWDOTM-MUPM*(ZWDOTM-1.))-WO*(ZUM*MWPM-MUPM*ZWM)
      E=32.2*(MUPM*ZWM-ZUM*MWPM)
C  SMULR IS A STANDARD 7094 COMPUTER PROGRAM OF THE SESCD FACILITY FOR
C  THE SOLUTION OF A POLYNOMIAL EQUATION OF AYY DEGREE. NX IS THE ORDER
C  OF THE EQUATION. ROOTR IS THE REAL PART OF ROOT AND ROOTI THE
C  IMAGINARNARY , IF ANY. IN THE PRINT OUT OF THE ROOTS R1 AND R5
C  COMPRISE ONE ROOT . SIMILLIARLY R2AND R6, R3 AND R7 , R4 AND R8.
      NX=4
      COE(1)=A
      COE(2)=B
      COE(3)=C
      COE(4)=D
      COE(5)=E
      CALL SMULR(COE,NX,ROOTR,ROOTI)
      WRITE(6,950)
  950 FORMAT(75H0    R1          R2          R3          R4          R5          R6
     1          R7          R8)
      WRITE(6,960)ROOTR,ROOTI
  960 FORMAT(1HC,8F10.5///)
C  THE NEW VALUE OF V IS NOW ASSIGNED AND THE ENTIRE CALCULATION
C  REPEATED FOR THE NEW FLIGHT CONDITIONS. THE TRANSITION IS COMPLETED
C  WHEN THE NOZZLE ANGLE REACHES ZERO.
  120 V=V+DELV
      U=V*COS(ALPHA)
      W=V*SIN(ALPHA)
      IF(DELJ.LE.0.)GO TO 70
      GO TO 1
   70 STOP
      END
```

Vita

Charles Peter Winters was born on [redacted] in [redacted] He graduated from high school in Owatonna, Minnesota in 1955. He received the Bachelor of Science degree from the United States Air Force Academy and a commission in the USAF in 1959. After receiving his pilot wings in July 1960, he attended advanced fighter training at Luke Air Force Base, Arizona and Nellis Air Force Base, Nevada. He subsequently was assigned to Misawa Air Base, Japan and Myrtle Beach Air Force Base, South Carolina flying the F-100.

Permanent address: [redacted]

This thesis was typed by Mrs. Imogene J. Hoffer.

UNCLASSIFIED

Security Classification

DOCUMENT CONTROL DATA - R & D

(Security classification of title, body of abstract and indexing annotation must be entered when the overall report is classified)

1. ORIGINATING ACTIVITY (Corporate author)

Air Force Institute of Technology (AFIT-SE)
Wright-Patterson AFB, Ohio 45433

2a. REPORT SECURITY CLASSIFICATION: Unclassified

2b. GROUP:

3. REPORT TITLE

The Approximate Logitudinal Stability Derivatives of a Vectored Thrust VTOL

4. DESCRIPTIVE NOTES (Type of report and inclusive dates)

AFIT Thesis

5. AUTHOR(S) (First name, middle initial, last name)

Charles P. Winters
Captain USAF

6. REPORT DATE	7a. TOTAL NO. OF PAGES	7b. NO. OF REFS
March 1968	150	9

8a. CONTRACT OR GRANT NO.	9a. ORIGINATOR'S REPORT NUMBER(S)
b. PROJECT NO.	GAM/AE/68-11
c. N/A	9b. OTHER REPORT NO(S) (Any other numbers that may be assigned this report)
d.	

10. DISTRIBUTION STATEMENT This document is subject to special export controls and each transmittal to foreign governments or foreign nationals may be made only with prior approval of the Dean of Engineering, Air Force Institute of Technology (AFIT-SE), Wright-Patterson Air Force Base, Ohio, 45433.

11. SUPPLEMENTARY NOTES	12. SPONSORING MILITARY ACTIVITY

13. ABSTRACT

The objective of this study was to investigate the stability derivatives and the stability of the vectored thrust P-1127 airplane. Expressions were derived for the derivatives. The performance, derivatives and stability were found for both an accelerating and nonaccelerating transition from hover to conventional flight. The results of the accelerating transition were compared to values available from Hawker Siddeley. Both transitions were unstable for many airspeeds but the times to double amplitude were such that a pilot could control the airplane.

DD FORM 1 NOV 68 1473

UNCLASSIFIED

Security Classification

14 KEY WORDS	LINK A		LINK B		LINK C	
	ROLE	WT	ROLE	WT	ROLE	WT
P-1127 - Transition Performance and Longitudinal Stability						
Longitudinal Stability						
VTOL Performance and Longitudinal Stability						